

**BAUXITE STABILIZATION USING
GYPSUM AND VERMICOMPOST AGAINST
LIQUEFACTION IN SOLID BULK CARGOES**



**MUHAMMAD FAT-HI AL JUWAINI BIN
PAHROL**

اونيورسيتي ملايسيا قهغ

UNIVERSITI MALAYSIA PAHANG

MASTER OF SCIENCE

UNIVERSITI MALAYSIA PAHANG

UNIVERSITI MALAYSIA PAHANG

DECLARATION OF THESIS AND COPYRIGHT

Author's Full Name : MUHAMMAD FAT-HI AL JUWAINI BIN PAHROL

Date of Birth : 23 NOVEMBER 1995

Title : BAUXITE STABILIZATION USING GYPSUM AND
VERMICOMPOST AGAINST LIQUEFACTION IN SOLID
BULK CARGOES

Academic Session : SEMESTER I 2020/2021

I declare that this thesis is classified as:

- CONFIDENTIAL (Contains confidential information under the Official Secret Act 1997)*
- RESTRICTED (Contains restricted information as specified by the organization where research was done)*
- OPEN ACCESS I agree that my thesis to be published as online open access (Full Text)

I acknowledge that Universiti Malaysia Pahang reserves the following rights:

1. The Thesis is the Property of Universiti Malaysia Pahang
2. The Library of Universiti Malaysia Pahang has the right to make copies of the thesis for the purpose of research only.
3. The Library has the right to make copies of the thesis for academic exchange.

Certified by:



(Student's Signature)

951123-10-5173

New IC/Passport Number

Date:

(Supervisor's Signature)

Assoc. Prof. Dr Muzamir
Bin Hasan

Name of Supervisor

Date:

NOTE : * If the thesis is CONFIDENTIAL or RESTRICTED, please attach a thesis declaration letter.

SUPERVISOR'S DECLARATION

We hereby declare that we have checked this thesis and in our opinion, this thesis is adequate in terms of scope and quality for the award of the degree of Master of Science.

(Supervisor's Signature)

Full Name : ASSOCIATE PROFESSOR DR MUZAMIR BIN HASAN

Position : SENIOR LECTURER

Date :



UMP

اونيورسيتي ملايسيا قهغ

UNIVERSITI MALAYSIA PAHANG

STUDENT'S DECLARATION

I hereby declare that the work in this thesis is based on my original work except for quotations and citations which have been duly acknowledged. I also declare that it has not been previously or concurrently submitted for any other degree at Universiti Malaysia Pahang or any other institutions.

(Student's Signature)

Full Name : MUHAMMAD FAT-HI AL JUWAINI BIN PAHROL

ID Number : MAG 18002

Date :

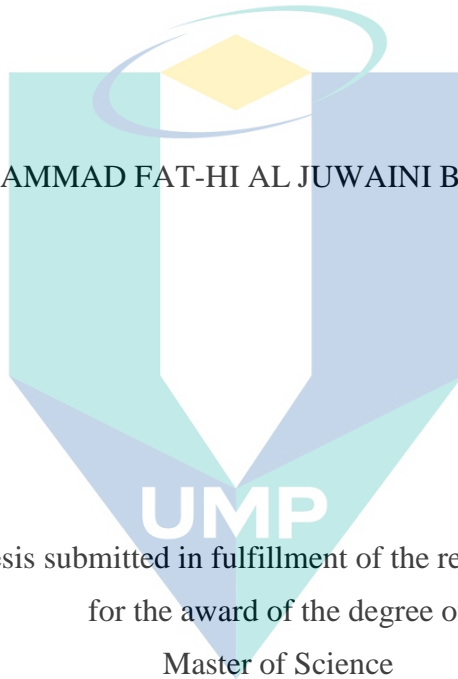
UMP

اونيورسيتي ملايسيا قهغ

UNIVERSITI MALAYSIA PAHANG

BAUXITE STABILIZATION USING GYPSUM AND VERMICOMPOST
AGAINST LIQUEFACTION IN SOLID BULK CARGOES

MUHAMMAD FAT-HI AL JUWAINI BIN PAHROL



Thesis submitted in fulfillment of the requirements
for the award of the degree of
Master of Science

اونيورسيتي مليسيا قهغ

UNIVERSITI MALAYSIA PAHANG

COLLEGE OF ENGINEERING
UNIVERSITI MALAYSIA PAHANG

OCTOBER 2020

ACKNOWLEDGEMENTS

Firstly, I would like to thank God for His greatness, give the ideas, energy, and dedication to me for complete this thesis. I would like to express my highest sincere appreciation to my supervisor Associate Prof Dr. Muzamir bin Hasan for his valuable supervision, continuous encouragement, cooperation and guide me to the right direction in making this research a success. His wide knowledge, experiences and skills in academic has allowed me to perform better and sharpen my capabilities in many areas, especially in the field of Geotechnical Engineering.

I would also like to thank all the lab assistants in Soil and Geotechnical Laboratory, University Malaysia Pahang, En. Ziunizan, En. Nor Azmi and En. Haliman who provided me trainings and equipment during my laboratory testing to complete my project.

Importantly to mention my beloved family in Residence College 4: En Nasrul Salim Pakheri, En Mohamad Najib, Che Muhammad Aizal, Aizat Azed, Balya Darohini, Hafizuddin, Dzul Iskandar, Syamsul Imran, Hilmi Hanoin, Abdul Rafiq, Irfan and Nabil for their support, taking care, and directly advice on both thesis work and life. Thank you for such a great moment as assistant fellow and friends.

Finally, thank you to my family members especially my parents and the special one: Pahrol Bin Mohd Juoi, Mastura Binti Bakar and Siti Nur Fatimah Binti Abd Nasir for their love, moral supports and encouragement in completing this research work.

اونيورسيتي ملايسيا قهغ

UNIVERSITI MALAYSIA PAHANG

ABSTRAK

Pencairan dalam kargo pepejal pukal adalah masalah serius yang disebabkan oleh kargo berbutir adalah disebabkan ketidakstabilan pasir bijih dan mineral di dalam agregat. Kajian ini bertujuan untuk menstabilkan bauksit menggunakan gipsium dan vermicompost untuk mengurangkan risiko pencairan dalam kargo pepejal pukal. Kaedah ini bermula dengan Factorial analysis di mana bauksit diubah oleh beberapa parameter seperti peratusan gipsium, vermicompost, air dan masa inkubasi. Pindaan-pindaan tersebut menjalani pengedaran agregat dan ujian spesifik graviti, hasil dari ujian ini kemudian diteruskan dengan menganalisis untuk menyaring parameter utama yang memberikan pengaruh yang signifikan terhadap kedua respon tersebut. Kedua-dua parameter utama (peratusan gipsium dan vermicompost) yang menyumbang kebanyakan tindak balas adalah parameter yang digunakan di kajian dalam center composite design di mana dua parameter lain (air di dalam sample 50% dan masa inkubasi selama 15 hari) tetap. Center composite design adalah penting untuk mengecilkan dan meningkatkan nilai permulaan analisa awal. Pada peringkat ini, nilai sasaran untuk pindaan yang memberikan sumbangan yang optimum diulangi sekurang-kurangnya empat kali untuk memastikan variasi data kecil. Nilai sasaran untuk pindaan untuk memberikan sumbangan yang optimum kemudiannya mengkaji dengan lebih terperinci yang merangkumi kestabilan agregat (Kaedah Le Bissonnais), jadual aliran, pengedaran zarah, graviti spesifik, mikroskop pelepasan pengimbasan dan sinaran penyebaran tenaga. Data ini menganalisis untuk menghasilkan nilai sasaran yang muktamad, yang memberikan sumbangan yang optimum. Analisis 39 sampel pindaan menunjukkan, pada 6% daripada gipsium dan 4% daripada vermicompost mengikut berat adalah keadaan optimum untuk meningkatkan kestabilan agregat dan mengurangkan risiko pencairan yang ketara. Peningkatan ketara dalam perkadaran taburan agregat pada 2.5 mm kepada 20.38%, manakala dalam graviti tertentu, pindaan yang dikurangkan sebanyak 20.67% yang menunjukkan jumlah kandungan halus dalam bauksit berkurang. Pindaan juga meningkatkan rintangan bauksit sebanyak 40% dan Mean Weight Diameter (MWD) pindaan dicatatkan peningkatan sebanyak 75.51% apabila dibandingkan dengan unjuran bauksit. Di samping itu, analisis jadual alir menunjukkan bahawa perubahan optimum mempunyai Transportable Moisture Limit (TML) yang lebih tinggi yang dicatatkan pada 26.97% apabila dibandingkan dengan kandungan lembapan semulajadi, 24.07%. Dalam morfologi yang dikaji, kombinasi gipsium dan vermicompost menukarkan agregat dari struktur lembaran seperti struktur agregat makro granular, sementara menukar agregat mikro dari bijirin ke struktur granular atau prisma. X-ray diffraction (XRD) menunjukkan bahawa jumlah aluminium oksida tidak dipengaruhi oleh pindaan yang dibuat dalam penyelidikan ini. Hasil kajian ini menunjukkan bahawa penggunaan gipsium dan vermicompost ke bauksit secara langsung mempengaruhi taburan ukuran agregat dan mikromorfologinya, mengakibatkan peningkatan kestabilan agregat untuk mengurangkan risiko pencairan tanpa mengubah kandungan aluminium oksida.

ABSTRACT

Liquefaction in solid bulk cargoes is a serious problem caused by granular cargoes such as crushed ore and minerals sands instability within aggregate. This study aim to stabilize bauxite using mixture of gypsum and vermicompost to reduce liquefaction risk in solid bulk cargoes. The method were initiated with factorial analysis in which the bauxites were amend by varies parameters such as percentage of gypsum, vermicompost, water intake and incubation days. The amendments undergo particle distribution and specific gravity test, the result from these test were then analyze for screening the main parameters that gives significant effect to both responses (particle distribution and specific gravity). The two main parameters (percentage of gypsum and vermicompost) that contribute most in the responses were study in central composite design where other two parameters (water intake of 50% and incubation days of 15 days) are remain fixed. Central composite design are important to narrowing and enhancing the initial value of preliminary analysis. At this stage, targeted value for the amendment to give optimal contributions were repeat for at least four times to ensure the variances are small. Targeted value for the mixtures to give optimal contributions (high value in 2.5 mm particle distribution) were then study in more details that includes aggregate stability (Le Bissonnais Method), flow table, particle distribution, specific gravity, scanning emission microscopy and energy dispersive x-ray. The data were analyze to produce the conclusive targeted value, which gives the optimal contribution. Analyses of 39 sample of amendment showed, at 6% of gypsum and 4% of vermicompost by weight is the optimal condition for increasing aggregate stability and significantly reduce liquefaction risk. Significantly improved its proportion of particle distribution at 2.5 mm by 20.38%, whereas in specific gravity, the amendments reduced by 20.67% which indicates the amount of 2.5 mm aggregate content in bauxite greatly reduced. Amendments also enhanced the erosion resistance of bauxite by 40% and the Mean Weight Diameter of amendment was recorded improvement by 75.51% when compare to unamend bauxite. In addition, flow table analysis showed that optimal amendment has higher Transportable Moisture Limit recorded at 26.97% when compare to natural moisture content, 24.07%. In the morphology studied, the combination of gypsum and vermicompost converted the aggregate from a sheet-like structure to a granular macro aggregated structure, whilst converting micro aggregates from a grain to a granular or prismatic structure. X-ray diffraction data shows that the amount of aluminum oxide not significantly affected by amendment made in this research. The findings of this work suggested that application of gypsum and vermicompost to bauxite directly influenced aggregate size distribution and its micromorphology, resulting in the improvement of aggregate stability to reduced liquefaction risk without changing its aluminum oxide content.

TABLE OF CONTENT

DECLARATION	
TITLE PAGE	
ACKNOWLEDGEMENTS	ii
ABSTRAK	iii
ABSTRACT	iv
TABLE OF CONTENT	v
LIST OF TABLES	viii
LIST OF FIGURES	ix
LIST OF SYMBOLS	xi
LIST OF ABBREVIATIONS	xii
CHAPTER 1 INTRODUCTION	1
1.1 Introduction	1
1.2 Problem statement	2
1.3 Objectives of Research	3
1.4 Scope of Research	4
1.5 Significant of Research	5
CHAPTER 2 LITERATURE REVIEW	6
2.1 Introduction	6
2.2 Liquefaction in Soil	6
2.2.1 Types of Solid Bulk Cargoes that Susceptible to Liquefy	8
2.2.2 Evaluate Liquefaction Potential: Past Researcher and IMSBC Code	9
2.2.3 Impact of Liquefaction of Solid Bulk Cargoes to Environmental	12
2.3 Review Studies on Bauxite	14

2.3.1	The Types of Bauxite in Malaysia	14
2.3.2	Liquefaction Potential in Bulk Cargoes	16
2.4	Studies on Aggregate Stability	18
2.4.1	Elements in Aggregate Stability	19
2.4.2	Relationship between Liquefaction and Aggregate Stability	23
2.5	Review Studies on Soil Stabilization for Liquefaction Mitigation	24
2.5.1	Materials to Stabilize Soil Sample against Liquefaction	25
2.5.2	Gypsum as Stabilizer	28
2.5.3	Vermicompost as Stabilizer	29
2.5.4	Gypsum and Vermicompost as Soil Stabilizer	30
CHAPTER 3 METHODOLOGY		32
3.1	Introduction	32
3.2	Selection of Materials	34
3.3	Preparation of Mixture	35
3.4	Description of Each Phase	36
3.4.1	Full Factorial Design	36
3.4.2	Central Composite Design	40
3.4.3	Validation and Comparing Result	42
3.5	Particle Size Distribution	42
3.6	Specific Gravity	43
3.7	Aggregate Stability Test	44
3.8	Flow Table Test	45
3.9	SEM and EDX	46

CHAPTER 4 RESULTS AND DISCUSSION	47
4.1 Introduction	47
4.2 Material and Sample Characterization	47
4.3 Full Factorial Design: Screening the Factor	48
4.3.1 Variable Contribution on Particle Distribution at 2.5 mm and Specific Gravity	51
4.3.2 Screening Variable that Effect on Both Responses	55
4.4 Central Composite Design: Optimization Analysis	59
4.4.1 Central Composite Design (CCD)	59
4.4.2 Modelling for Optimization Stage	61
4.4.3 Regression Model	62
4.4.4 Response Surface Plot	63
4.5 Validation: Aggregate Stability and Flow Table Analysis	64
4.5.1 Aggregate Stability Analysis	65
4.5.2 Flow Table Analysis	68
4.5.3 Scanning Emission Microscopy and Energy Dispersive X-Ray	70
CHAPTER 5 CONCLUSION	73
5.1 Introduction	73
5.2 Recommendations	74
REFERENCES	76
APPENDIX A	84
APPENDIX B	93
APPENDIX C	100

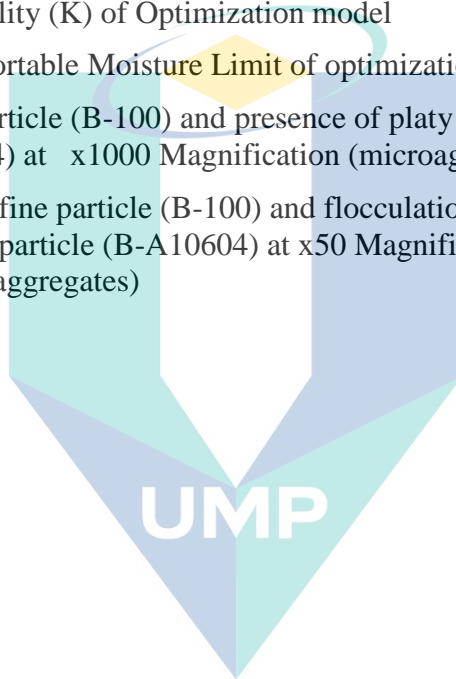
LIST OF TABLES

Table 2.1	Chemical compositions of Bauxite in Peninsular Malaysia	15
Table 2.2	Industries Specification to Process Bauxite	15
Table 2.3	Ship stability failures related to liquefaction in cargo	16
Table 2.4	Summary of the applied methodologies for evaluating aggregate stability	20
Table 2.5	Main breakdown mechanism in the modified Le Bissonnais' method	20
Table 2.6	Properties of soil affecting liquefaction	21
Table 2.7	Types of material recently used for liquefaction mitigation	26
Table 3.1	Materials used	34
Table 3.2	Central Composite Design Table	40
Table 3.3	Validation and Modelling Table	42
Table 4.1	Basic Properties of Material	48
Table 4.2	Basic Properties of Material	48
Table 4.3	Initial value of each variable	49
Table 4.4	Finalized output for each parameter to be screening	50
Table 4.5	Estimated Effect of Variable to Particle Distribution at 2.5 mm	54
Table 4.6	Estimated Effect of Variable to Specific Gravity	54
Table 4.7	ANOVA for factorial analysis for Particle Distribution at 2.5 mm	55
Table 4.8	ANOVA for factorial analysis for Specific Gravity	56
Table 4.9	The value of factors used in Central Composite Design	59
Table 4.10	Finalized output for each parameter to be screening	60
Table 4.11	ANOVA of model for particle distribution at 2.5 mm	61
Table 4.12	ANOVA of model for specific gravity	62
Table 4.13	Validation and Modelling Table	64
Table 4.14	Samples and each of disruptive test in term of MWD, GMD and Erodibility Factor	65
Table 4.15	Tranportable Moisture Limit of Optimziation model	69
Table 4.16	X-ray diffraction of amended bauxite (B-A10604)	71
Table 4.17	X-ray diffraction of unamend bauxite (B-100)	72

LIST OF FIGURES

Figure 2.1	Liquefaction at Palu (soil slide to right), Indonesia on 28 September 2018.	7
Figure 2.2	Compaction causes water to push aggregate leading to liquefaction	7
Figure 2.3	Liquefaction in solid bulk cargoes caused by rapid loading from wave Source: Munro & Mohajerani, (2017)	8
Figure 2.4	Potential solid bulk cargo to liquefy	9
Figure 2.5	Representation of the tested lateritic soils on Seed et al. (2003) recommended chart	10
Figure 2.6	Showing increase in diameter plotted against moisture content.	11
Figure 2.7	Bauxite washing pond showing red water in Malaysia	13
Figure 2.8	Illustrate summarize accidents that involving liquefaction in bulk cargoes	17
Figure 2.9	Trending of liquefaction in solid bulk cargoes Source: Hou et al. (2014)	17
Figure 2.10	Pore pressure ratio versus shear strain from strain-controlled triaxial test Source: Ju et al., (2018)	23
Figure 2.11	Soil structure change into platy and from machine at x1000 magnification	31
Figure 3.1	Flowchart of research	33
Figure 3.2	Mixing Method and Apparatus	35
Figure 3.3	Incubation Preparation at Soil Mechanics Engineering Lab UMP	35
Figure 3.4	Selection of factorial design box in Design Expert software	36
Figure 3.5	Factors and their designated low and high actual value	37
Figure 3.6	Response to evaluate the physical changes of amended bauxite.	37
Figure 3.7	Factorial Design table with responses value	38
Figure 3.8	Desirability of solutions in factorial design	38
Figure 3.9	All the interaction of factors according to the response	39
Figure 3.10	Targeted value from screening phase are at the center of CCD phase.	40
Figure 3.11	Targeted value from target value for optimum effect to amend bauxite	41
Figure 3.12	Sieve analysis apparatus	43
Figure 3.13	Vacuum chamber and specific gravity of sample	43
Figure 3.14	Flow table apparatus	45
Figure 3.15	Benchtop SEM, Hitachi TM3030 Plus used for morphological analysis	46

Figure 4.1	Effect on Particle Distribution at 2.5 mm	52
Figure 4.2	Effect on Specific Gravity	52
Figure 4.3	Interaction of Gypsum (%) and Vermicompost (%) on specific gravity and particle density (%)	53
Figure 4.4	Predicted versus actual regression model graph for Particle Distribution at 2.5 mm	58
Figure 4.5	Predicted versus actual regression model graph for Specific Gravity	58
Figure 4.6	Optimization of 3D Contour Plot	63
Figure 4.7	Mean Weight Diameter of Optimization model	67
Figure 4.8	Erodibility (K) of Optimization model	68
Figure 4.9	Transportable Moisture Limit of optimization model	69
Figure 4.10	Fine particle (B-100) and presence of platy arrangement (B-A10604) at x1000 Magnification (microaggregates)	70
Figure 4.11	Scatter fine particle (B-100) and flocculation of fines particle to dense particle (B-A10604) at x50 Magnification (macroaggregates)	71

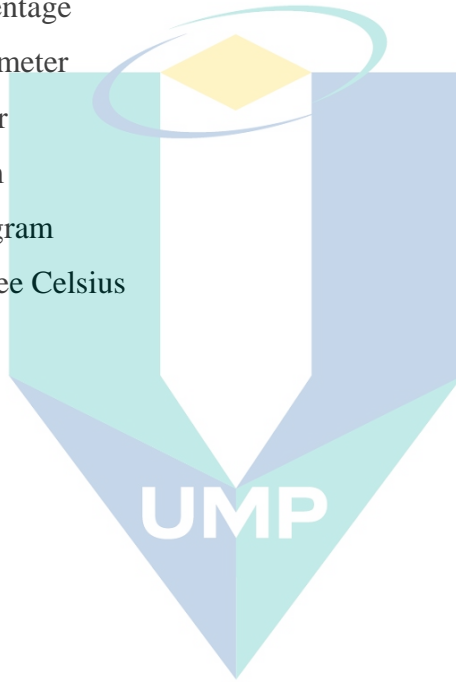


اونيورسيتي مليسيا قهغ

UNIVERSITI MALAYSIA PAHANG

LIST OF SYMBOLS

c'	Cohesion angle
ϕ'	Friction angle
τ_f	Effective stress
u	Pore water pressure
ω	Moisture content
c'	Cohesion angle
%	Percentage
mm	Millimeter
m	Meter
g	Gram
kg	Kilogram
$^{\circ}\text{C}$	Degree Celsius



اونيورسيتي ملايسيا قهغ

UNIVERSITI MALAYSIA PAHANG

LIST OF ABBREVIATIONS

Al	Aluminum
ANOVA	Analysis of Variance
ASTM	American Society for Testing and Materials
CCD	Central Composite Design
EDX	Energy Dispersive X-Ray
Fe	Iron
FMP	Flow Moisture Point
FW	Fast Wetting
GA ₃	Gibberellic Acid
IAA	Indole-3-Acetic Acid
IMSBC	International Maritime of Solid Bulk Cargoes
LI	Liquidity Index
LL	Liquid Limit
MWD	Mean Weight Diameter
Na	Sodium
O	Oxygen
pH	Potential Hydrogen
PI	Plasticity Index
RSM	Response Surface Method
SEM	Scanning Electron Microscope
Si	Silicon
SW	Slow Wetting
Ti	Titanium
TML	Transportable Moisture Limit
wc	Water content
WS	Wet Stirring
XRD	X-Ray Diffraction
XRF	X-Ray Fluorescence

CHAPTER 1

INTRODUCTION

1.1 Introduction

The word “liquefied” was first used for soil in 1918 by Allen Hazen in response to the failure of Calaveras Dam in California and that spark the interest of many scholars and researcher to explore the phenomena more (Patrick Koester, 1994; Derakhshandi et al., 2008; Ju et al., 2018). Liquefaction is phenomena that occur from earthquake as induces seismic waves cyclically shear the soil (Wang & Dreger, 2004). In general, liquefaction occurs when the aggregate of loose, saturated sand breaks down due to a rapidly applied load (Mahmood & Mulligan, 2016). Two conditions that need to be present for the phenomena to occur are: 1) increase in soil water pressure, which reduces the contact forces between the individual soil particles 2) subjected to transient or periodic loading (Ju et al., 2018)

However, liquefaction can also occur in cargoes carrying item across sea for shipping purpose and with increasing incidence as recorded by Ju et al, 2018. Bauxite is a rock formed from reddish clay material called laterite soil commonly found in tropical or subtropical regions and exportation of bauxite usually in form of granular ore, minerals sand or crushed ore (Gore, 2015). Crushed ore and mineral sands such as bauxite, iron ores, and nickel ore are responsible for the loss of numerous ships every years (Gourvenec, 2018).

For example, the MS (Motor Ship) Bulk Jupiter that departed from Kuantan, Malaysia on 30 December 2014 carrying 56 000 tons of bauxites has sunk the coast of Vung Tau, Vietnam on 2 January 2015 with 16 loss; two dead and one survived. Substantially to note that if two conditions mention earlier occurs in soil aggregate; liquefaction can happen. Munro & Mohajerani (2017) explained that the liquefaction of solid bulk cargoes on bulk carrier is a reoccurring problem whereby a combination of fine particles, moisture and changing pore pressure within a cargo resulted in the mass acting like liquid.

International Maritime of Solid Bulk Cargoes (IMSBC) under International Maritime Organization (IMO) outlined a few mandatory test methods to minimize the risk of liquefaction within solid bulk cargoes by determining the Transportable Moisture Limit (TML) of liquefiable cargoes (Walton. 2015). However, this do not stop the increasing number of the incidents. Therefore, some researchers start to explore on different factors that could lead to this phenomenon. Burbank et al (2001) look into soil structure of the dry bulk cargoes, which depends on the presence of aggregate and their stability. For example, bauxite residue have poor soil structure and low hydraulic conductivity and this is a major factor of disaggregation within vessel (Djurić et al., 2010). This may cause severe effect of liquefaction in solid bulk cargoes. Existing technology for stabilizing soils to mitigate liquefaction include cementation (e.g., permeation grouting), densification (e.g. Vibro replacement, deep dynamic compaction, or compaction grouting), drainage, and thermal stabilization (Burbank et al., 2011). Although many of these approaches have proven successful but these methods are limited in liquefaction mitigation of solid bulk cargoes (Mitchell & Baxter, 1995).

Preliminary work on using soil stabilization to strengthen liquefiable soils was led by Burbank et al. (2011) in which he had found that calcite precipitation increases soils resistance to seismic-induced liquefaction. On the other hand, Zhu et al. (2017) suggested that application of gypsum and vermicompost to bauxite residue might directly influence aggregate size distribution and its micromorphology. Thus, this will affect the aggregate stability and structure. This thesis critically focus on how improvement of aggregate stability and structure of bauxite can reduce liquefaction risk in solid bulk cargoes.

1.2 Problem statement

Liquefaction in solid bulk cargoes that are cause by granular cargoes such as crushed ore and mineral sands instability within aggregate is an important issue to addressed (Derakhshandi et al., 2008; Maurer et al., 2014; Munro & Mohajerani, 2016). In 2015, the 56,000-tonne bulk carrier Bulk Jupiter carrying bauxite from Malaysia rapidly sunk around 300 km south-west of Vietnam, with only one of its 19 crew survived. Statistically, ten solid bulk cargoes have been lost at sea each year for the last decade as found by Ju et al., 2018. Gourvenec (2018) commented that the existing guidance on stowing and shipping solid bulk cargoes is too simple, as it does not take the strength of inter-particle cohesion into account. The variety of soil physical, chemical and biological

influences neglected in the guide. Therefore, a new perspective has brought into this matter, the study of aggregate stability of soil. Aggregate stability is ability of soil aggregate to resist deterioration when external forces are applied (Goebel et al., 2012). Study by Zhu et al., 2017 look into aggregate stability of bauxite residue for agricultural shows, the use of gypsum and vermicompost stimulate aggregate formation and improve aggregate stability. The focus of the study was agricultural purposes and the sample use are the residue of bauxite, which is the by-product of Bayer Process (Cabllk, 2007). Raw bauxite have poor aggregate structure and stability, which resulted in the excessive fines particles appear after mining (Guo et al., 2016). Surprisingly, the findings by Zhu et al., 2017 do not test any raw bauxite sample for reducing liquefaction risk in solid bulk cargoes.

Liquefaction risk in solid bulk cargoes can be quantify by the standard test of IMSBC Code through flow table test to obtain the TML value. Moisture content of the soil must be lower than its own TML in order to have permit to be in cargoes. Presence of fine particles in soils are the reason of low TML (Cheng et al., 2014). However, weak aggregate stability, present of viscous material (such as kaolin and laterite ore), and poor drainage between aggregate should be in focus as these can contribute to such incidents (Cheng et al., 2014; Munro & Mohajerani, 2018). This worsening the problem with the drastic measure taken to reduce fines particles within soils by washing it (beneficiation), resulted in pollution of water supply (Abdullah et al., 2016).

Therefore, there is a need to find solution to reduce soil liquefaction in solid bulk cargoes without beneficiation process that focus on improving stability within aggregate. This study attempts to assess the aggregate stability performance of raw bauxite under treatment of gypsum and vermicompost. Thus, it is important to find the optimal value for using gypsum and vermicompost by weight to reduce significant amount of TML and liquefaction risk.

1.3 Objectives of Research

The objectives of this research are:

- i. To determine which parameters (incubation days, water intake, gypsum and vermicompost) give the highest contribution to amend bauxite's physical properties.

- ii. To enhance the target value data of the parameters (incubation days, water intake, gypsum and vermicompost) by using Central Composite Design (CCD) To quantify the dry index for 80 years (2020 – 2099) for long-term duration.
- iii. To investigate the performance of amended bauxite and raw bauxite on Mean Weight Diameter and Transportable Moisture Limit.

1.4 Scope of Research

The scopes of research are as follows:

1. Investigate liquefaction problems in solid bulk cargoes carrying bauxite by propose analytical method on using gypsum and vermicompost as stabilizer to reduce liquefaction risk in bauxite.
2. Highlighted the weak aggregate stability of bauxite has led to slaking, differential swelling and mechanical dispersion that resulting in water entrapped and increased pore water pressure. Ultimately liquefaction within the vessel of cargoes.
3. Fresh-deposited bauxite were taken during September 2017 from Gebeng, Kuantan, Pahang, which is located approximately 38km from Kuantan city. Around five seal cap container were used to store the bauxite in Soil Mechanics and Geotechnical Lab, University Malaysia Pahang.
4. Amendment of raw bauxite by using gypsum and vermicompost was focus on improving physical properties that gives significant changes on Transportable Moisture Limit and Mean Weight Diameter. The chosen physical test were used to evaluate the changes of amend bauxite are particle size distribution at 2.5mm, specific gravity, Le Bissonnais Method (slow wetting, fast wetting and wet stirring) and Flow Table, . The highest contribution will see as positive result.

1.5 Significant of Research

The transportation industry such as sea exportation must tackle the challenges in meeting the growing worldwide demand of cargoes such as bauxite, iron ores, lead ore, and nickel ore, which surely will increase the incident of capsizing due to liquefaction in the next decades if the authority (sea marshal) are solely depends on TML of cargoes before it been shipped. The issues of environmental pollution due to beneficiation process should be in focus to maintain the sustainability of mining industry. To resolve both issues regarding liquefaction in bauxite bulk cargoes and beneficiation process, this research will provide an alternative ways to reduce liquefaction risk by significant increase aggregate stability of bauxite that directly affect its TML and MWD. The amended bauxite has lower fines particles from raw bauxite will contribute to less water pollution.

This study shows bauxite has poor aggregate stability that were suspected to be one of reasons on liquefaction in solid bulk cargoes. This is because when aggregate breaks into finer aggregate, water entrapped within soil and severely increase pore water pressure and liquefaction risk. Therefore, this study provides an alternative to amend bauxite by addition of gypsum and vermicompost that stimulate aggregate formation. Eventually, the cost to implement the idea is low and easy to replicate in industry scale, and soon will attract foreign investor while benefitting the environment and mining industry.

The main novelty of this study is in its findings on the relationship of aggregate stability and liquefaction risk within bulk cargoes. Aggregate stability are one of the main factor for liquefaction in solid bulk cargoes. The aim of this study was to outline the weak aggregate stability has led to slaking, differential swelling, mechanical dispersion and physicochemical dispersion that resulted in water entrapped and increased pore water pressure. Ultimately, all of these will cause liquefaction. Quantitative analysis of the gypsum and vermicompost to be use to amend bauxite will share an important output for the future researcher, mining industry and transportation.

CHAPTER 2

LITERATURE REVIEW

2.1 Introduction

This chapter presents relevant literature review to date in order to gain knowledge to support the present study objectives. This is important for researcher to find the way to overcome liquefaction in solid bulk cargoes as it influences the surrounding environment at nearly every scale. The mechanics of soil is always depending on its morphological and its reaction toward changes from its surrounding therefore to amend bauxite; we must first understand the bauxite physical stability and morphology. The review provided in this chapter were organized chronologically and offer much deeper insight. Compilation of the contemporary study published will give better perspective on the subject of liquefaction and bauxite stabilization. The review consist of topics to discuss the gravity of the problem occurs due to liquefaction in solid bulk cargoes, the type of cargoes that contributed to liquefaction, the soil mechanics of solid bulk cargoes especially bauxite are exemplify, the role of gypsum and vermicompost as proposed solution.

2.2 Liquefaction in Soil

Liquefaction is a phenomenon in which the strength and stiffness of a soil is reduced by earthquake shaking or other rapid loading. Liquefaction has been responsible for great amounts of damage in historical earthquake around the world as shown in Figure 2.1, the soil from its initial place has been shifted to the left due to earthquake as soil behave like liquid. Liquefaction occurs in saturated soils where the space between individual particles in the soil were filled with water. This water exerts a pressure on the soil particles that influences how tightly the particles pressed together. Prior to an earthquake, the water pressure is relatively low but earthquake shaking caused the water pressure to increase. This will continue until the soil particles have no contact within aggregates, thus decreasing the soil shear stress.

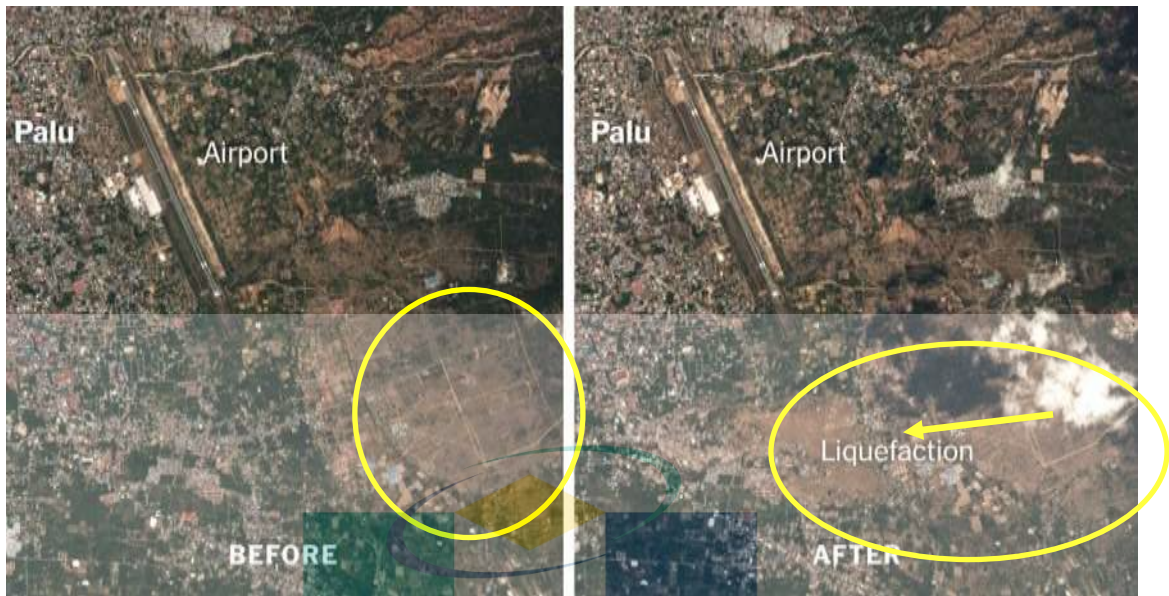


Figure 2.1 Liquefaction at Palu (soil slide to right), Indonesia on 28 September 2018.

Source: Fountain, (2010)

Shear stress of soil is dependent on its contact between aggregates. As soil been compacted due to movement, pore water pressure increase causing the aggregate to lose contact between themselves and eventually decrease the tendency of soil to maintain its shape. This is the main reason soil behave like liquid and cause structure above it to collapse. Figure 2.2 shown the close image of aggregate when liquefaction occurred.

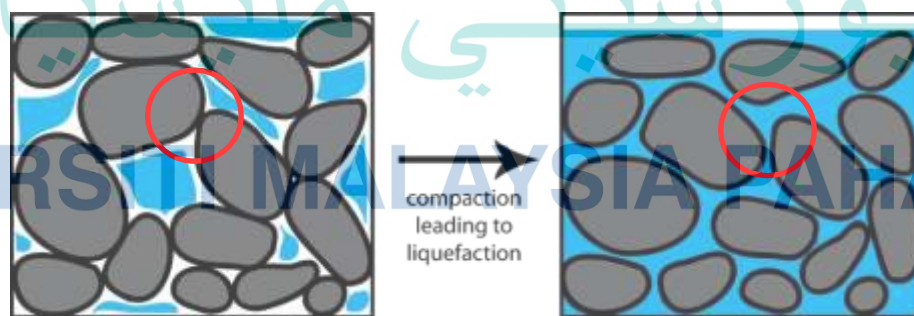


Figure 2.2 Compaction causes water to push aggregate leading to liquefaction

Source: Maurer et al., (2014)

Liquefaction can occur in cargoes carrying item across sea for shipping purpose and as recorded by Ju et al (2018) many incidents that occurs in recent years due to increase of exporting materials that liquefy inside the cargoes. For example, the MS (Motor Ship) Bulk Jupiter that was depart from Kuantan, Malaysia on 30 December 2014 sank off the coast of Vietnam on 2 January 2015 with 16 loss; two dead and one survivor. Substantially to note that if two conditions mention earlier occurs in soil aggregate; liquefaction can happened. Munro & Mohajerani (2017) explain the liquefaction of solid bulk cargoes on ships is a common problem as the combination of fine particles and changing pore pressure within a cargo will result in the mass acting like liquid and manipulate the center of gravity (G) of ships. Ships are stable if mass (M) and buoyancy (B) are equilibrium, but when ship are tilt right/left the restoring moment (M_r) cannot cancel out the overturning moment (M_o), ship will becomes unstable as shown in Figure 2.3.

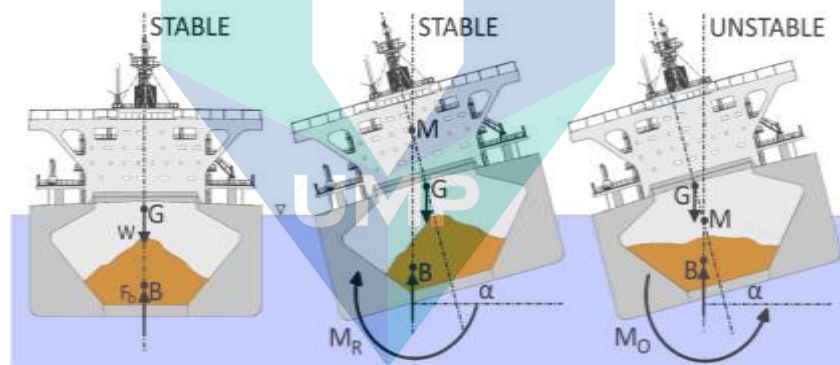


Figure 2.3 Liquefaction in solid bulk cargoes caused by rapid loading from wave
Source: Munro & Mohajerani, (2017)

2.2.1 Types of Solid Bulk Cargoes that Susceptible to Liquefy

Types of solid bulk cargoes also influence the liquefaction. Hou et al. (2014) highlighted that traffic volume of cargoes that are in its naturally state of ore are more likely to cause accidents as it accounts for about 46% of overall accidents. Even if the traffic volume of nickel mines and kaolin was small, their accidents resulted approximately to be 9% and 25% respectively (Hou et al., 2014) which is expressed in Figure 2.4. Meanwhile, bauxite (aluminum ore) was recently recorded in 2015 as liquefiable dry bulk cargo and its shows similar properties with iron ores poses the same threat (Munro & Mohajerani, 2016a).

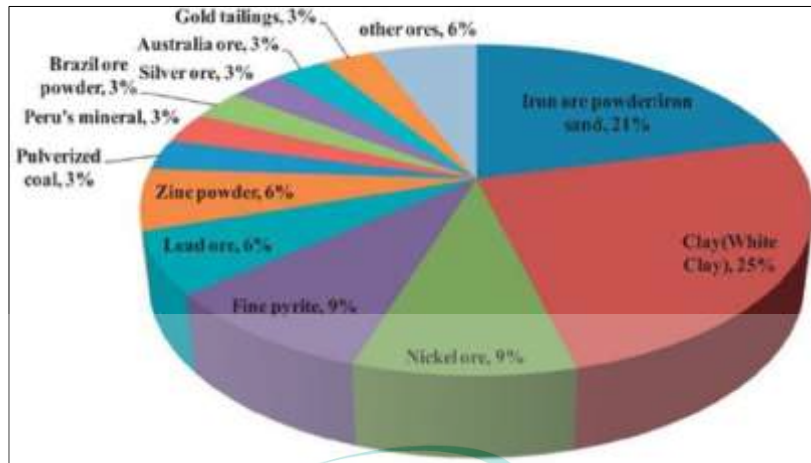


Figure 2.4 Potential solid bulk cargo to liquefy
Source: Hou et al. (2014)

Many researchers has investigated the relationship between types of solid bulk cargoes and liquefaction for example (Bao et al., 2019; Derakhshandi et al., 2008; Munro & Mohajerani, 2016) and outline that strong hygroscopic cargoes lead to poor drainage and increase poor water pressure. Hygroscopic in cargoes are shows in tendency of its bulk to retain water content in standard temperature and pressure (Cheng et al., 2014). Whereas, mechanism of soil disaggregation play an important aspect to be consider as it affect in many soil properties including how liquefaction can take place in any solid bulk cargoes (Xiao et al., 2018). Gore, (2015) state that bauxite ore has strong hygroscopicity and weak aggregate stability, this has lead into bauxite marked as liquefiable soil under IMSBC Code.

2.2.2 Evaluate Liquefaction Potential: Past Researcher and IMSBC Code

Methods have been developed since the first incident regarding liquefaction occurred to predict the liquefaction potential of soils. Many approaches have been developed to assess the soil potential liquefaction using different combination of soil physical characteristic.

To begin with, Tsuchida (1970) proposed particle size distribution boundary curves that used the results of sieve analyses on soils that did or did not liquefy during past earthquake. Methodically, grain size curve of any soil should be presented on the graph to deduce its liquefaction potential. Meanwhile, Seed & Idriss (1982) stated that cohesive soil which are prone to liquefaction must fulfil the following criteria: Percent Finer than 0.005 mm < 15% and $(w_c) > 0.9 \times \text{Liquid Limit}$. Andrews & Martin (2000)

developed an empirical approach based on LL and percentage of fraction passing 2 um presented in the following table. Last but not least, Seed et al., (2003) recommended an assessment chart shown in Figure 2.5 which is divided into three zones: Zone A where soils are considered potentially susceptible to liquefaction if $w_c > 80\%$ LL; Zone B where soils are considered potentially liquefiable with detailed laboratory testing recommended if $w_c > 85\%$ LL and Zone C where soils are considered generally not susceptible to classic cyclic liquefaction, although they should be checked for potential sensitivity..

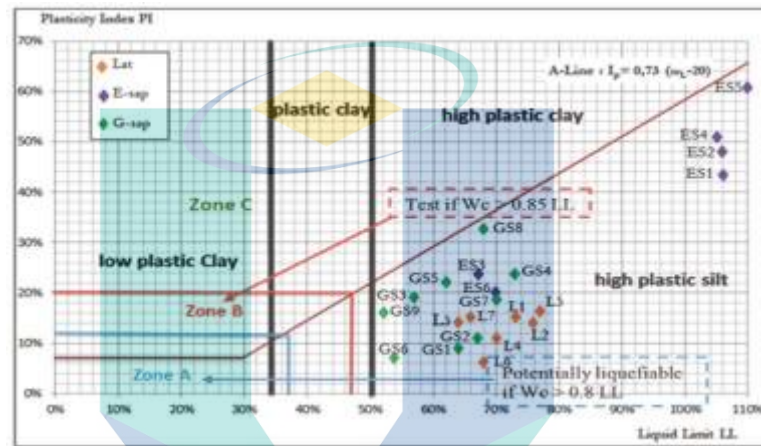


Figure 2.5 Representation of the tested lateritic soils on Seed et al. (2003) recommended chart

Source: Daoud et al., (2017)

In January 2011, the International Maritime Solid Bulk Cargoes (IMSBC) Code became part of a mandatory requirement that is to be followed by all owners of vessels carrying solid bulk cargo. The IMSBC code outlines dangers associated with certain types of solid bulk cargos and provides procedures to be followed when transporting these materials. The code includes test methods used to determine the TML of Group A cargoes, which are cargoes with the potential to liquefy due to the proportion of fine particles and moisture that they contain. The IMSBC Code provides three test methods that can be used to obtain TML; flow table test, penetration test and proctor/ Fagerberg test. However, only flow table test were widely used in maritime test due to its flexibility. The Flow Table test is as series of test that determine the maximum increase of diameter of cone displacement when moisture content is zero. The test needed at least two point to use extrapolation in finding the value of intersecting graph increase in diameter versus moisture content shown in Figure 2.6.

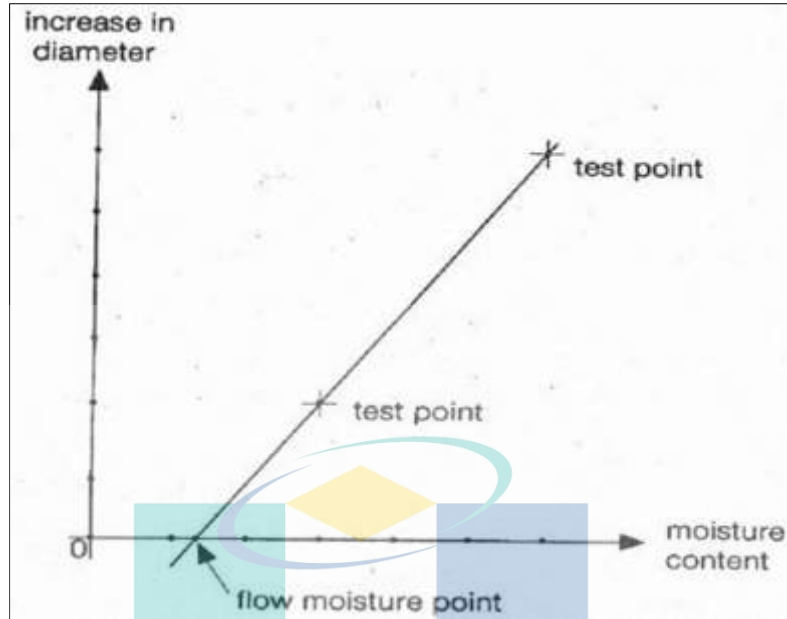


Figure 2.6 Showing increase in diameter plotted against moisture content.
 Source: Munro & Mohajerani (2016)

Moreover, FMP also can be obtained by using mathematical equation shown in Eq 2.1. This can be done after the flow state has been reached as the moisture content would be determined on two samples; one with moisture content just above the FMP and the other with moisture content just below the FMP. The difference between the two values should then be 0.5% or less, and the FMP has taken as the mean of these two values.

$$FMP = \frac{(m_1 - m_2)}{m_1} + \frac{(m_3 - m_4)}{m_3} \quad 2.1$$

FMP = flow moisture point

m1 = the exact mass of the sample just above flow state

m2 = the exact mass of the sample just above flow state, after

drying m3 = the exact mass of the sample just below flow state

m4 = the exact mass of the sample just below flow state, after drying

With reference to Koromila et al., (2013), cargoes must have lower water content than its TML as the risk to liquefy increases as the water content grows over its TML. At time of loading, cargoes of such would be in granular state and appear dry. However at sea, they are subject to agitation due to the engine vibration; ship is rolling as well as swell impact. The oscillatory ship movement cause the resettling of the cargo particles and compaction of the inter-granular spaces. This compaction raises the water pressure while forcing the particles apart and potentially would lead to lose direct contact. The condition for the cargo to liquefy would exist as it loses its shear strength IMSBC (2008). As a result, this later can lead to a “free surface effect” that lead to dynamic separation.

2.2.3 Impact of Liquefaction of Solid Bulk Cargoes to Environmental

Dr. Martin Jonas, a marine consultant considers some of the technical issues behind the causalities involving the carriage of unprocessed natural ores from Indonesia and Philippines as he published in Gard News of 197 (Jonas, 2015). The focus of the paper was cargoes carrying unprocessed ores that were mostly found to be iron ore fines that were exported from Indonesia, Philippines and New Caledonia. These are element that is not concentrates, raw and unprocessed. In Indonesia, the Philippines and New Caledonia, mining locations are typically very remote as loading takes place at natural anchorages close to the mines. The mines operate their own flow table for TML testing in their in-house laboratories that are poorly and are not abiding to the IMSBC Code.

Normally unprocessed natural ores will undergo beneficiation in order to be consider as processed. Beneficiation is a method of washing natural to reduce fines content and remove impurities. In Malaysia, they are specify washing pond to perform beneficiation (Abdullah et al., 2016). It is not environmental friendly as it causes water pollution and extensive washing of bauxite would produce effluent, which flows into nearby river. Stockpile of bauxite in large quantities was found polluting the rivers, as there was no proper drainage system (Abdullah et al., 2016). The amount of water pollution is shown in Figure 2.7.



Figure 2.7 Bauxite washing pond showing red water in Malaysia

Source: Abdullah et al. (2016)

Despite the pollution and harm, this method still being used by many natural ore mining sites as alternative to increase TML. Beneficiation can reduce fines content that decrease liquefaction risk. However, it is affecting the environment negatively which could be hazardous to people. Bauxite contains aluminum oxide, ferric oxide, silica, iron and high-level exposure of such elements to stomach might prevent the absorption of phosphate, a chemical compound required for healthy bones. This is dangerous as it may cause bone diseases in children (Services, 2010). These matters become dilemma for the developer whether to perform beneficiation or not, as this method enriched natural ores and reduce liquefaction risk at the same time create a massive water pollution.

On the other hand, climate in Southeast Asia can be described as tropical, meaning that the weather tends to be hot and humid most part of the year. The region receives plenty of rain throughout the year, especially during the wet monsoon season because of tropical rain belt and the seasonal shifting of wind. This make processed natural ore through beneficiation pointless, as the moisture is still high even after the process. Accordingly, the present study attempts to have better alternatives to enrich natural ore and reduce liquefaction risk without affecting the environment.

2.3 Review Studies on Bauxite

Generally, bauxite is found in abundance at many locations around the world, which includes the location of those major commercial deposits are found such as Australia, China, Brazil, Guyana, France, Ghana, Guinea, Hungary, India, Malaysia, Jamaica and Suriname (Brown et al., 2015).

Each location will have their own bauxitization due to chemical weathering. Chemical weathering is a major mechanism that partitions element between crustal rocks and natural water; it is completely dependent on the (climate-driven) water cycle (Yuste et al., 2017).

That is why it has been claim by Vassiliadou (2015); bauxite does not have specific composition. Even though, the definition by Valetton (1972) on bauxite can be our reference, “The term bauxite ore is applied to bauxite which are economically mineable at present or in the foreseeable future; containing not less than 40-50% Aluminum Oxide Al_2O_3 and not more than 20% Iron (III) Oxide Fe_2O_3 , and 3-5% combined silica”. The morphological and geotechnical of bauxite literature from ore to its residue will be review and analyze to gain more idea about its nature.

2.3.1 The Types of Bauxite in Malaysia

Malaysia bauxite is mostly associated with weathered intermediate to basic rocks such as gabbro, diorite, andesite, and basalt. These rocks are classified as igneous rocks where it can be further be grouped into two, intrusive and extrusive igneous rock. Igneous rocks have many uses in construction as aggregates. The bauxite found in Malaysia is a residual product and it occurs as a superficial crust of nodules in clay as shown in Table 2.1.

According to Harben (1998), the uses of bauxite in industry were dependent on its amount of Aluminum Oxide, Al_2O_3 and Silicon Oxide, SiO_2 . Based on Table 2.2, only Pengerang – Teluk Ramunia and Batu Pahat can be considered as producing bauxite with metallic quality. Bauxite deposits were formed mainly by weathering of aluminous rock.

Table 2.1 Chemical compositions of Bauxite in Peninsular Malaysia

Bauxite Properties (Malay Peninsular)					
Location/Area	Constituent Percentages				
	Al ₂ O ₃	SiO ₂	Fe ₂ O ₃	TiO ₂	LOI
Bauxite in Johore					
Pengerang Teluk Ramunia	45.30 - 59.10	2.80 - 8.00	5.43 - 24.0	0.30 - 3.0	27.0 - 30.65
Batu Pahat	52.60 - 56.60	1.60 -8.99	2.60 - 5.80	0.01 - 0.8	27.30 -30.4
Bauxite in Pahang and Terengganu					
Bukit Tanah Merah	33.0 - 44.0	1.0 - 7.0	21.0 - 30.0	2.56 - 4.88	21.4 - 27.0
Kuantan	21.0 - 39.0	1.9 - 21.8	25.0 - 40.0	3.60- 5.20	20.6 - 27.1
Ladang Bukit Goh	26.0 - 48.0	1.44 - 25.2	22.0 - 26.0	2.40 - 4.96	20.1 - 28.3
Lembah Jabor	30.0 - 48.0	2.28 - 24.1	23.0 - 27.0	2.00 - 4.56	20.0 - 28.4

Source: Eki et al., (2014)

Table 2.2 Industries Specification to Process Bauxite

Known Malaysian (Malay Peninsula) Bauxite Compared To Specification (Harben,1998)						
Specification of Bauxite For Industries (Harben,1998)			Bauxite (Malay Peninsula)			
Oxide %	Metal	Chemical	Pengerang – Teluk Ramunia	Ladang Jeram Kuantan	Ladang Bukit Goh	Batu Pahat
Al ₂ O ₃	50-55	Min.55	45.3-59.1	21.0-39.0	26.0-48.0	52.6-56.6
SiO ₂	0-15	5-18	2.80-8.00	1.9-21.8	1.44-25.2	1.60-8.99
Fe ₂ O ₃	5-30	Max.2	5.43-24.00	25.0-40.0	22.0-26.0	2.60-5.80
TiO ₂	0-6	0-6	0.30-3.00	3.60-5.20	2.40-4.96	0.01-0.80

Source: Eki et al., (2014)

Known bauxite deposits in Malaysia occurs in five states, which are Johore, Pahang, Terengganu, Sarawak and Sabah. However, among all the bauxite deposits in Malaysia, only Pengerang, Teluk Ramunia, Batu Pahat, Bukit Gebong, Munggu Belian, Tanjung Serabang and Telupid areas are considered as metallic quality.

2.3.2 Liquefaction Potential in Bulk Cargoes

The transportation of bulk cargoes has an important share over the commodities transported on board vessel all around the world (Maurer et al., 2014). Issues has arisen since Jonas (2010) reported the relation of severe consequences of the bulk cargoes liquefaction with the type of cargoes. Every bulk cargo has their own properties that are influencing pore water pressure. According to International Maritime Solid Bulk Cargoes (IMSBC), bulk cargoes that were transported on board vessels can be divided in two categories: bulk cargoes with small particles and high-density bulk cargoes.

Liquefaction in solid bulk cargoes cause many problems such as properties damage, environmental problem, and loss of people life. Approximately 9.5 billion ton of goods is transported over the world oceans annually with dry bulk representing the largest cargo group (Höfer et al., 2016). MS Bulk Jupiter is an important case to be highlighted as it was departed from Kuantan, Malaysia on 30 December 2014 and sank off near the coast of Vung Tau, Vietnam on 2 January 2015 with 16 loss: two dead and one survived (Walton, 2015). Recently, Stellar Daisy from South Korea capsized due to cargo liquefaction in March 2017 is another highlight to this matter. The above tragic accidents are not the only of its kind and unfortunately there are no comprehensive or practical solution yet is taken by authority. The incidents occurred over the decades shown in the Table 2.3 below illustrate the casualties that happened involving severe ship stability failure led capsizing, due to cargo liquefaction.

Table 2.3 Ship stability failures related to liquefaction in cargo

Year	Vessel	Cargo loaded	Incident	Location
2009	Hodasco 15	6,000 tons iron ore	Capsizing	Malaysia
2009	Black Rose	23,000 tons iron ore	Capsizing	Paradip Port (India)
2009	Asian Forest	13,000 tons iron ore	Capsizing	Mangalore (India)
2010	Jian Fu Star	43,000 tons nickel ore	Capsizing	West Of Taiwan
2010	Nasco	55,150 tons nickel ore	Capsizing	East Of Taiwan
2010	Hong Wei	40,000 tons nickel ore	Capsizing	South Of Taiwan
2011	Bright Ruby	25,000 tons iron ore	Capsizing	South Of Taiwan
2011	Vinalines	54,000 tons nickel ore	Capsizing	South China Sea

Source: Hou et al. (2014)

Over the past decades, there has been dramatic increase in capsizing cargoes in the area of Southeast Asia region regarding liquefaction in solid bulk cargoes as shown in Figure 2.8. This raise the question by the Lloyd’s Maritime Academy on the reason for such incidents to keep occurring in Southeast Asia region



Figure 2.8 Illustrate summarize accidents that involving liquefaction in bulk cargoes

Source: Hou et al. (2014)

On the other hand, according to Hou et al. (2014) there were 20 sunken ship caused by liquefiable solid bulk cargoes in past ten years. It can be seen from Figure 2.9, the number of accidents showed significantly upward trend due to lack of understanding on mechanism of liquefaction in solid bulk cargoes.



Figure 2.9 Trending of liquefaction in solid bulk cargoes

Source: Hou et al. (2014)

This has become more serious as it because more life to be loss as recorded by to Hou et al. (2014) that 25 people dead, 74 people missed and 231 people rescued in 23 wreck accidents. That caused direct material losses of over RM 88.05 million. This statistical data does not include recent accidents such as MV Bulk Jupiter and MS Stellar Daisy that will add another 16 deaths, which conclude 41 deaths in the past 15 years. The process of liquefaction can be often identified when the cargo leaned to one side without any symptom. In a few minutes later, the ships suddenly capsized, in fact of many regulations provided the issues are still yet incur in our society.

After all, these increasing trends brought the world to discuss about the regulation in more details; the International Maritime Organization (IMO) is the specialized agency of the United Nation dealing with safety of shipping, navigating and the reduction and prevention of marine pollution from ships. IMO launch International Convention for the Safety of Life at Sea (SOLAS), which then become direct guidelines and regulation in IMSBC Code toward the safety of dry goods transported in bulk (Höfer et al., 2016). Technical objectives of IMSBC Code in regarding liquefaction are control of the moisture content. Transportable Moisture Limit (TML) is a value of bulk cargoes need to be obtained before it can be shipped. The value is obtained from Flow table test and it must exceed initial water content. TML represent the limit in which the pore water pressure already cancels out the surface contact between aggregates, which can lead to liquefaction. That is the basic precaution to ensure the safety of exportation in cargoes (Hou et al., 2014).

2.4 Studies on Aggregate Stability

Xiao et al. (2018) points out that aggregate disintegration mechanism during mechanical loading could give impact performance of aggregate will afterwards. This great view of how unstable aggregate will affect soil liquefaction are maybe the answer of why liquefaction in solid bulk cargoes are still happening even after IMSBC Code were implemented. The contribution of different mechanism of aggregate breakdown to cargo liquefaction are still obscure. It is possible to hypothesize that weak aggregate stability can influence aggregate to build up excessive pore water pressure that can cause liquefaction.

Liquefaction is the phenomena when there is loss of strength in saturated and cohesion- less soils because of increased pore water pressure and hence reduced effective stressed due to dynamic loading. It is a phenomenon in which the strength and stiffness of a soil is reduced by earthquake shaking or other rapid loading such as sway motion of a ship. The theory can be applied to cargo liquefaction, in which it will not occur if the cargo contains a sufficiently low inherent moisture content with sufficiently high interstitial air that. Thus, even in its most compacted state, there are still sufficient interstitial spaces to accommodate all of the moisture so that the increase in water pressure is inhibited (Jonas, 2010). This sub topic will divide and discuss the recent research on the relationship of aggregate stability with liquefaction.

2.4.1 Elements in Aggregate Stability

Structure is a fundamental property of productive soils due to its influence on many areas of studies as geotechnical, plantation and civil engineering. Many researchers believe aggregated soil structure can advance plant growth and increase resistance to soil erosion (Y. Wang, Zhang, & Zhang, 2015). Soil structure rely on the presence of aggregates and their stability (An et al., 2013).

Soil aggregate stability impacts several soil physical processes including soil erosion, water infiltration, soil aeration and biological activity (Karami et al., 2012). In order to preserve the productivity of soil and minimise erosion and degradation, it is important to install high soil aggregate stability. (Stanchi et al., 2015; H. Xiao et al., 2018).

Aggregate stability is a significant factor leading to soil erosion. Aggregate stability of soil can be accessed using two method (Le Bissonnais, 1996; Yoder, 1936). Among these two, the modified Le Bissonnais' method was more appropriate to determine the susceptibility to disaggregation mechanism.

This is due to the fact that Yoder (1936) separates aggregates by slaking and mechanical breakdown while Le Bissonnais (1996) combines three disruptive test that are characterized by different wetting conditions and energies which differentiate three disaggregation mechanism: slaking, mechanical breakdown and swelling index. Le Bissonnais' method is shown in Table 2.4.

Table 2.4 Summary of the applied methodologies for evaluating aggregate stability

Methodology	Initial aggregate sizes before wet sieving	Treatments before wet sieving	Used sub sieve sizes to obtain MWD values
Modified Yoder's method	<2 mm	Immersion of soil aggregates in distilled water with shaking	1 ,0.2, 0.05 mm
Fast Wetting (FW)	1-2 mm	Direct immersion of soil aggregates into water	1 ,0.2, 0.05 mm
Slow Wetting (SW)	1-2 mm	Immersion of soil aggregation into ethanol	1, 0.2, 0.05 mm
Wetting Stirring (WS)	1-2 mm	Pre-wetting of soil aggregates at matric potential	1, 0.2, 0.05 mm

According to the characteristic of the main breakdown mechanism in the Le Bissonnais' method, different tests involved different types of forces. The FW test intricate internal pressure by air entrapment during wetting and was used to stimulate the disaggregation of soil aggregates under rainstorm events or cyclic loading. The SW test involved internal pressure by clay differential swelling and was used to determine disaggregation of soil aggregates under conditions of reduced precipitation as ethanol prevented slaking and swelling due to its relatively low surface tension. SW test use much smaller dielectric constant with respect to that of water. The WS test used external pressure by raindrop impact and was used to determine the effect of mechanical breakdown on soil aggregate (Amezket, 1999). Table 2.5 shown the summary of the test.

Table 2.5 Main breakdown mechanism in the modified Le Bissonnais' method

Test Perspective	FW Test	SW Test	WS Test
Mechanism	Slaking	Breakdown by differential swelling	Breakdown by raindrop impact
Types of forces involved	Internal pressure by air entrapment during wetting	Internal pressure by clay differential swelling	External pressure by raindrop impact

Table 2.5 Continued

Test Perspective	FW Test	SW Test	WS Test
Soil properties controlling the mechanism	Porosity, wettability, internal cohesion	Swelling potential, wetting conditions, cohesion	Wet cohesion (clay, organic matter, oxides)
Resulting fragments	Micro-aggregate	Macro and Micro aggregates	Elementary particles
Intensity of the disaggregation	Large	Limited	Cumulative

Slaking of aggregate can contribute to excessive pore water pressure as aggregate disintegrate as it occupies the interstitial void and entrap the water more effectively. Thus creating severe contributions to liquefaction (Majou, 2008). Subsequently breakdown by differential swelling which surge up the pore water pressure as clay of soil begin to increase it is volumetric compressibility (Derakhshandi et al., 2008). Breakdown by raindrop can be consider as direct forces which then can be in this research context as sway motion of ship when it hit waves. There are widely research on how biologically induced soil modification can be used to decrease permeability, decrease compressibility, increase strength and alter volumetric behavior during shearing (Dejong et al., 2006). Hence, it could be conceivably hypothesized that better aggregate stability can sustain higher liquefaction risk.

Table 2.6 Properties of soil affecting liquefaction

Properties	Explanation	References
Pore water pressure	Pore water pressure generation during cyclic motion of ships initiates liquefaction and affects the shear strength of soil directly. Recent studies show that pore pressure dissipation are influenced by threshold shear strain and volumetric compressibility of the soil. This raise an interest in researcher to study how plastic fines affect the pore pressure generation characteristic of saturated sands.	(Ni & Fan, 2002) (Derakhshandi, et al., 2008) (Ju et al., 2018)

Table 2.6 Continued

Properties	Explanation	References
Slaking	Slaking is caused by the compression of air entrapped inside aggregates during wetting. Slaking usually occurred mainly during the initial few minutes under fast wetting condition by using an image recognition algorithm method. It was then confirmed by researcher the importance of slaking on soil disaggregation.	(Han et al., 2016) (Xiao et al., 2018)
Differential Swelling of clay	Breakdown by differential swelling via internal pressure when shrinkage of clays occurs during wetting and drying and results micro cracking of aggregates. The degree of differential swelling increases the amount of slaking proportionally.	(Guo et al., 2015) (Almajmaie et al., 2017)
Mechanical dispersion	This perhaps is the most direct forces make it impact to the soils. As stated by researcher, this mechanical breakdown due to rain impact and splashing water causing external pressure, which affects elementary particles cumulatively. Hence erodibility usually used to indicate the resistance of soil aggregates stability against irrigation and cyclic motion	(Geeves, 1997) (Guo et al., 2015)
Physicochemical dispersion	The scope of this research is to study and implement the biologically induced precipitation of calcite found in gypsum to alter soil characteristic. Naturally found in vermicompost such as urease-positive bacteria can be hydrolyze in the presence of calcite within the pores. This potentially is one of key factor to reduce pore water pressure the substantially enhance soil shear strength. This method has great influence on decrease permeability, decrease compressibility, increase strength and alter volumetric behavior during shearing.	(Dejong et al., 2006) (Burbank et al., 2011)

However, there has been scarce discussion about improving aggregate stability to reduce liquefaction risk. Therefore, this thesis comes with more details on how weak aggregate stability can affect directly shear strength with dispersion and excess pore water

pressure as shown in Table 2.6. Therefore, the effort to increase aggregate stability of minerals soils such as nickel ore and aluminum ore can be certain.

2.4.2 Relationship between Liquefaction and Aggregate Stability

As clearly, liquefaction occurs due to an increase in excess pore water pressure and a corresponding decrease in effective stress in a soil deposit. To increase the spectrum, pore pressure generation is caused by the rearrangement of soil particles under undrained condition, and this rearrangement of particles is best characterized by shear strain. From many incidents happened in the last decades regarding liquefaction, many researchers focus their study on how fines contents of soil affecting threshold shear strain. Since then, the area of study was then enlarge to relationship of plastic and non-plastic fines affecting cyclic resistance (Hazirbaba, 2019a)

Early researcher on this field accommodate cyclic shear strain rather than cyclic shear stress as it controls the densification and volume change of sands, presumably the pore pressure response (Silver & Seed, 1971). Wang & Dreger (2004) extended this work to measure pore pressure response of saturated sands under strain-controlled, undrained loading. The results demonstrated that pore pressure generation generally initiates at shear strains greater than 0.01% and excess pore pressure ratios grows at shear strain larger than this threshold strain, and shear strains as small as 0.3-1% can generate pore pressure ratio close to one. Figure 2.10 plotted as excess pre pressure ratio versus the logarithm of shear strain for different number strain cycles.

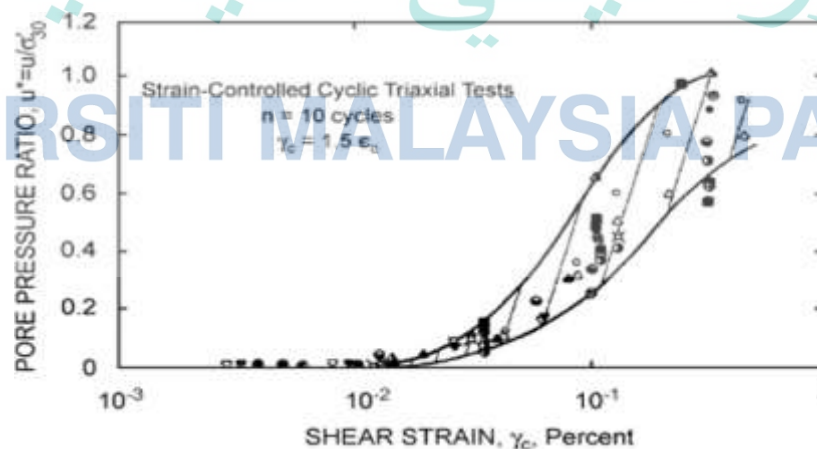


Figure 2.10 Pore pressure ratio versus shear strain from strain-controlled triaxial test
Source: Ju et al., (2018)

Various experimental studies focused on systematically evaluating the effect of plastic fines on liquefaction resistance; however most of these studies employed cyclic stress-controlled testing. Koester (1994) investigate stress-controlled testing on reconstituted samples of sand/silt/clay mixture. Specimens were tested at a constant overall void ratio representing 50% relative density for the clean san and plasticity index (PI) of the fines ranged from 4-40. There are two suggestion were then made. Firstly, cyclic strength generally decreases with increasing fines content up to 20% fines, after which the cyclic strength increases. Secondly, cyclic strength increases with increasing PI.

However, Prakash & Puri, (1999) synthesized data from various studies on the liquefaction potential of undisturbed and reconstituted silts and silty clays. They concluded that PI is an important parameter affecting the liquefaction resistance of soils, with the cyclic strength decreasing with increasing PI at low level of plasticity ($PI = 0-5$), but increasing with increasing PI at larger levels of plasticity ($PI > \text{about } 10$). It was supported by recent researcher like Derakhshandi et al. (2008) and Hazirbaba (2019a). A strong relationship between cyclic resistance to fines content and PI has been reported in the above literature review. Overall evaluation has shown different fines content (plastic or non-plastic) indicated decreasing pore water pressure, in general, with increasing fines content up to 20% fines and start changing trend as it is approaching 30%. This support regulation made by IMSBC Code that limit the cumulative value of particle distribution at 2.5 mm must be below 30% in order to be classified as non-liquefiable.

Reducing fines content on soil lower the liquefaction risks. Furthermore, altering the PI value through stabilization could add more to the positive result. The aims of this research are to align with the recent studies and it is important to note that excessive pore water pressure in soil could significantly amended by the soil stabilization using gypsum and vermicompost.

2.5 Review Studies on Soil Stabilization for Liquefaction Mitigation

Lately, new liquefaction mitigation methods are constantly emerging due to the rapid development of science, technology and multi-disciplinary engineering approaches. New concepts like passive site remediation, microbial geotechnical and induced partial saturation have been proposed. Meanwhile, new methods of liquefaction mitigation have been developed based on these concepts, such as nanomaterial suspension grouting, bio

cementation, air injection, biogas and liquefaction mitigation using other geomaterials (Maithilli KL, 2017). In particular, the availability of new materials and techniques has promoted the development of liquefaction mitigation technologies.

In order to sufficiently understand the progress of liquefaction resistance in present literature, investigation into recently developed liquefaction mitigation methods were reviewed in this paper with a focus on soil improvement with new concepts and materials. First, the mitigating mechanism, characteristic, effectiveness, possible executive problems in engineering practice were analyzed and discussed in detail. Then, the applicability and uniformity in soils with different pore sizes and any possible disturbance to nearby structures were presented.

Further, the duration time and potential cost of the mitigation measures for site construction were simply discussed based on laboratory tests' results. It was recommended that long term in-site testing should be performed to investigate mitigation effectiveness and duration time.

This review does not attempt to discuss all available soil improvement techniques and points; instead, it will raise some important questions and encourage further research and discussion. Many of the recent developed techniques the paper will presents are still in the stage of laboratory investigation and not used in the engineering practice for mitigation of seismic- hazard, thus, not all the points, e.g. duration time, exact cost assessment for on-site practice, can be sufficiently addressed. However, based on the presented research trend of liquefaction mitigation in this study, researchers can fully understand the relationship between the development of science, technology, new materials and multidisciplinary engineering approaches, and encourage further explore of new methods and techniques, which could be effective, easy for on-site construction, with low cost, environment-friendly and highly durable.

2.5.1 Materials to Stabilize Soil Sample against Liquefaction

With the development of new technology and multidisciplinary engineering approaches, the use of nanomaterials has shown superior performance in geotechnical engineering. This is due to the nano-scale particle size being able to penetrate finer soils without the use of high- pressure infusion that reduce the disturbance effect on surrounding environments as compared to traditional materials (Huang et al. 2016). For

liquefaction mitigation, the nanomaterials investigated mostly are colloidal silica (CS), bentonite and laponite. These nanomaterials are non-toxic to soil and groundwater. Hence, this section mainly describes the application of these three kinds of nanomaterials in the application of liquefaction mitigation, including mitigation effects, mechanism and potential problems.

The use of these materials in soil mixtures increases strength, swelling index and compressibility, while decreasing permeability, liquefaction risk, settlement and volumetric strains. Soil strength improvement by the inclusions of nanomaterials does not cause a large disturbance in the surrounding ground or structures and is an environment-friendly method. Furthermore, considering the cost of cement and chemical solutions, colloidal silica, bentonite, and laponite can be estimated to be an economical solution. According to the performance ratio report Huang et al. (2016), nanomaterials have a better price/performance ratio than traditional chemical grouting materials despite their relatively high unit price. Only small volume of nanomaterials is required for effective strengthening for the same grouting conditions and soil porosity as other materials. In these cases, the nanomaterials would completely fill the pore without any grouting waste in the soil treatment. In addition, the price of nanomaterials is expected to drop lower with the availability of advanced production techniques and improved manufacturing. Thus, as a new technology; the application of nanomaterials in geotechnical engineering can benefit the economic and social outcomes.

Table 2.7 Types of material recently used for liquefaction mitigation

Material	Explanation	References
Colloidal Silica (CS)	Electrical inter-particle forces dictate the behavior and fabric formation of the particles, and chemical bonding continues after the initial resonating gel state was reached. Therefore, based on these advantages, CS particles gel in low concentrations can effectively alleviate liquefaction of sand by cementing individual grains together and fixing the pore fluid. Experiments showed that the strength of the treated sand increased with an increasing concentration of CS. The shear strength would continue to increase as the time of gel increases as well.	(Gallagher et al., 2009) (Conlee et al., 2012)

Table 2.7 Continued

Material	Explanation	References
Colloidal Silica (CS)	<p>Electrical inter-particle forces dictate the behavior and fabric formation of the particles, and chemical bonding continues after the initial resonating gel state was reached. Therefore, based on these advantages, CS particles gel in low concentrations can effectively alleviate liquefaction of sand by cementing individual grains together and fixing the pore fluid. Experiments showed that the strength of the treated sand increased with an increasing concentration of CS. The shear strength would continue to increase as the time of gel increases as well.</p>	<p>(Gallagher et al., 2009)</p> <p>(Conlee et al., 2012)</p>
Bentonite	<p>Bentonite can effectively enhance the sand liquefaction resistance. This is because bentonite has the rheological properties of pore fluid and the formation of a bentonite gel with soil-like properties in the pore space could restrain the motion of sand grains under the action of earthquakes. Because bentonite dispersion has a high initial yield stress and viscosity, and the time of gelation is very short, it will affect the permeability coefficient of sand. This results in a reduced performance for large areas and non-uniform transmission in liquefiable sand.</p>	<p>(Ochoa et al., 2014) (Xu et al., 2016)</p>
Laponite	<p>Laponite particles are typically 25 nm in diameter and 1 nm in thickness, and are almost one-tenth the size of bentonite. Laponite suspensions prepared with deionized water have a cellular microstructure formed by elongated cells of a size several orders of magnitude greater than the natural clay particles, which is consistent with the structure of an attractive gel. Formation of the laponite suspension in the pore space shows solid-like properties. The suspensions not only fill the pores as a pore fluid, but also show solid-like properties to bond the sand particles together.</p>	<p>(Howayek et al., 2014)</p> <p>(Ochoa et al., 2016)</p>

2.5.2 Gypsum as Stabilizer

Gypsum is calcium sulphate. The most common form of it is dehydrate which means that each molecule of calcium sulphate has two water molecules associated with it. It is expressed as $\text{Ca}(\text{SO}_4) \cdot 2(\text{H}_2\text{O})$. The structure of gypsum consists of parallel layers of $(\text{SO}_4)^{-2}$ groups strongly bonded to $(\text{Ca})^{+2}$. These layers are separated by sheets of (H_2O) molecules with weak bonds existing between the H_2O molecules in neighboring sheets (Kuttah & Sato., 2015). Kuttah & Sato (2015) pointed out that gypsum is either colorless or it may be white, grey, red, brown or having various shades of yellow resulting from impurities. Regarding the specific gravity, Horta (1989) reported that gypsum has specific gravity of 2.32.

Subhi (1987) pointed out that the mixing of gypsum with the sandy silty clay may involve cation exchange. It may also produce flocculation and agglomeration of the soil and decrease the optimum moisture content due to the decrease in the surface area and increase in edge to face contacts of the particles. Courtney & Kirwan (2014) demonstrated that gypsum was a source of calcium and could precipitate solution alkalinity and suppress the solubility of solid phase alkalinity. Zhu et al. (2016) for example, found that an increase in organic carbon and calcium could stimulate macro aggregate stability of bauxite residue under natural weathering processes. Kamei et al. (2012) reported that the dry unit weight increased and moisture content decrease with the increase of recycled basanite content ($\text{CaSO}_4 \cdot 1/2 \text{H}_2\text{O}$) in the very soft clay soil mixture. The increase in dry unit weight when the amount of basanite increases is attracted to the potential of basanite for absorbing the water from the test soil. Furthermore, the developed hardening between soil particles prevents or reduces the penetration of water inside the soil sample and then no more or little water can be further absorbed by the sample (Kamei et al., 2012).

Overall, gypsum has effects on soil compaction characteristic, soil permeability, soil strength, swelling and heaving. However, the information of gypsum content on bauxite to reduce liquefaction risk is not establish. Alani & Dudas (1988) stated that an understanding of the mechanism involved was needed for better management of soil structure. Calcium carbonate was added to soil samples to bring the calcium carbonate content to 0, 2, 4, 8, 16, and 32% on a dry weight basis.

Increasing calcium carbonate content from 0 to 4% decreased the specific absorption rate of water but increased the MWD of aggregates. Further increase in calcium carbonate content increased specific absorption rate and decreased MWD.

Despite of the variation in the research findings with respect to the effect of gypsum content on different soil properties, it is agreed that there is an optimal gypsum content in the soil, which could lead to the best performance of that soil. However the percentage would differ from one soil to another depending on many factors such as the type of the soil and its particle size distribution, the type of gypsum component and its fineness, the presence of other salts in the soil, the drying and soaking condition. These factors have played a large role in the agreement and the contradiction among the researcher findings in the field.

2.5.3 Vermicompost as Stabilizer

Vermicompost is produced by earthworm's digestion of organic waste (e.g., food waste, horticultural waste, poultry droppings, and food industry sludge) (Yadav & Garg, 2013). This material has received increase attention in recent years because of its interesting physical, chemical and biological characteristics. Vermicompost is a sustainable source of macro and micro nutrients, mineral nutrient elements in vermicompost also are easily absorbed by plants (Edwards et al., 1988). Furthermore, vermicompost has fine granular structure with a large surface area and benefit it to be able to absorb and retain nutrients thus help it to be used as stabilizer (Zhao et al., 1991). A large number of plant hormones are found in vermicompost (e.g., IAA, GA3, and kinetin) and their presence may be the result of jointing activity of earthworms and microorganisms (Balasubramani et al., 2016). Overall vermicompost has the basic characteristics associated with a material that could be employed to improved soil quality.

Effect of vermicompost on related chemical and physical conditions of bauxite is found to be scarce and hinder for academic purposes. However, past studies that investigate the effects of vermicompost to soil can be use as references. This subtopic will discuss and present past paper that can be use as support argument to choose the best factor of amended on raw bauxites that lead to significant effect on improving aggregate stability against liquefaction.

However, to date, little research has focused on quantification and interpretation of aggregate formation and aggregate stability of bauxite following the addition of amendments.

Vermicompost have been suggested as excellent amendments to remediate soils and to improve organic carbon content and fertility, whilst alleviating salinity and improving crop growth (Stanchi et al., 2015). Vermicompost is a bio-oxidative process that has been reported as an effective technique for the efficient management of organic solid wastes (Fornes et al., 2012). Vermicompost are stabilized organic materials produced by interactions between earthworms and microorganisms; high concentrations macronutrients and micronutrients, high porosity and microbial activity (Coman et al., 2012). It is important to decide on suitable particle size fraction and shape of particles size fraction and shape of particles for operational cost of sieving and for the effect of that compost fraction in soil (Han et al., 2016). Vermicompost has demonstrate to achieve finer and more homogenous final product compared to classical composting (Hanc & Dreslova, 2016).

Addition of vermicompost significantly reduced bulk density and increased total porosity of bauxite residue and at higher rates the change on was more obvious. Changes in bulk density and porosity in the amended residues were of importance as they improve physical conditions including increase drainage and aeration (Duval et al., 2008). Courtney (2008) reported that organic compost application to soil would also reduce bulk density. Aksakal et al. (2015) observed that addition of vermicompost cause lowest mean bulk density and the increase total porosity.

2.5.4 Gypsum and Vermicompost as Soil Stabilizer

There are several researcher such as suggest the used of combination between vermicompost and gypsum to improves soils aggregate stability. Important research has initiates by Zhu et al., (2017), study about effect on bauxite aggregates when amended with vermicompost and gypsum. The findings shows combination gypsum and vermicompost converted the bauxite from a sheet-like structure to granular macro aggregated structure, whilst converting micro aggregates from grain to a granular or prismatic structure (Zhu et al., 2017). Zhu et al., (2017) also suggest that application of gypsum and vermicompost to bauxite may directly influence aggregate size distribution

and its micro morphology, resulting in the improvement of both aggregate stability and structure.

Addition of gypsum significantly reduced pH and increased soil electrical conductivity (EC), whilst addition of vermicompost had a positive effect on bulk density, porosity and organic carbon content. The selected amendments improved aggregate stability and micro aggregate stability of the residue. Both gypsum and vermicompost may well improve the proportion of water-stable aggregates and mean weight diameter (MWD), nevertheless, the improvement effect from vermicompost addition was exceptional.

Vermicompost significantly increased the fraction of 250-50 μm micro aggregates, and gypsum stimulated the flocculation of $<20 \mu\text{m}$ particles. On the other hand, in perspective of morphology under SEM analysis, researcher such as Burbank et al., (2011), Guo et al., (2016) and Zhu et al., (2017) states that with the addition of gypsum and vermicompost, the quantity of macro aggregates of the sheet-like structure increased significantly.

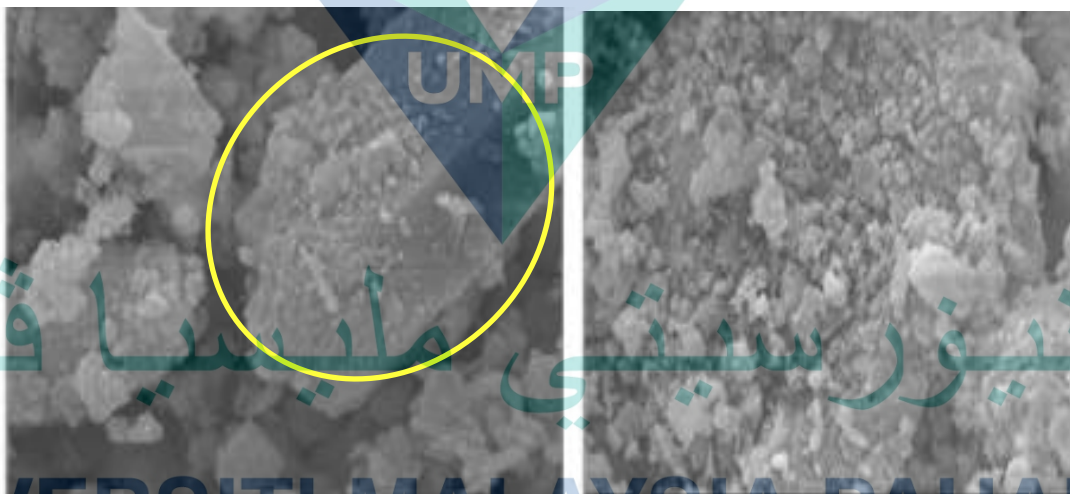


Figure 2.11 Soil structure change into platy and from machine at x1000 magnification

The size of the sheet-like structure became larger and the major fraction were the 2-5 μm particles. The combination of vermicompost and gypsum changed the bauxite to a denser structure and form platy arrangement as a formation of calcite in amendment of bauxite as shown in Figure 2.11.

CHAPTER 3

METHODOLOGY

3.1 Introduction

This chapter presents methods that have been conducted in this research. In order to achieve the objectives of the study, the entire work is divided into three major phases. The first phase was screening the four variables (incubation days, water intake, gypsum percentage and vermicompost percentage) to amend the raw bauxite using factorial design table. The physical changes of the amended bauxite were evaluated and the highest contribution among the variables used as the main variable in the second phase. In the second phase, the central value of the main variable tested using the method called Central Composite Design (CCD), four times repetitively.

Central value data were optimized to obtain optimum effect on its amended physical properties. In the third phase, the output from the CCD was then tested on its physical changes in detail. For example, aggregate stability test, flow table test and morphological perspective were investigated to give more understanding on how this central value can amend bauxite to significant result. The result also being compared to raw bauxite. The details of each phase will explain in Section 3.4.

Laboratory works such as particle distribution, specific gravity, aggregate stability, flow table test and morphological studies were carried on November 2018 until July 2019 followed procedure as shown in Figure 3.1. The climate is temperate continental monsoon, with a mean annual daily temperature of 26-36°C. Average annual rainfall ranges from 600 to 1000 mm. The sample of bauxite from Gebeng was fresh on 23 November 2018 and tagged with code GB01#, GB02# and GB03#. Samples were sealed tight in container to maintain its moisture content and composition of aggregate. Incubation process follows specific manipulated variable state in Design Expert software.

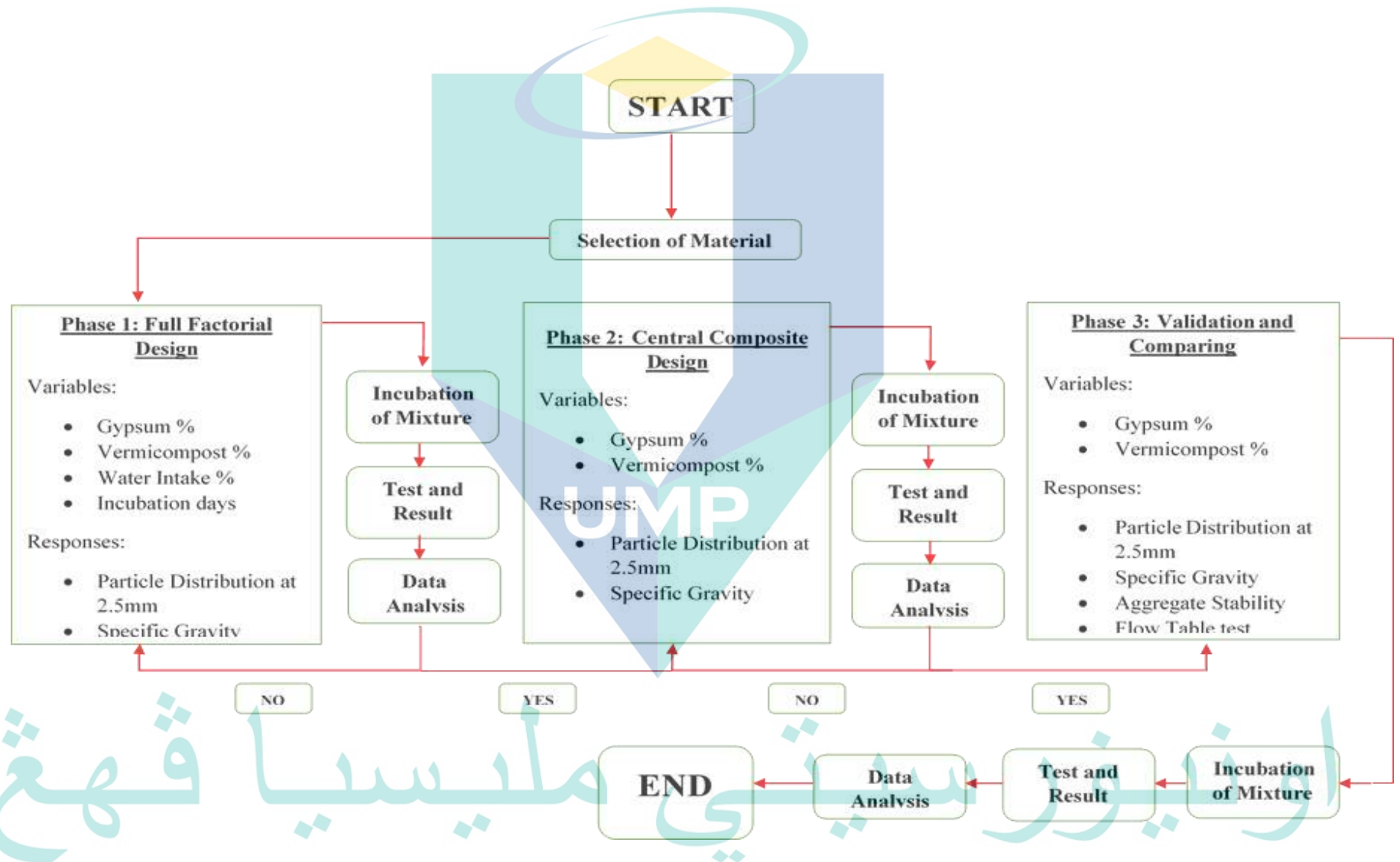


Figure 3.1 Flowchart of research

3.2 Selection of Materials

Approximately around 80 kg of bauxite samples from Gebeng, Pahang, Malaysia were used in this study. The samples were stored in sealed containers to maintain originality of the bauxite on site.. The gypsum were in powder form, supplied by BisChem Technology Sdn Bhd. The gypsum used in this experiment are calcium sulfate dehydrate commonly used in agricultural. Early material characterization shows it has size of <63um and has 2.33 of specific gravity. Gypsum (calcium sulfate) prevents soil erosion by increase aggregate stability thus improves the soil drainage. Whereas, the compost used in this experiment was produced by the pure worm composting. The vermicompost used in this experiment has average size of 0.02-0.25 mm and pH of 6.5 with 30.7% organic carbon(Aksakal, sari, & Angin, 2015). Burbank (2011) stated hydrolyze urea in the presence of divalent calcium ions cause the precipitation of calcite within the pores of liquefiable soils. This process also alters in soil properties that indicate that the potential for liquefaction was reduced as a result of bio mineralization (Burbank et al., 2011)

Table 3.1 Materials used

Materials	Picture
Bauxite	
Gypsum	
Vermicompost	

3.3 Preparation of Mixture

Bauxite were incubated according to variables study and its values that are design statistically using Design Expert v7, which will be explained in Section 3.4. Each step cannot be performed simultaneously as each phase can only be conducted after result from the previous phase has been analysed. Samples were tagged using numbering code for each phase. Incubation process will add percentage of gypsum, vermicompost and water intake to 2 kg of bauxite as shown in Figure 3.2.



Figure 3.2 Mixing Method and Apparatus

Several holes with diameter of 0.5 mm were drilled in the bottom of containers. After mixing, the samples were transferred to its container and arranged on a rack for incubation according to their incubation period as shown in Figure 3.3.



Figure 3.3 Incubation Preparation at Soil Mechanics Engineering Lab UMP

At the end of incubation period, each container or samples were divided for the physical test and morphological test. Finally, process was repeated for each phase and each sample was manipulated according to the variable to achieve the objective of research.

3.4 Description of Each Phase

There are three phase of this experiment, Phase 1: Full Factorial, Phase 2: Central Composite and Phase 3: Validation and Comparing were performed in orderly steps. It is important to ensure the quantitative analysis of the experiment can be carried out. The analysis of factorial design and central composite design aim to determine the most effective parameters and central value to amend bauxite. The analysis used was Design Expert software. However, validation phase was conducted to investigate performance of amended bauxite in comparison to raw bauxite. It was also to ensure the effect from amended bauxite are significant on reducing liquefaction risk.

3.4.1 Full Factorial Design

Factorial Design used to narrow the initial value of variable and to decide which variable give more contribution to responses. Therefore 2^4 were selected in this phase as shown in Figure 3.4. This will include 16 run of experiments with using four variables and two responses. Variables are: 1) Vermicompost percentage (4% and 10%), 2) Gypsum percentage (2% and 6%), 3), Incubation periods (15 day & 22 day), and 4) Water intake percentage (50% & 80%). The samples were amended with its designated variable according to factorial design. For example, sample with 2kg mass were amended with 2% and 4% of gypsum and vermicompost by weigh accordingly, then the sample were wetted to 50% of water percentage by weigh before its incubate for 15 days. Percentage of aggregate accumulated at 2.5mm and value of specific gravity will be the responding variable.

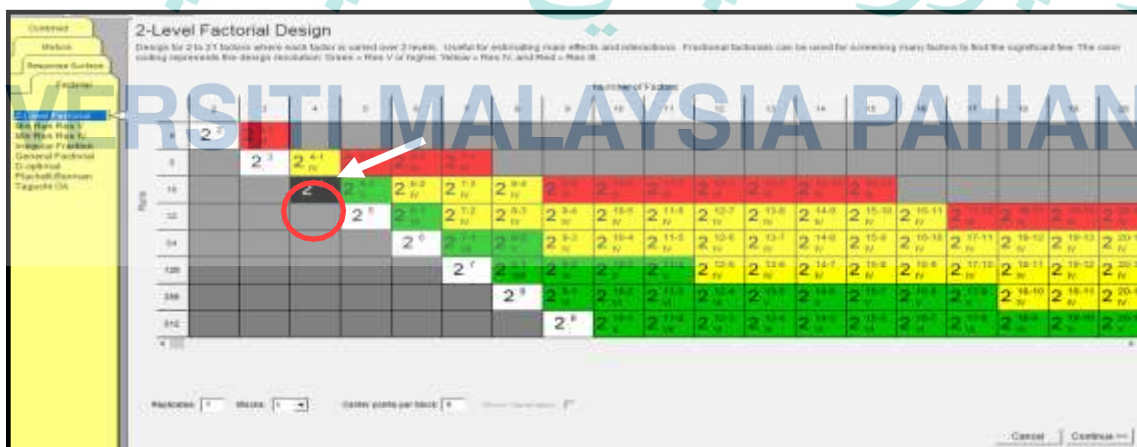


Figure 3.4 Selection of factorial design box in Design Expert software

Study Type	Factorial	Runs	16
Initial Design	2 Level Factorial	Blocks	No Blocks
Center Points	0		
Design Model	4FI		

Factor	Name	Units	Type	Low Actual	High Actual	Low Coded	High Coded	Mean	Std. Dev.
A	Gypsum	%	Numeric	2.00	6.00	-1.000	1.000	4.000	2.000
B	Vermicompost	%	Numeric	4.00	10.00	-1.000	1.000	7.000	3.000
C	Water Holding C	%	Numeric	50.00	80.00	-1.000	1.000	65.000	15.000
D	Incubation Days	days	Numeric	15.00	22.00	-1.000	1.000	18.500	3.500

Figure 3.5 Factors and their designated low and high actual value

2-Level Factorial Design

Optional Power Wizard: For each response, you may enter the minimum change the design should detect as statistically significant and also the estimated standard deviation of each response (generally obtained from historical data). The ratio will then be calculated in the Delta/Sigma field. Press Continue to see the calculated power for each response. A probability of 80% or higher is recommended. If power is low, consider adding runs by choosing a larger design or replication, or reconcile yourself to not detecting a signal this small.

Leave Sigma and Delta fields blank to skip power calculation.

Responses: (1 to 999)

Name	Units	Diff. to detect Delta ("Signal")	Est. Std. Dev. Sigma ("Noise")	Delta/Sigma (Signal/Noise Ratio)
Particle Size Distribution at 2.5 mm	%			
Specific Gravity				

Figure 3.6 Response to evaluate the physical changes of amended bauxite.

The design-generated 16 experimental run estimated the model coefficients effect and interaction of the factors (Table 3.3). Each experimental run was conducted in triplicate and the average was taken as response. The incubation process will execute following the value shown in Table 3.2. Each raw value data from experiment particle distribution at 2.5 mm and specific gravity were fill in the response tab to compute using Design Expert software as shown in Figure 3.6.

Select	Std	Run	Factor 1 A:Gypsum %	Factor 2 B:Vermicompo %	Factor 3 C:Water Holding %	Factor 4 D:Incubation D days	Response 1 Particle Density %	Response 2 Specific Gravit
1		13	2.00	4.00	50.00	15.00	32.1	1.75
	2	16	6.00	4.00	50.00	15.00	27.5	2.15
	3	12	2.00	10.00	50.00	15.00	26.5	2.77
	4	7	6.00	10.00	50.00	15.00	29.24	2.04
	5	3	2.00	4.00	80.00	15.00	26.72	2.08
	6	5	6.00	4.00	80.00	15.00	25.1	2.31
	7	4	2.00	10.00	80.00	15.00	29.41	2.85
	8	1	6.00	10.00	80.00	15.00	27.11	2.04
	9	6	2.00	4.00	50.00	22.00	27.27	2.39
	10	10	6.00	4.00	50.00	22.00	25.35	2.65
	11	14	2.00	10.00	50.00	22.00	25.67	2.3
	12	11	6.00	10.00	50.00	22.00	25	2.69
	13	2	2.00	4.00	80.00	22.00	25.38	2.42
	14	8	6.00	4.00	80.00	22.00	22.82	1.9
	15	15	2.00	10.00	80.00	22.00	22.81	2.83
	16	9	6.00	10.00	80.00	22.00	27.73	2.55

Figure 3.7 Factorial Design table with responses value

The factorial design were computed and solution are sort according to its degree of desirability. Desirability are solution that tell which value of variable will give the best responds. For example at how many gypsum (%) will gives the highest amount of particle distribution at 2.5mm. The highest desirability among samples as shown in Figure 3.8 are selected as central value for the next phase.

Number	Gypsum	Vermicompos	Water Holding	Incubation Day	Particle Densit	Specific Gravit	Desirability
1	6.00	4.00	80.00	15.00	25.0991	2.32107	0.829
2	6.00	4.00	79.74	15.00	25.1209	2.31966	0.826
3	6.00	4.00	79.60	15.00	25.432	2.31882	0.827
4	6.00	4.03	80.00	15.00	25.1099	2.31981	0.827
5	6.00	4.01	79.45	15.00	25.1473	2.31894	0.826
6	5.93	4.00	80.00	15.00	25.1291	2.31872	0.824
7	6.00	4.08	79.01	15.00	25.2057	2.31143	0.821
8	5.85	4.00	80.00	15.03	25.1533	2.30872	0.817
9	6.00	4.00	76.75	15.00	25.36	2.30147	0.817
10	6.00	4.00	75.68	15.00	25.4299	2.29616	0.814
11	6.00	4.02	80.00	15.60	24.9132	2.28555	0.807
12	6.00	4.00	72.61	15.00	25.6911	2.2763	0.801

Figure 3.8 Desirability of solutions in factorial design

As shown in Figure 3.9, the interaction of gypsum and vermicompost percentage (black box) are the only significant to study further. This is due to the intersection points between the value studies. Whereas, interaction between water holding capacity and vermicompost are not selected as it is beyond the scope of this study. For incubation days, its shows no interaction for both gypsum and vermicompost as it no intersection between variables.

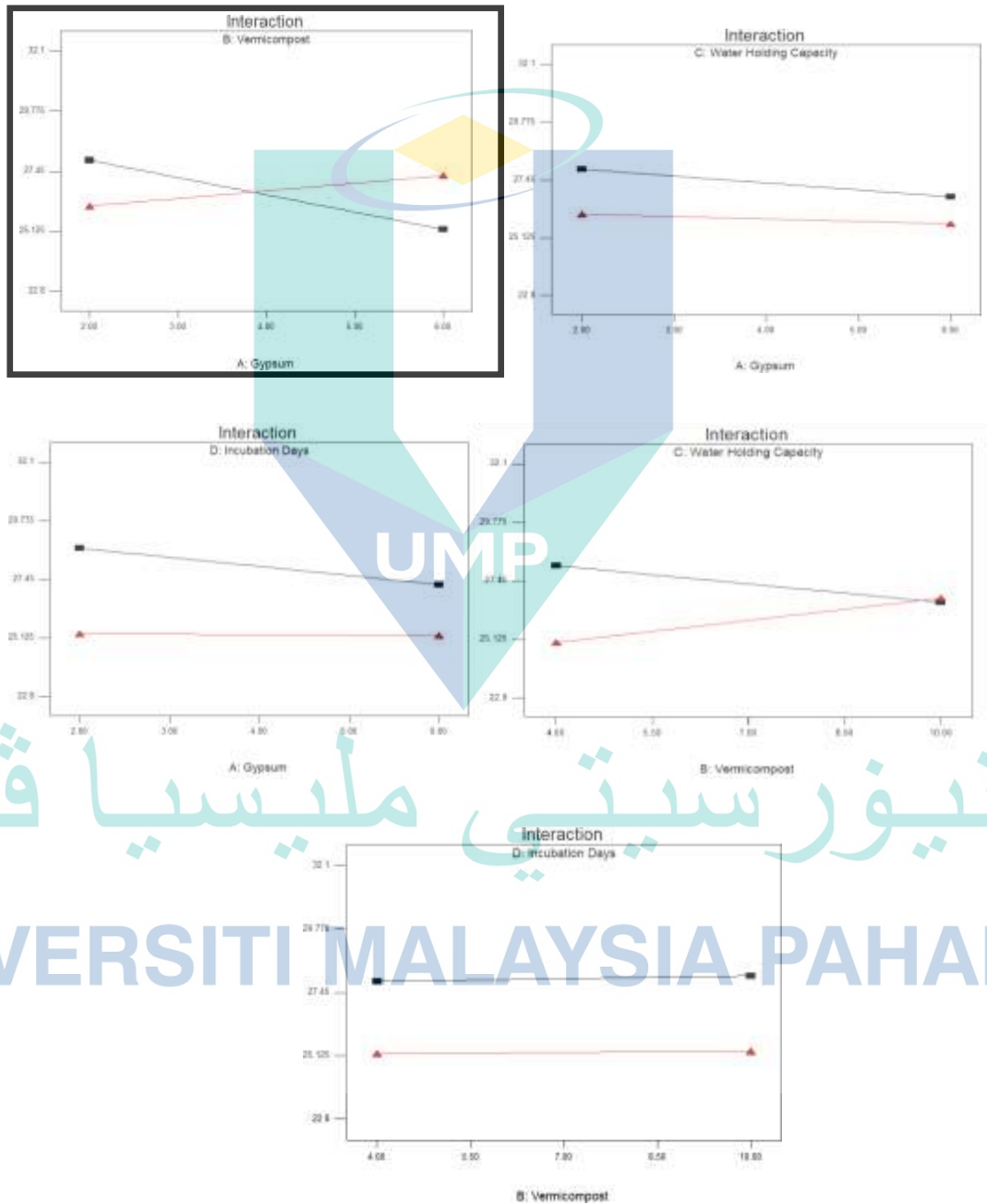


Figure 3.9 All the interaction of factors according to the response

3.4.2 Central Composite Design

Central Composite Design (CCD) are used to enhance and improve the accuracy of targeted value (Gypsum 6% and Vermicompost 4%) obtained from Phase 1: Factorial Design, which was at center value as shown in Figure 3.10. This phase is also known as optimization as prior of this phase we can see the targeted value for the variable that give

$$S = \sum_{i=1}^d SPI_i \quad 3.1$$

optimal contributions to responses. Optimization are repeated for at least four times to ensure the variance are little.

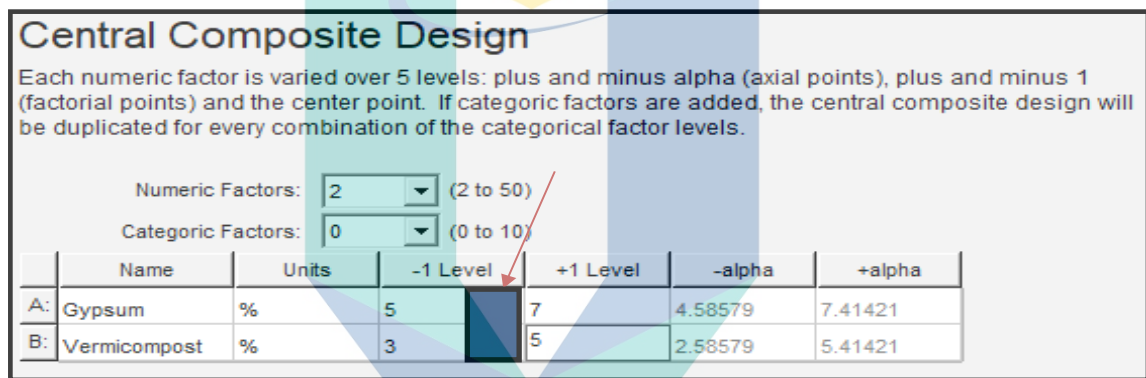


Figure 3.10 Targeted value from screening phase are at the center of CCD phase.

This phase include 13 runs of experiment with using two variables and two responses selected in the previous phase.

The water intake and incubation day are fix to 50% and 15 days respectively. The central composite design box includes specific amount of value of two factors that needs 13 samples are shown in Table 3.2.

Table 3.2 Central Composite Design Table

Sample	Gypsum %	Vermicompost %
1	5.00	3.00
2	7.00	3.00
3	5.00	5.00
4	7.00	5.00
5	4.00	4.00
6	8.00	4.00
7	6.00	2.00
8	6.00	6.00
9	6.00	4.00
10	6.00	4.00

Table 3.2 Continued

Sample	Gypsum %	Vermicompost %
11	6.00	4.00
12	6.00	4.00
13	6.00	4.00

As shown in Figure 3.11, the targeted value for optimum effect to amend bauxite is at 5.5% of gypsum and 3.0% of vermicompost with highest desirability of 0.730. However, this value (optimal value) need to be validated through more details experiments to see the changes in its physical and morphological properties.

Name	Goal	Lower	Upper	Lower	Upper	Importance
		Limit	Limit	Weight	Weight	
Gypsum	minimize	5	7	1	1	3
Vermicompost	minimize	3	5	1	1	3
Particle Density	minimize	23.15	26.87	1	1	3
Specific Gravity	maximize	2.01	2.52	1	1	3

Solutions						
Number	Gypsum	Vermicompos	Particle Densit	Specific Graviti	Desirability	
1	5.49	3.00	24.93	2.38	0.730	Selected
2	5.54	3.00	24.89	2.38	0.730	
3	5.40	3.00	25.00	2.37	0.729	
4	6.02	3.00	24.56	2.42	0.704	

4 Solutions found

Figure 3.11 Targeted value from target value for optimum effect to amend bauxite

3.4.3 Validation and Comparing Result

Validation phase was used to advance the response of optimal value from previous phase into physical and morphological properties test. The outcome of this phase is the performance of amended bauxite on aggregate stability, flow table test, SEM and EDX. The output was evaluated to detect significant changes in reduced liquefaction. Ten runs of experiment including control samples with using two variable and four responses, the water intake and incubation days are fix to 50% and 15 days respectively. The validation design needed specific amount of value of two factors and 10 samples as shown in Table 3.3.

Table 3.3 Validation and Modelling Table

Sample	Gypsum %	Vermicompost %
B-200 (Control)	-	-
B-20503	5.00	3.00
B-20505	5.00	5.00
B-20705	7.00	5.00
B-20404	4.00	4.00
B-20606	6.00	6.00
B-A20604	6.00	4.00
B-B20604	6.00	4.00
B-C20604	6.00	4.00
B-20204	2.00	4.00

Since validation phase was more straightforward, each sample will be tested and evaluated with unamend bauxite control sample.

3.5 Particle Size Distribution

To determine the relative properties of the different grain sizes that make up the material use and amended bauxite sample, a quantitative test to assess particle size distribution was carried out. Dry sieve analysis was conducted to determining the particle size distribution in a cohesion less soil down to the fine-sand size accordance to Geospec 3: Part 2; 8, Clause 3.5. Sieve analysis having the following aperture sizes: 6.3mm, 5 mm, 3.35 mm, 2 mm, 1.18 mm, 600 μm , 425 μm , 300 μm , 212 μm , 150 μm , 63 μm and pan for the material used as shown in Figure 3.12. The soil was first dried in an oven to remove it from any cohesion properties of water.

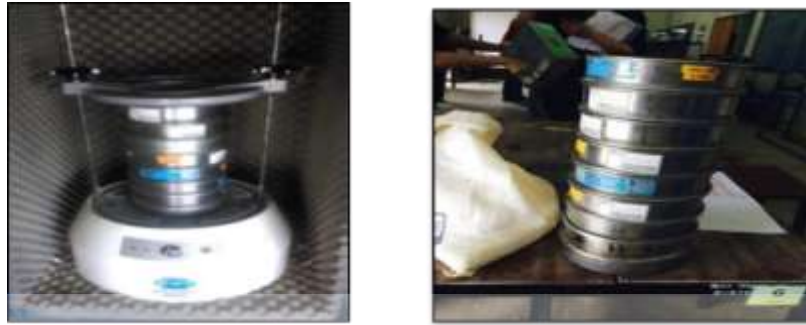


Figure 3.12 Sieve analysis apparatus

Then, the sample was placed in the sieve shaker and shaken where the particle fell through the sieves with mesh size reducing gradually, and the mass of the sample retained on each of the sieve were weighed. The finest range of sieve size is usually $63\mu\text{m}$ and the hydrometer method was used to determine the grain size distribution of the material passing $63\mu\text{m}$ and below.

3.6 Specific Gravity

Specific gravity test was conducted to determine the particle density of soil. Determination of amended bauxite, gypsum and vermicompost density was done using small pycnometer, also known as density bottle test. It accurate as it uses a working liquid with well-known density like water. Small pycnometer method is appropriate for particles of soil smaller than 2 mm in accordance to Geospec 3: Part 2; 7, Clause 3.4. Bigger material need to crush down to smaller size before testing.



Figure 3.13 Vacuum chamber and specific gravity of sample

During the experiment, the sample was weighted and recorded. Next, bauxite were placed inside pycnometer that filled by purified liquid. Lastly, to remove the air existed

in the sample, all the small pycnometer were placed in a vacuum chamber in the soil laboratory as shown in Figure 3.13.

3.7 Aggregate Stability Test

The aggregate stability of bauxite obtained by using the modified Le Bissonnais' method to test aggregate stability of amended samples (Xiao et al., 2018). This method combined three disruptive test: fast wetting (FW), slow wetting (SW) and wet stirring (WS) (Xiao et al., 2018).

FW test is sensitive to the slaking process thus 1-2 mm of samples (6 g) were quickly immersed in deionized water for 10 min. For the SW test which determined aggregate sensitivity for differential clay swelling, 1-2 mm bauxite samples (6 g) were placed on filter paper resting upon a sponge soaked in ethanol for 30 min. WS test is sensitive to mechanism breakdown processes. 1-2 mm (6 g) of samples aggregate were gently immersed in ethanol prior to being transferred to conical flask of deionized water and shaken. Aggregate size distribution of the samples was determined by sieving (1 mm, 0.25 mm, and 0.55 mm) in ethanol. The aggregates obtained from each sieve were collected and dried at 40°C for 48h (Saygin et al., 2012). Mean weight diameter (MWD), geometric mean diameter (GMD), and the erodibility factor (K) were selected as the parameters to evaluate aggregate stability and erosion resistance of the treated bauxites. The three parameters were calculated using the following equations (Le Bissonnais, 1996) shown in Equation 3.1, 3.2 and 3.3:

$$MWD = \sum_{i=1}^n Xi \times Wi \quad 3.1$$

$$GMD = \exp\left(\frac{\sum_{i=1}^n Wi \ln Xi}{\sum_{i=1}^n Wi}\right) \quad 3.2$$

$$K = 7.954 \times \{0.0017 + 0.0494 \times \exp[-0.5 \times (\lg [GMD + 1.675]) / 0.6986]^2\} \quad 3.3$$

Le Bissonnais' method: Where X I was the mean diameter over the adjacent sieves (mm), W I was the percentage of residue aggregates in the size range and n was the number of sample sieves.

3.8 Flow Table Test

The flow table test is a test for cement mortar, performed to calculate the amount of water required to gauge the strength of masonry cement. The test is also useful for drying shrinkage test of cement. Based on the BS EN 12350-5, the slump used is more than 175 mm. The 700 mm square flow table was hinged to a rigid base with a stop that gives the far end an uplift of 40 mm. A cone similarly used in slump testing is used but truncated is filled with two layers of the sample. Each layer is tamped with a multiply of 10 with a specially designed wooden bar and the concrete of the upper layer is finished off with the top of the cone. Any excessive sample is removed and cleaned off from the outside of the cone. The cone is then lifted to allow the concrete or sample to flow out and spread out a little on the flow table. The table is raised up to the stop and allowed to freely drop 15 times. This causes the sample to spread further in a circular form and shape. The flow diameter is the mean of the maximum diameter of the pool of the sample and the diameter at the right angles. Figure 3.14 below shows the apparatus needed for the flow table test.

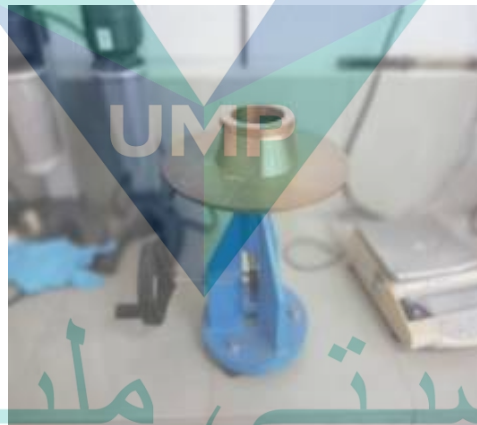


Figure 3.14 Flow table apparatus

In order to get the accurate measurement of the workability of the soil, the flow test acts as a cohesion indicator. A mix that is prone to segregation forms a non-circular pool of concrete or sample. A ring of clear water may form after a few minutes if the mix is prone to bleeding. In equation 3.4

$$FMP = \frac{(m1 - m2)}{m1} + \frac{(m3 - m4)}{m3} \quad 3.4$$

FMP = Flow Moisture Point

m1 = the exact mass of the sample just above flow state

m2 = the exact mass of the sample just above flow state, after

drying m3 = the exact mass of the sample just below flow state

m4 = the exact mass of the sample just below flow state, after drying

3.9 SEM and EDX

For better understanding of the changes of amended bauxite affect the value of TML and MWD, the targeted percentage value of gypsum and vermicompost were investigated using scanning electron microscopy (SEM). The sample of amended and unamend bauxite were sent to UMP Central Laboratory, Malaysia for morphological analysis. . The main objective of this analysis is to gain a knowledge on how the bauxite has altered its aggregate stability on microscopic perspective after amendment from using mixture gypsum and vermicompost.

Secondly, it is crucial to acknowledge value of aluminum oxide on bauxite after amendment. The sample were secure on the specimen holder with aluminum tape and then sputtered with gold in sputter coated (BAL-TEC SCD 005, Balzers, Switzerland). All the specimens were examined with a Hitachi TM3030 Plus, benchtop scanning electron microscope under high vacuum condition, at an accelerating voltage of 20.0 kV and working distance of 8-10 m



Figure 3.15 Benchtop SEM, Hitachi TM3030 Plus used for morphological analysis

CHAPTER 4

RESULTS AND DISCUSSION

4.1 Introduction

In this chapter, the result and discussion will provide a better understanding of the bauxite stabilization using gypsum and vermicompost as treatment against liquefaction in solid bulk cargoes. It covers screening study by using factorial analysis, optimization using CCD and validation by comparing result with unamend bauxite. In screening phase, factorial analysis of four parameters effecting physical properties of amended bauxite was carried out to determine the contribution of each parameters, analysis of variance (ANOVA), and interaction between parameters.

Based on screening phase, two parameters were chosen to be proceed in optimization part. Central Composite Design (CCD) was applied to optimize two factors, which are vermicompost and gypsum percentage. The optimization phase was determined by ANOVA where lack of fit and response surface plot used to obtain optimal condition (central value data) for physical properties of bauxite. Lastly, the result were tested by comparing amend with the unamend bauxite to see the significant changes in its Mean Weight Diameter (MWD), Transportable Moisture Limit (TML) and morphological.

4.2 Material and Sample Characterization

Important to state the condition and properties of material and sample used in this experiment. Therefore, materials used such as gypsum and vermicompost has undergo several test to obtain its basic properties as state in Table 4.1.

Table 4.1 Basic Properties of Material

Properties	Gypsum	Vermicompost
Particle Distribution	Clay	Sand
> 425 μm (%)	100	100
> 63 μm (%)	100	45
> 2 μm (%)	97	8
Specific gravity, G_s	2.33	0.56
pH	7.3	6.5

On the other hand, bauxite used in this experiment has undergone x-ray diffraction to ensure the amount content of aluminum oxide are present and significant. Table 4.2 shows the raw bauxite used in this experiment can quantify as medium grade of bauxite and the data from XRD taken from morphology analysis done prior experiment using Hitachi TM3030 Plus.

Table 4.2 Basic Properties of Material

Element	Apparent Concentration	Wt.%	Standard Label
Carbon	0.36	19.22	C
Oxygen	3.19	38.92	SiO ₂
Aluminum	0.83	19.76	Al ₂ O ₃
Si	0.15	2.60	SiO ₂
Ti	0.08	1.82	TiO ₂
Fe	0.57	12.46	Fe ₂ O ₃
Zr	0.64	5.22	Zr

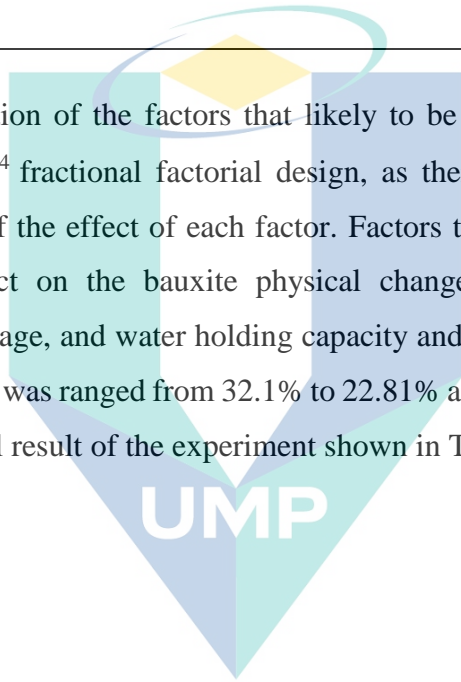
4.3 Full Factorial Design: Screening the Factor

The factorial design used to screen the factors studied in this study. The factors involved at this stage were percentage of gypsum, vermicompost, and water intake and incubation period shown in Table 4.1. These responding variables were chosen to represent the aggregate stability and IMSBC Code. Starting value of variable used are determined by prior study according literature review section. Table 4.3 shows summarized data input and output for fractional factorial design.

Table 4.3 Initial value of each variable

Factor	Range	Respond
Gypsum (%)	2%-6%	Particle Passing at 2.5 mm
Vermicompost (%)	4%-10%	
Water Intake (%)	50%-80%	Specific Gravity
Incubation Period (Days)	15 days-22 days	

The identification of the factors that likely to be effective on the bauxite was carried out through 2^4 fractional factorial design, as there are four factor. This is to establish the degree of the effect of each factor. Factors that was taken into account to investigate their effect on the bauxite physical changes were gypsum percentage, vermicompost percentage, and water holding capacity and incubation days. The particle distribution of 2.5 mm was ranged from 32.1% to 22.81% and specific gravity was ranged from 2.85 to 1.75. Full result of the experiment shown in Table 4.4.



اونيورسيتي ملايسيا قهغ

UNIVERSITI MALAYSIA PAHANG

Table 4.4 Finalized output for each parameter to be screening

Std	Factor 1	Factor 2	Factor 3	Factor 4	Response			
	Gypsum %	Vermicompost %	Water Holding %	Incubation Days	Actual Particle Distribution at 2.5 mm	Predicted Particle Distribution at 2.5 mm	Actual Specific Gravity	Predicted Specific Gravity
1	2	4	50	15	32.1	31.81	1.75	1.75
2	6	4	50	15	27.5	27.54	2.15	2.16
3	2	10	50	15	26.5	26.12	2.77	2.73
4	6	10	50	15	29.24	29.26	2.04	2.02
5	2	4	80	15	26.72	27.32	2.08	2.09
6	6	4	80	15	25.1	24.90	2.31	2.35
7	2	10	80	15	29.41	29.47	2.85	2.84
8	6	10	80	15	27.11	27.30	2.04	2.00
9	2	4	50	22	27.27	26.97	2.39	2.38
10	6	4	50	22	25.35	25.90	2.65	2.61
11	2	10	50	22	25.67	25.91	2.3	2.31
12	6	10	50	22	25	25.12	2.69	2.73
13	2	4	80	22	25.38	25.36	2.42	2.38
14	6	4	80	22	22.82	22.48	1.9	1.89
15	2	10	80	22	22.81	22.88	2.83	2.87
16	6	10	80	22	27.73	27.41	2.55	2.56

4.3.1 Variable Contribution on Particle Distribution at 2.5 mm and Specific Gravity

The relative size of effect are shown as in Pareto chart, where the bar length is proportional to absolute value of estimated effect. Effect of t-value limit (black line) are considered statistically significant at 95% confidence level whereas the effect below t-value limit are not likely to be significant. Effect above Bonferroni's corrected t-value limit (red line) is highly significant. A quick analysis was performed on the selected effect using Pareto chart statistically check for significance of selected effect at 95% confidence level.

For the response on particle distribution at 2.5 mm, the selected effect (D, AB, ABCD, BC and C) shown to be significant at both t-value limit and Bonferroni's corrected t-value limit as in Figure 4.1. Most interactions (AB, ABCD, BC, ACD, AD, and B) gave a positive effect to the particle distribution at 2.5 mm (refer to orange bar chart). Meanwhile, interaction factors (BCD, A, C, and D) resulted in negative effect (blue bar chart). A positive effect means that when increasing a parameter value, the particle distribution at 2.5 mm also increases while the negative effect is when the parameter value increases the response value decreases. If the factor value is below the T-value limit line the factor has no significance to the particle distribution at 2.5 mm. However, if the factor value is above the Bonferroni's limit the parameter is highly contributes to the particle distribution at 2.5 mm. The factor values between T-value limit and Bonferroni's limit lines also contributes to the response.

Pareto chart was used for response on specific gravity, the selected effect (ABD and B) shown to be significant at both t value limit and Bonferroni's corrected t-value limit as in Figure 4.2. Most interactions (ABD, B, D, BCD, AD, BC and C) gave the positive effect to the contributions on specific gravity. Meanwhile, some interaction factors (AB, AC, ACD, A and CD) gave negative effect. A positive effect means that when increasing a parameter value, the specific gravity also increases while the negative effect causes response value to decrease when the parameter value increases. If the factor value is below the T-value limit line the factor has no significance to the specific gravity. However, if the factor value is above the Bonferroni's limit the parameter highly contributes to the specific gravity.

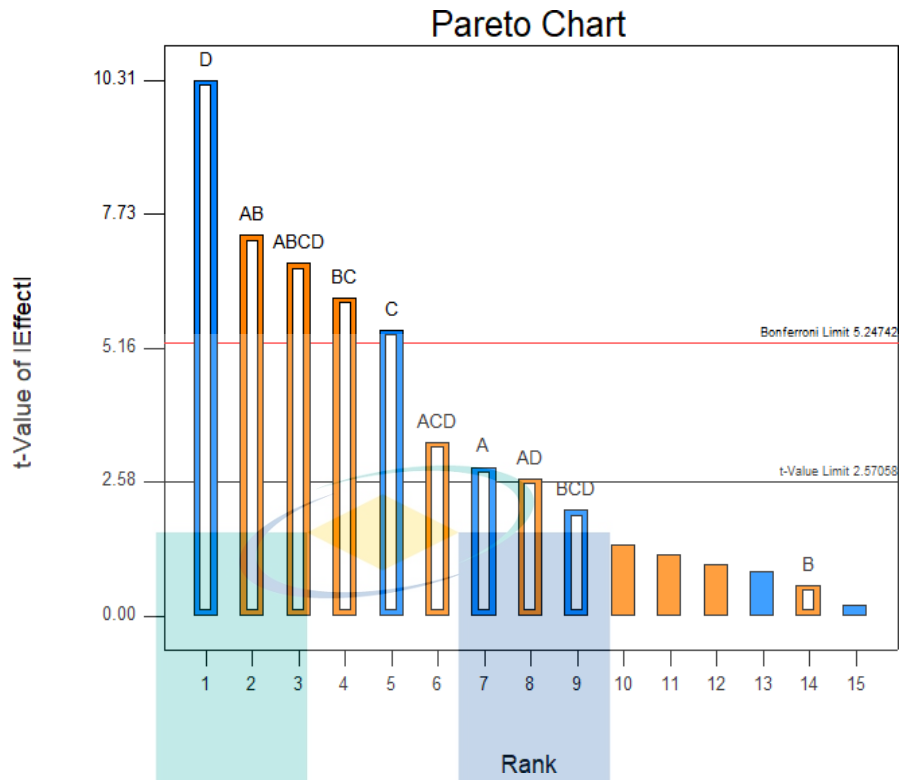


Figure 4.1 Effect on Particle Distribution at 2.5 mm

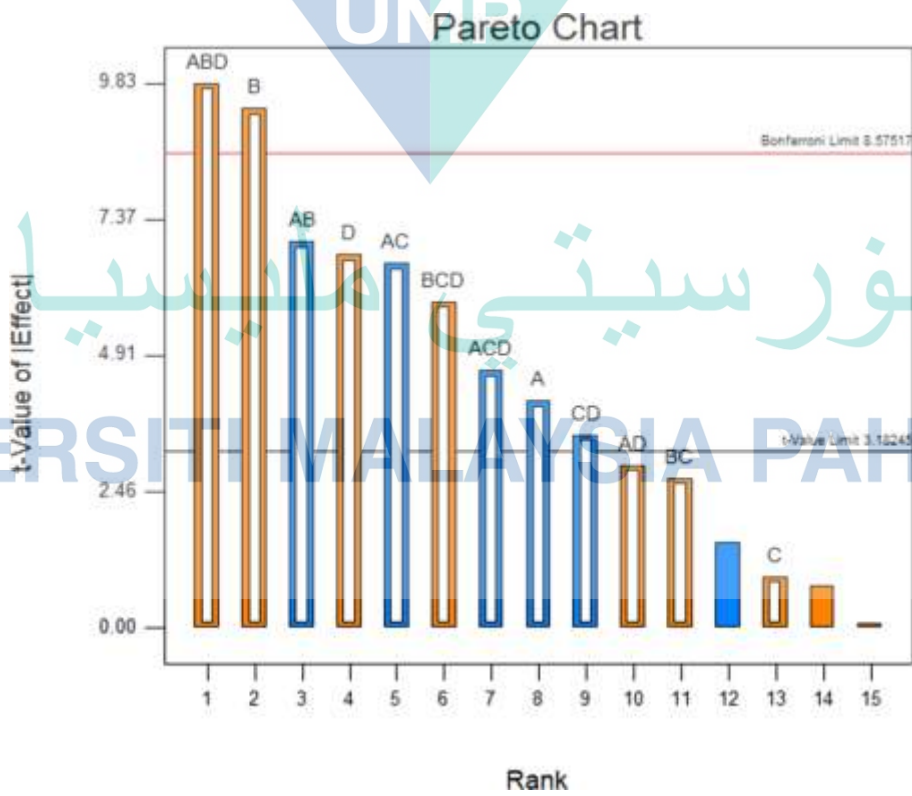


Figure 4.2 Effect on Specific Gravity

Figure 4.1 and Figure 4.2 describes the percentage contribution of each factor and interaction factors to the particle distribution at 2.5 mm and specific gravity respectively. Incubation days (D) and vermicompost (B) are the main contributing factors which gives about 34.34% and 20.57% affect to the responses. Incubation day which refers to the day stockpile been kept in port are consider to be out of scope since it is depends on transportation schedule. However, the model shows that higher days gives the proportional effects to contributions of other variable and interaction on the responses. Interestingly, both responses recorded highest interaction between gypsum and vermicompost (AB) which prove that this variable are dependent of each other and it is clearly shown in Figure 4.3 that interaction AB is significant.

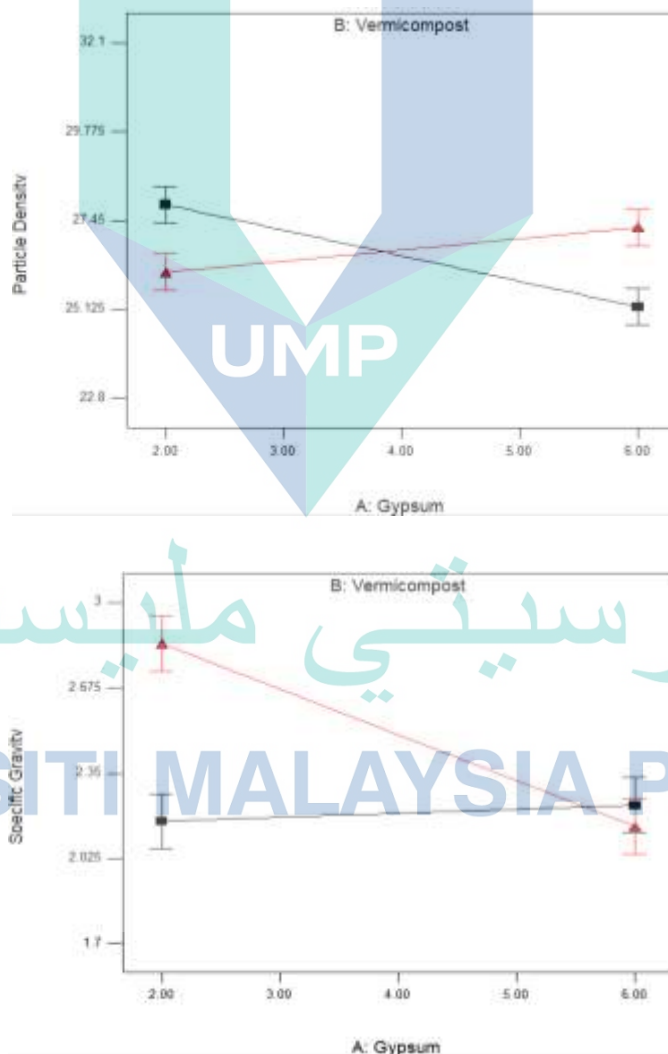


Figure 4.3 Interaction of Gypsum (%) and Vermicompost (%) on specific gravity and particle density (%)

As observed from the intersection lines on both charts, value lies on 4% to ~6% which indicates that the best interaction can be replicate when the value of both variable are in the range. Thus, gypsum at 6% and vermicompost at 4% are among the highest desirability of the model.

On the other hand, the correlation of AB is unique as particle distribution at 2.5 mm shows positive effect whereas in specific gravity, AB contributes negative effect. The opposite effects should be studied in more depth to investigate the best solution on using gypsum and vermicompost for reducing liquefaction risks. It is only rational for AB to undergo Central Composite Design (CCD)

Table 4.5 Estimated Effect of Variable to Particle Distribution at 2.5 mm

Parameters	Effect Estimate	Sum of Square	% Contribution
A: Gypsum	-0.75	2.26	2.65
B: Vermicompost	0.15	0.095	0.11
C: Water Intake	-1.44	8.34	9.77
D: Incubation Days	-2.71	29.30	34.34
AB	1.92	14.80	17.35
AD	0.69	1.93	2.26
BC	1.61	10.32	12.10
ABC	0.88	3.07	3.60
BCD	-0.53	1.14	1.34
ABCD	1.78	12.69	14.88

Table 4.6 Estimated Effect of Variable to Specific Gravity

Parameters	Effect Estimate	Sum of Square	% Contribution
A: Gypsum	-0.13	0.070	3.95
B: Vermicompost	0.30	0.37	20.57
C: Water Intake	0.0030	3.6 E -3	0.20
D: Incubation Days	0.22	0.19	10.63
AB	-0.23	0.20	11.38
AC	-0.21	0.18	10.15
AD	0.095	0.036	2.03
BC	0.087	0.031	1.72
CD	-0.11	0.051	2.84
ABD	0.32	0.40	22.66
ACD	-0.15	0.090	5.06
BCD	0.19	0.14	8.11

Conclusively for this subtopic, AB had the highest contribution between two ways interactions and AB is in the acceptable contribution range. These two variables were selected for the CCD (Section 4.4). This factorial design was setup with the aim of accessing the importance interaction of variables. Therefore, it is clear that interaction of gypsum between vermicompost is the important to be looked on in more details.

4.3.2 Screening Variable that Effect on Both Responses

The result has modelled and analyzed using ANOVA to analyse the parameters that influence the particle distribution at 2.5 mm and specific gravity. The ANOVA was carried out to determine the significant effect of the variables to the responses. A significance model where the p-value is less than 0.05, showing 5% chance of the model to be insignificant due to noise was used. The p-value describes the mutual interaction between each variable (Gan et al., 2007).

The smaller p-values define the mutual interaction between variables in the model (Alzorqi et al., 2017). Table 4.5 and 4.6 shows the model developed for the CCD. Both of the model showed high significance with p-value <0.0001 ($P < 0.05$). All the variables in the model were significant ($P < 0.005$) except B for the model. All the interactions variables were also showed to be significant. The results suggest that the factors and interactions produce significant effect to the responses.

Table 4.7 ANOVA for factorial analysis for Particle Distribution at 2.5 mm

Source	Degree of Freedom	Sum of Square	Mean of Square	F value	p-Value	
Model	10	83.94	8.39	30.46	0.0007	significant
A Gypsum	1	2.26	2.26	8.19	0.0353	
B Vermicompost	1	0.095	0.095	0.34	0.5835	
C Water Holding	1	8.34	8.34	30.26	0.0027	
D Incubation	1	29.30	29.30	106.31	0.0001	
AB	1	14.80	14.80	53.72	0.0007	
AD	1	1.93	1.93	6.99	0.0458	
BC	1	10.32	10.32	37.45	0.0017	
ACD	1	3.07	3.07	11.14	0.0206	
BCD	1	1.14	1.14	4.14	0.0977	
ABCD	1	12.69	12.69	46.05	0.0011	
Residual Error	5	1.38	0.28			
Total	15	85.31				

Table 4.8 ANOVA for factorial analysis for Specific Gravity

Source	Degree of Freedom	Sum of Square	Mean of Square	F value	p-Value	
Model	12	1.77	0.15	35.27	0.0068	significant
A Gypsum	1	0.070	0.070	16.82	0.0262	
B Vermicompost	1	0.37	0.37	87.67	0.4216	
C Water Holding	1	3.6E-03	3.6E-03	0.86	0.0067	
D Incubation	1	0.19	0.19	45.32	0.0061	
AB	1	0.20	0.20	48.50	0.0071	
AC	1	0.18	0.18	43.26	0.0605	
AD	1	0.036	0.036	8.65	0.0733	
BC	1	0.031	0.031	7.34	0.040	
CD	1	0.051	0.051	12.13	0.0022	
ABD	1	0.40	0.40	96.58	0.0188	
ACD	1	0.090	0.090	21.56	0.0098	
BCD	1	0.14	0.14	34.59		
Residual Error	3	0.013	4.175E-03			
Total	15	1.78				

Coefficient of determination (R^2) shows the ration of the described variation to the total variation and determines the agreement between the experimental and predicted results (Yang et al., 2017). R^2 is must be more than 80% for it to be considered as a good fit model (E. Gan et al., 2007).

The adjusted R^2 describe the degree of fitness and it is more reliable than R^2 as it compare models with different numbers of independent variables. In these models, R^2 value was 0.8345 and 0.7998, which are reliable while the adjusted R^2 value are 0.9515 and 0.9648. High R^2 value indicates that the model was well adapted to the response as the regression model could offer decent prediction as its values approaches $R^2 = 1$. Coefficient of determination (R^2) is defined as the ration of the described variation

In addition, a quadratic polynomial equation is used to explain the mathematical relationship between variables and their response (E. Gan et al., 2007). Based on the ANOVA results (Table 4.7 and 4.8) a quadratic model was drawn for this screening study. Equation 4.1 and 4.2 shows the response surface quadratic model for particle distribution at 2.5 mm and specific gravity which can be presented in terms of coded factors and as in the following equation

$$Y = 26.61 - 0.38(A) + 0.077(B) - 0.72(C) - 1.35(D) + 0.96(AB) + 0.35(AD) + 0.80(BC) + 0.44(ACD) - 0.27(BCD) + 0.89(ABCD) \quad 4.1$$

$$X = 2.36 - 0.066(A) + 0.15(B) - 0.015(C) + 0.11(D) - 0.11(AB) - 0.11(AC) + 0.047(AD) + 0.044(BC) - 0.056(CD) + 0.16(ABD) - 0.075(ACD) + 0.095(BCD) \quad 4.2$$

where:

- Y : Particle Distribution
- X : Specific Gravity
- A : Gypsum
- B : Vermicompost
- C : Water Intake
- D : Incubation Days

The unknown A, B, C and D were referred to the main effect, while AB, AD, BC, ACD, BCD, CD, ABD and ABCD were the interaction effects contributed in particle distribution at 2.5 mm and specific gravity. Based on first-order linear equation, coefficient of A to D is lesser, comparing to constant in both equation.

This gives an indicator that the model equation is good even with small error and can be used for further analysis. A regression model can be used to foresee expected new observations on both responses that corresponding to experimental values of the factors.

Meanwhile, the data that extrapolate beyond the straight line generated by Design Expert show high possibility that a model is no longer fit in the regression model.

Moreover, the higher values of R² of the models will show a close agreement between the experimental results and the theoretical values predicted by the model. Thus, the experimental data for the particle distribution at 2.5 mm and specific gravity from the empirical model is in good agreement with the observed ones in the range of the operating factors as shown in Figure 4.4 and 4.5.

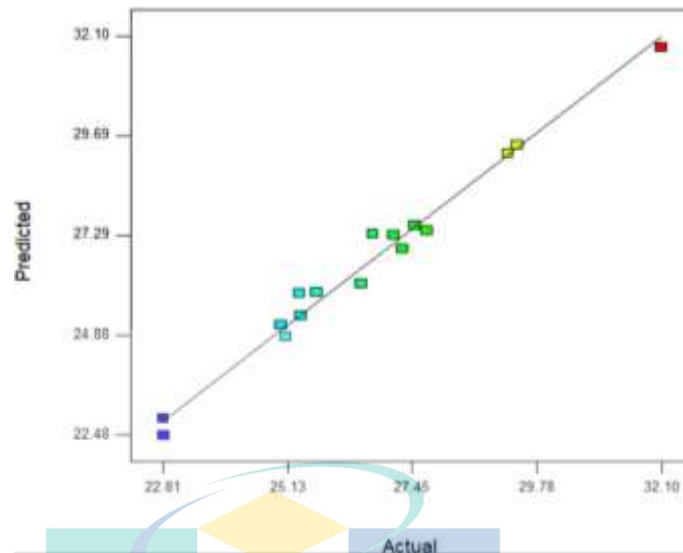


Figure 4.4 Predicted versus actual regression model graph for Particle Distribution at 2.5 mm

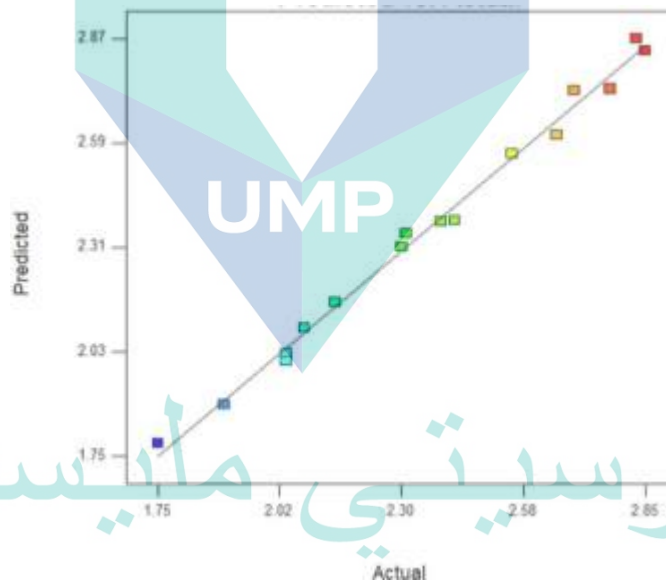


Figure 4.5 Predicted versus actual regression model graph for Specific Gravity

As conclusion, this technique is a combination of mathematical and statistical techniques that are helpful for modelling experimental data where the response variable was influenced by the factors of experiment. The objective is to narrow initial value and select the most contributable variables. All the laboratory data for Phase 1 are shown in **Appendix A**.

4.4 Central Composite Design: Optimization Analysis

Optimization touch on the improvement of performance of a model, a process, or a product in order to gain the maximum benefit from it while optimizing levels of variables in order to accomplish the best system performance (Bezerra et al., 2008). Optimization on optimum factors conditions that effect responses was selected based on the previous phase (Section 4.2). Based on factorial analysis (Section 4.2), two factors that were selected for optimization are gypsum and vermicompost. The optimization was carried out using Design Expert and central composite design (CCD). It was employed to determine the optimum condition for the interaction to gain lower particle distribution at 2.5 mm specific gravity. The previous phase results showed that percentage of gypsum and vermicompost optimum at 6% and 4% respectively based on the desirability of the optimum condition. Therefore, the optimum value was used as central composite design for optimization study.

4.4.1 Central Composite Design (CCD)

A set of 13 experiments including five replicates at the center points were designed from two parameters which are gypsum and vermicompost by using CCD to optimize the responses using method as, summarized in Table 4.9. The center points were performed to determine the experimental and pure error required for the ANOVA as well as to observe the existence of curvature in the RSM plot (Alzorqi et al., 2017). The range of the two parameters and the center points are presented in Table 4.10, based on results from factorial analysis. For example, the two factors at the center points were set at 6% of gypsum and 4% of vermicompost. The particle distribution at 2.5 mm and specific gravity was determined as the response of parameters while the optimum responses was obtained at one of the five-center point.

Table 4.9 The value of factors used in Central Composite Design

Factor	Low level (-)	High level (+)
A: Gypsum (%)	5	7
B: Vermicompost (%)	3	5

Table 4.10 Finalized output for each parameter to be screening

Std	Factor		Response			
	Gypsum %	Vermicompost %	Actual Particle Distribution at 2.5 mm	Predicted Particle Distribution at 2.5 mm	Actual Specific Gravity	Predicted Specific Gravity
1	5	3	25.22	25.32	2.32	2.33
2	7	3	24.04	23.99	2.41	2.45
3	5	5	26.42	24.46	2.01	2.10
4	7	5	24.32	23.98	2.10	2.23
5	4	4	26.87	26.86	2.05	2.04
6	8	4	23.15	23.28	2.35	2.29
7	6	2	24.65	26.23	2.52	2.53
8	6	6	25.26	25.46	2.18	2.10
9	6	4	24.42	24.73	2.41	2.31
10	6	4	25.15	24.73	2.39	2.31
11	6	4	24.69	24.73	2.36	2.31
12	6	4	24.26	24.73	2.29	2.31
13	6	4	24.87	24.73	2.24	2.31

اونيورسيتي ملايسيا قهق

4.4.2 Modelling for Optimization Stage

The precision of a test can be evaluated by ANOVA with referring to the model analysis and lack of fit test, as well as by using coefficient of determination (R^2) analysis (Bezerra et al., 2008; Nath et al., 2007; Yang et al., 2017)

The ANOVA results for the optimization study in perspective of particle distribution at 2.5 mm is shown in Table 4.11. The model generated for this study was highly significant ($p = 0.0005$). A model is considered significant if the p-value is less than 0.05 indicating that only 5% chance of noise can occur in the model (Yang et al., 2017) P-value is used to identify the significance of the effect of each linear, quadratic and interaction term toward the response (Yang et al., 2017) The quadratic terms of main factors, A^2 and B^2 were moderate significant with p-value more than 0.005. However, the main factors A were significant ($p < 0.0001$).

Table 4.11 ANOVA of model for particle distribution at 2.5 mm

Model	Degree of Freedom	Mean square	F-value	P-value	
Model	5	2.12	20.12	0.0005	Significant
A	1	9.58	90.71	<	0.0001
B	1	0.61	5.75	0.0475	
AB	1	0.21	2.00	0.1998	
A^2	1	0.17	1.60	0.2460	
B^2	1	0.12	1.13	0.3229	
Residual	7	0.11			
Lack of fit	3	0.079	0.63	0.6315	Not Significant
Pure error	4	0.13			
Cor total	12				

The ANOVA results for the optimization study in perspective of specific gravity is shown in Table 4.12. The model generated for this study was significant ($p = 0.027$). The quadratic terms of main factors, A^2 and B^2 were not significant with p-value more than 0.05. However, the main factors (A and B) were significant ($p < 0.05$).

Table 4.12 ANOVA of model for specific gravity

Model	Degree of Freedom	Mean square	F-value	P-value	
Model	5	0.045	5.12	0.0270	Significant
A	1	0.051	5.78	0.0472	
B	1	0.14	16.05	0.0052	
AB	1	0.000	0.000	1.000	
A ²	1	0.030	3.41	0.1071	
B ²	1	4.091E-005	4..6E-003	0.9475	
Residual	7	8.777E-003			
Lack of fit	3	0.014	2.71	0.1802	Not Significant
Pure error	4	5.07E-003			
Cor total	12				

The lack of fit can be tested when experimental design performed with reliable repetition such as center point and the response predictor is rejected. The lack of fit of the model for this study was not significant for both responses, particle distribution at 2.5 mm and specific gravity as the p- value were 0.635 and 0.1802 respectively.

Important to highlight, this model used R² value obtained in this study. The R² value of the generated model for both responses recorded at 0.9350 and 0.789 implied that the experimental data confirm the compatibility with the data predicted by the model. The adjusted coefficient of determination (R² Adj.) was 0.885 and 0.6321 which are in high value and further supports the significance of the model. Based on Yemiş et al. (2011) a good fit for a model is value of R² above 0.80. Furthermore, the model with high value of R² presented a close agreement between theoretical values predicted by the model and experimental data as shown in Figure 4.11. These statistical tests showed that the model was suitable to represent the data and able to explain the relationship between the process variables and response. Similar report by Teng et al. (2016) also stated that high R² values represent a good model as it will demonstrate high computability with theoretical data. Thus, the generated model was applicable to predict the experimental data of responses using gypsum and vermicompost.

4.4.3 Regression Model

The response surface quadratic model for particle distribution at 2.5 mm (X) and specific gravity (Y) in this optimization study are presented in term of coded factors as shown in equation 4.2 and 4.3.

$$X = 24.72 - 0.89 A + 0.22 B - 0.23 AB + 0.086 A^2 + 0.072 B^2 \quad 4.3$$

$$Y = 2.31 + 0.065 A - 0.11 B + 0.010 AB - 0.036 A^2 + 0.013 B^2 \quad 4.4$$

In the equation, X is the particle distribution at 2.5 mm (%) and Y act as specific gravity. A is the gypsum (%) and B is vermicompost (%), where both are the main effects. Whereas AB, A², and B² were the interaction effect that contribute in both responses.

4.4.4 Response Surface Plot

Since the model shows good fitting, the response value is sufficiently explained by the regression equation (Equation 4.3 and 4.4). To demonstrate the interactions of the variables and to determine the optimal value of each variable for the maximum response, the response surface curves were plotted. Correlation between responses and experimental level of each variables and interaction between two test variable can be presented by regression equation which can be obtained by graphical plots that include 2D contour plot and 3D response surface (Qiao et al., 2009)

Figure 4.6 shows the experimental result in 3D response surface plots representing the relationship between two variables and their responses.

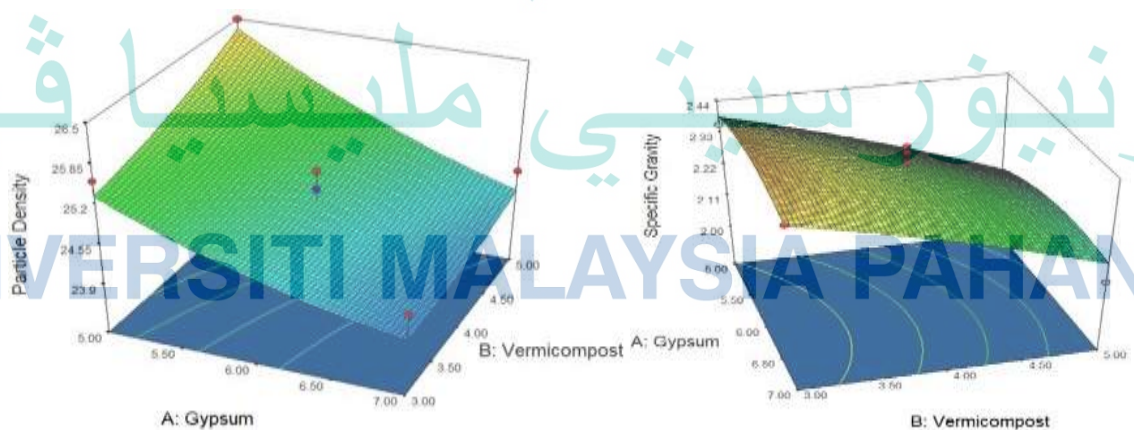


Figure 4.6 Optimization of 3D Contour Plot

This 3D plot illustrates the surface where the maximum point is placed inside the experimental region. As the gypsum (%) increases the particle distribution increases as well. It was found to be optimum at 6% of gypsum and 4% of vermicompost. Afterward, the gypsum shown to be gradually decreased as the vermicompost increased. Therefore, the gypsum and vermicompost has significant effect on the responses which agrees with the findings of Zhu et al. (2017) who reported that the interaction of gypsum and vermicompost is one of the main interaction that has significant effect on the physical aspect of soil. All the laboratory data for Phase 2 are shown in **Appendix B**.

4.5 Validation: Aggregate Stability and Flow Table Analysis

This phase are usually not required in the mainly factorial design as it already undergo one factor analysis or screening phase and optimization by central composite design. However, the findings from the previous phase from this study provide optimization effects of interaction between gypsum and vermicompost. It was then undergo important geotechnical and morphological analysis. It is important to breakdown the information as soil stabilization using gypsum and vermicompost need a further review on how it affects soil physically, chemically and biologically. This phase provide analysis of aggregate stability, flow table, SEM and XRD. There are 10 samples, which contained the highest desirability from the previous phase as shown in Table 4.13. The targeted optimization mixture (Gypsum 6%: Vermicompost 4%) percentage were tested for triplicate to reduce human error.

Table 4.13 Validation and Modelling Table

Sample	Desirability	Gypsum %	Vermicompost %
B-200 (Control)	-	-	-
B-20503	0.730	5.00	3.00
B-20505	0.563	5.00	5.00
B-20705	0.763	7.00	5.00
B-20404	0.587	4.00	4.00
B-20606	0.603	6.00	6.00
B-A20604	0.764	6.00	4.00
B-B20604	0.764	6.00	4.00
B-C20604	0.764	6.00	4.00
B-20204	0.517	2.00	4.00

4.5.1 Aggregate Stability Analysis

The aggregate stability of bauxite obtained by using the modified Le Bissonnais' (LB) method is shown in Table 4.14. This method was selected to test aggregate stability of amended samples which included three disruptive test: fast wetting (FW), slow wetting (SW) and wet stirring (WS) (Xiao et al., 2018). The relative importance of slaking y differential swelling is known to be strongly influenced by soil moisture content, soil particle size and clay mineral type. Comparison between different moisture pre-treatments and fluids indicates that when dry aggregate was sieve in water, aggregate breakdown principally resulted from differential clay swelling. This is followed by dispersion with only contribution from air entrapment and mechanical abrasion. Lower stability of the air-dried aggregates was attributed to increased slaking (Le Bissonnais, 1996; Leelamanie et al., 2013). In this study, breakdown of bauxite principally resulted from alternate force from ship motion which increase the force between aggregate due to weakness on aggregate stability.

Table 4.14 Samples and each of disruptive test in term of MWD, GMD and Erodibility Factor

Sample	Disruptive Test	MWD (mm)	GMD	Erodibility Factor (K)
B-10503	FW	1.510671	1.43471	0.026152
	SW	1.386553	1.374998	0.027053
	WS	1.436859	1.417888	0.026396
B-10505	FW	1.505245	1.429984	0.026220
	SW	1.4432	1.469105	0.025672
	WS	1.3892	1.3737	0.027074
B-10705	FW	1.561486	1.53468	0.024828
	SW	1.529971	1.490404	0.025388
	WS	1.456358	1.440572	0.026068
B-10404	FW	1.407412	1.471749	0.025636
	SW	1.411235	1.379959	0.026975
	WS	1.453528	1.40609	0.026572
B-10606	FW	1.559683	1.53476	0.024819
	SW	1.436941	1.475623	0.025584
	WS	1.50222	1.4404	0.026070

Table 4.14 Continued

Sample	Disruptive Test	MWD (mm)	GMD	Erodibility Factor (K)
B-A10604	FW	1.544384	1.512237	0.025107
	SW	1.538372	1.510867	0.025124
	WS	1.537169	1.525063	0.024947
B-B10604	FW	1.545358	1.509608	0.025140
	SW	1.527624	1.48739	0.025428
	WS	1.525616	1.505309	0.025195
B-C10604	FW	1.548266	1.532841	0.024851
	SW	1.513017	1.479638	0.025530
	WS	1.525956	1.482926	0.025487
B-10204	FW	1.26929	1.146156	0.031557
	SW	1.323259	1.235272	0.029572
	WS	1.253427	1.333827	0.027731
B-100	FW	1.146685	0.882231	0.040177
	SW	1.299351	1.201966	0.030274
	WS	1.187248	1.207405	0.030156

As shown in Figure 4.7, the highest MWD (mm) in fast wetting test is record B-C10606 at 1.548, whereas: the lowest MWD (mm) in fast wetting test record in control sample at 0.882. The FW and WS test had significant effects on particle disaggregation. Higher MWD with addition of vermicompost and gypsum indicated that interaction between AB can give better aggregate stability which is essential in order to reduce liquefaction risk (Zhu et al., 2017).

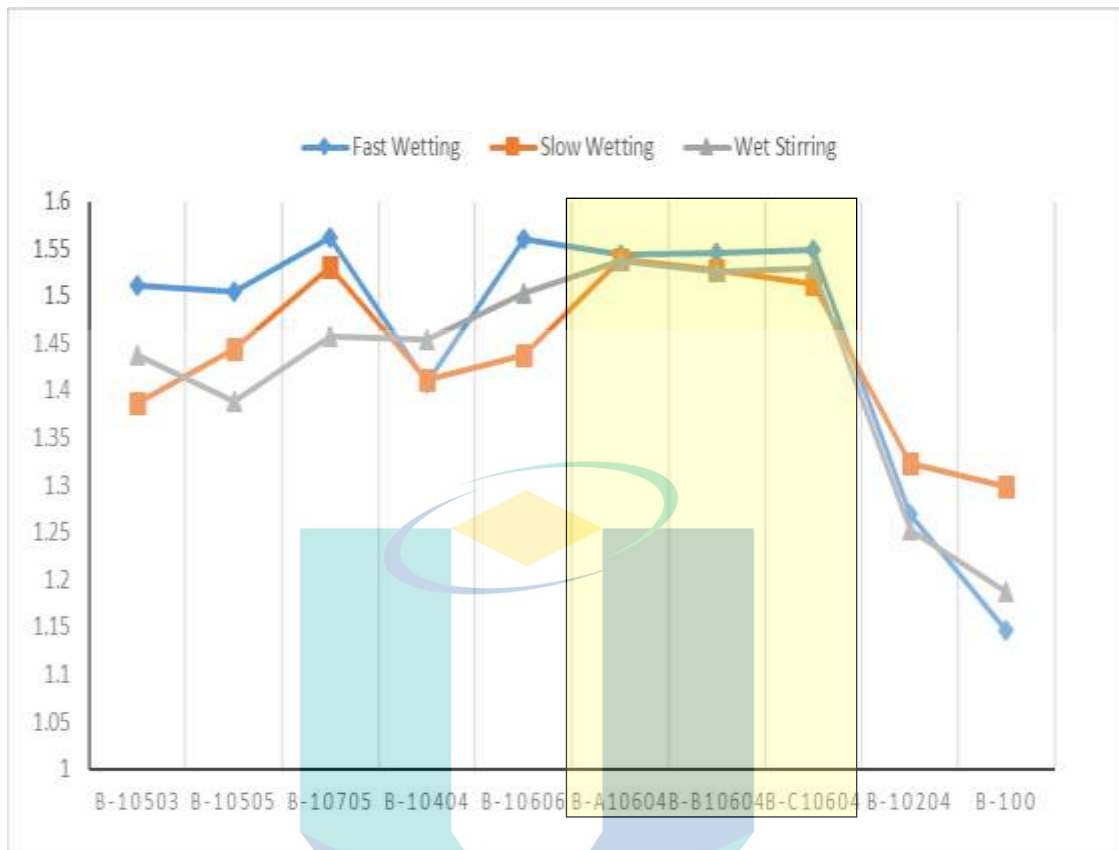


Figure 4.7 Mean Weight Diameter of Optimization model

On the other hand, high value of erodibility factor (K) indicate a less stable physical structure. Significant differences in K of the samples was presented in Figure 4.8. Control sample was recorded to have the highest value of K in fast wetting test which was 0.04.

Whereas, the lowest value of K in fast wetting in record was 0.024. The erodibility factor (K) embodies both susceptibility of soil to erosion and disaggregation, as measured under the three disruptive tests.

The factor reflected that different soil eroded at different rates when the other factors involved were infiltration, permeability, total water capacity and dispersion. The soil erodibility factor range in value from 0.02 to 0.69 (Goldman et al., 1986).

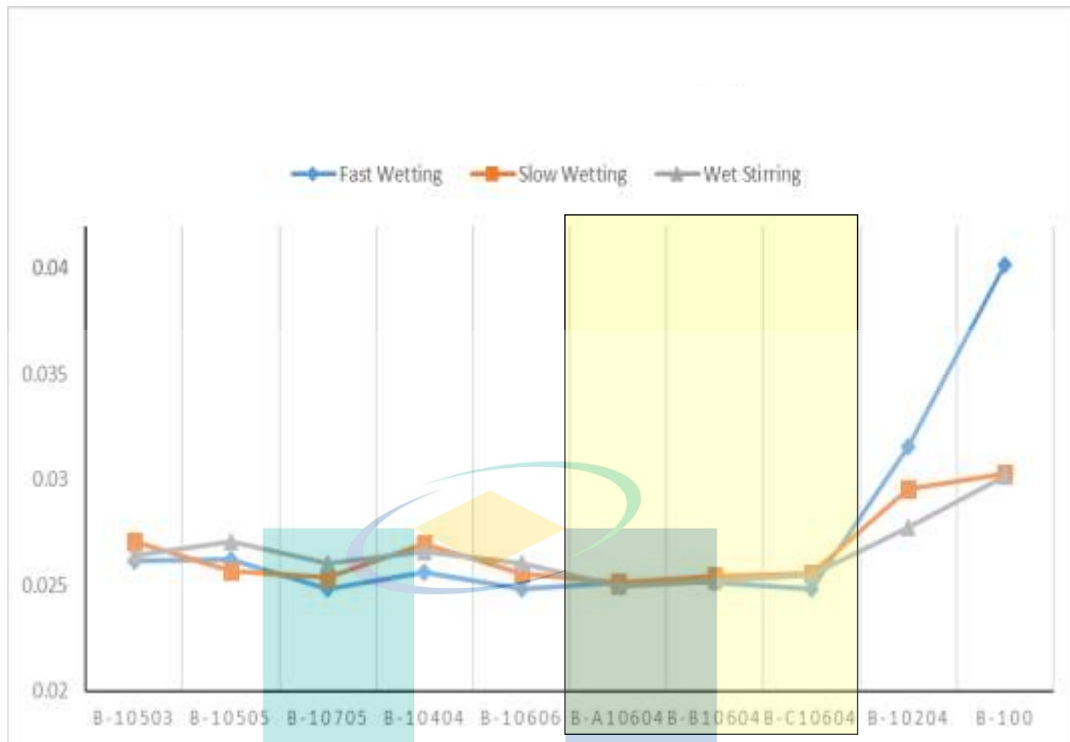


Figure 4.8 Erodibility (K) of Optimization model

The optimization model improved the MWD (mm) compare to control at rate of 75.5% and the erodibility factor (K) at rate 66.7%. The evidence in this study suggest that at optimization level from previous phase which gypsum percent at 6% and vermicompost percent at 4% by weight that used to amend bauxite will significantly improve its overall aggregate stability.

4.5.2 Flow Table Analysis

In the flow table test, the flow moisture point is determined in order to calculate the transportable moisture limit in accordance to the IMSBC Code. The flow moisture point represents the percentage of moisture content when the flow state is in progress which is when a sample from the cargo starts to lose its shear strength. The cargoes typically have moisture content beyond o above flow moisture point may liquefy as per IMSBC Code state. In this test, 10 sample from optimization were tested and the result were shown in Table 4.15. After that, the results were compared with the moisture limit of the batch bauxite taken for the experiment. Transportable moisture limit (TML) of the sample is 90% of the flow moisture point (FMP).

Table 4.15 Tranportable Moisture Limit of Optimziation model

Sample	Flow Moisture Point	Transportable Moisture Limit
B-10503	25.82%	23.24%
B-10505	26.18%	23.56%
B-10705	26.07%	23.47%
B-10404	25.37%	22.83%
B-10606	27.46%	24.71%
B-A10604	29.06%	26.15%
B-B10604	29.69%	26.72%
B-C10604	29.97%	26.97%
B-10204	23.86%	21.48%
B-100	22.97%	20.67%

As shown in Section 2.5, the TML of the specimen must exceeds moisture limit in order to pass the requirement according to IMSBC Code (Figure 4.9). Therefore, the specimen from the same batch were tested to obtain moisture limit with value average 24.07%. This adequate for optimization model to pass the code by at most margin of +2.9%.

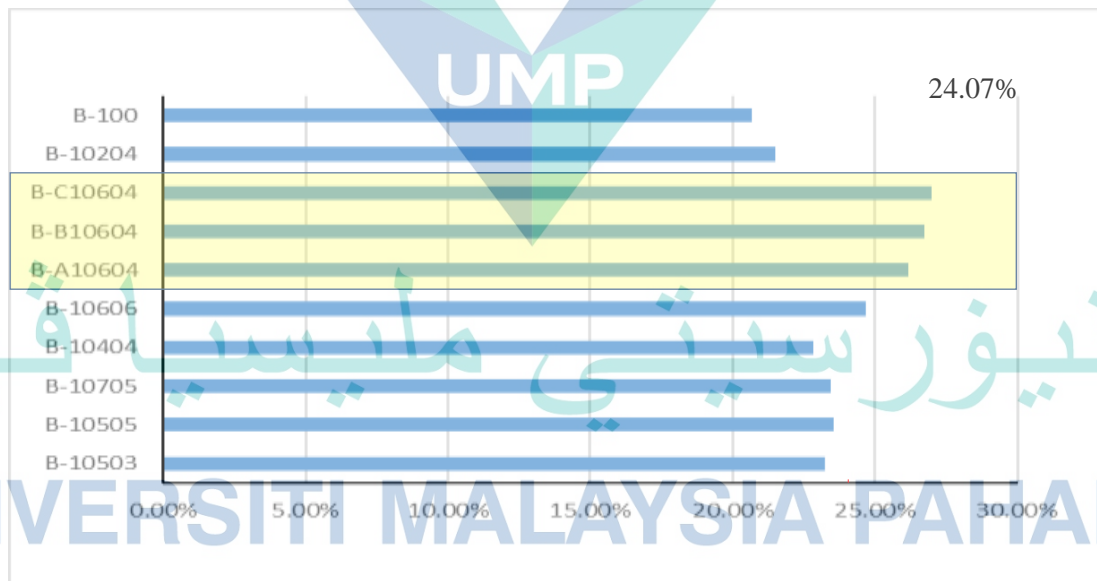


Figure 4.9 Tranportable Moisture Limit of optimization model

Concisely, it is important to determine the transportable moisture limit before every voyage as it is a matter of safety. Based on the analysis above, it is seen that the four sample (B-A10604, B-B10604, B-C10604 and B-10606) from optimization mode using gypsum and vermicompost amend the sample have greater TML and surpass the moisture limit indicating that samples have lower risk of liquefaction.

4.5.3 Scanning Emission Microscopy and Energy Dispersive X-Ray

Scanning Electron Microscopy with Energy Dispersive X-Ray analysis (SEM-EDX) was carried out by Hitachi TM3030 Plus machine in the UMP Central Laboratory to determine the morphological properties of samples. The micromorphology of samples in macro aggregates (2-1 mm) were suitable to observe for changes on its structure. SEM imaging comparing of control micro aggregate (B-100) with the B-A10604 (Figure 4.10) revealed that the particles of 0.5-1 μm were the major fraction. Residue macro aggregates of control sample had a sheet-like structure with many fine fragments. With the addition of gypsum and vermicompost, the quantity of macro aggregates of the sheet-like structure increased significantly. The size of the sheet-like structure became larger and the major fraction were the 2-5 μm particles. The combination of vermicompost and gypsum changed the bauxite to a denser structure. A large number of fine particles with granular structures attached to macro aggregate surfaces was found (Zhu et al., 2017). As shown in Figure 4.10 addition of vermicompost and gypsum improved aggregate structure from a sheet-like assembly to a platy arrangement as present of calcite in gypsum, whilst the 1-3 μm fraction of micro aggregates significantly decreased.

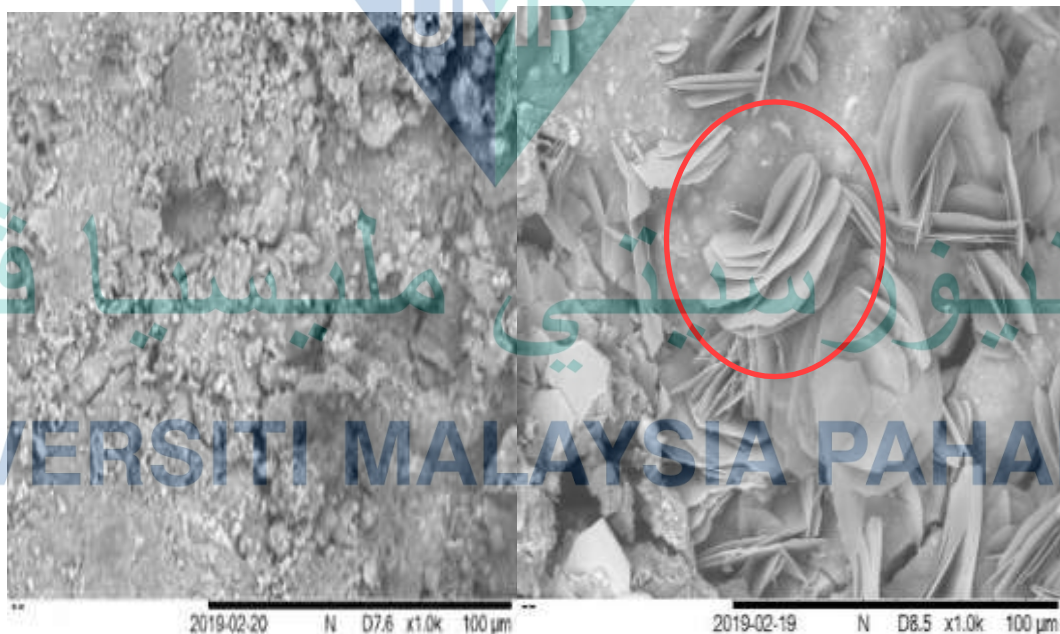


Figure 4.10 Fine particle (B-100) and presence of platy arrangement (B-A10604) at x1000 Magnification (microaggregates)

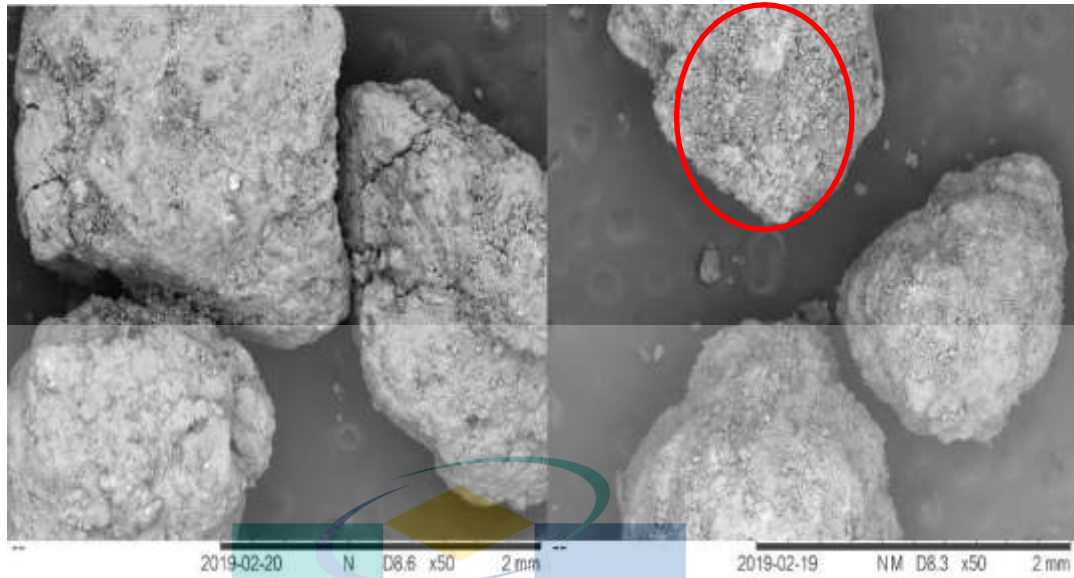


Figure 4.11 Scatter fine particle (B-100) and flocculation of fines particle to dense particle (B-A10604) at x50 Magnification (macroaggregates)

The EDX has provide the apparent concentration and percentage of aluminum of sample bauxites. This information is crucial for this phase, as the percentage of aluminum of bauxite has to be consistent before and after the addition of vermicompost and gypsum. Table 4.11 proves that uses of gypsum and vermicompost did not alter the chemical of aluminum oxide, which is the main ingredient in bauxite for industry purposes. Control sample record about 19.76%, which is the actual weightage of the sample from Gebeng’s bauxite as shown in Table 4.16. Whereas sample of optimization model of B-A10604 shows the presence of aluminum 15.23% of weightage from the mended bauxite as shown in Table 4.17.

Table 4.16 X-ray diffraction of amended bauxite (B-A10604)

Element	Apparent Concentration	Wt. %	Standard Label
Carbon	0.10	30.88	C
Oxygen	0.37	40.12	SiO ₂
Aluminum	0.75	15.23	Al ₂ O ₃
Ferum	0.15	9.01	Fe ₂ O ₃
Zirconium	0.07	4.71	Zr

Table 4.17 X-ray diffraction of unamend bauxite (B-100)

Element	Apparent Concentration	Wt.%	Standard Label
Carbon	0.36	19.22	C
Oxygen	3.19	38.92	SiO ₂
Aluminum	0.83	19.76	Al ₂ O ₃
Si	0.15	2.60	SiO ₂
Ti	0.08	1.82	TiO ₂
Fe	0.57	12.46	Fe ₂ O ₃
Zr	0.64	5.22	Zr

As the conclusion, this study found that the granular or lump sizes of bauxite create a stable array sand with a better cementation ability resulting in the ability to prevent soil from liquefying. This explain the condition of the optimization sample that has better aggregate stability and high transportable moisture limit comparing to control sample. This method of stabilization using gypsum and vermicompost are different from beneficiation process, which widely used for reducing liquefaction risk. However, soil stabilization method used in this study is a greener alternative that can be implemented to conserve our domestic water. All the laboratory data for Phase 3 are shown in **Appendix C**.

اونيورسيتي ملايسيا قهغ

UNIVERSITI MALAYSIA PAHANG

CHAPTER 5

CONCLUSION

5.1 Introduction

In Malaysia, the moratorium of bauxite activities has ended since the end of 2018. This is crucial point where the method studied in this research to be implement as an alternative for safer mining industry.

This research aimed to find the most effective factors to improve physical properties of raw bauxite. Differences in particle distribution at 2.5 mm and specific gravity were then analyzed. The result of analysis shows that gypsum and vermicompost percentage by weight of 6% and 4% respectively shown the highest contributions in improving physical properties of raw bauxite. Relationship between gypsum and vermicompost, which at its targeted value (6% and 4 % respectively) were then analyze with Mean Weight Diameter (MWD) and Transportable Moisture Limit (TML).

The information from TML and MWD are important to explain the liquefaction risk in solid bulk cargoes. This stage was performed using central composite design, which enhance the targeted value data that was obtained in the previous stage. In terms of MWD, amended bauxite (B-C10604) shows significant positive result, showing improvement from 0.882mm to 1.548mm. Total improvement was 75.5%, which greatly influence its capability to disaggregate towards external forces. Meanwhile, the improvement on its TML also gives significant improvement, passing the terms of IMSBC Code. This is because, TML of raw bauxite, which recorded at 20.67%, improve to 26.61%, showing nearly 28.73% of improvement.

Initial water content of raw bauxite recorded at 24.07%, value of TML above initial water content also found to pass the IMSBC Code. Therefore, it can be concluded that bauxite stabilization using gypsum and vermicompost can give positive result of MWD and TML.

The study continued to validate the output by comparing micromorphology of amended and unamend bauxite. Scanning emission microscopy (SEM) was conducted to give image of microstructure of amended and unamend bauxite. The result shows that the combination of vermicompost and gypsum changed the bauxite to be in more dense structure. There was a large number of fine particles with granular structures attached to macro aggregate surfaces. Addition of vermicompost and gypsum also improved aggregate structure from a sheet-like assembly to platy arrangement, whilst the 1- 3um fraction of micro aggregates significantly decreased. Control sample record about 19.76%, which is the actual weightage of the sample from Gebeng's bauxite. Whereas sample of optimization model of B-A10604 shows the presence of aluminum 15.23% of weightage from the mended bauxite. Coefficient Variation (CV) of 0.119, as a rule of thumb, a CV less than 1 indicates as relatively low which conclude that aluminum content after stabilization are not affected.

New perspectives of understanding liquefaction especially in solid bulk cargoes by investigate its aggregate stability. By using stabilization of gypsum and vermicompost at its own unique target value, it is proven that liquefaction risk of bauxite is decrease as TML of bauxite increase. The finer particles of bauxite also drastically decrease with increases of MWD, which surely affect the soil aggregate response to any external forces, Using this approach, any soil with risk of increased pore water pressure can be stabilize using this set of experiment to obtain its own unique targeted value on using gypsum and vermicompost.

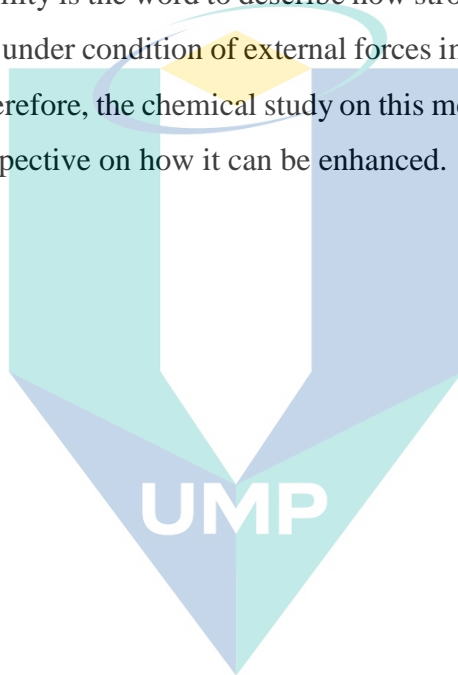
5.2 Recommendations

This study has embarked the possible alternative, which gives better environment protection with excellent result on reducing liquefaction risk. However, this soil stabilization under this development should be carried out in the future under a larger scale with real case scenario testing to test and analysis on the real performance and outcomes. Some recommendation are made to ensure that Gebeng bauxites and this research can be improved:

1. The incubation period of gypsum and vermicompost in bauxite should be increased to 16 weeks instead of only 2 and 3 weeks as used in this research. Natural weathering process which in this study converted as water intake

percentage (variable C) should be free from any value for certain period of season, for example rainy monsoon season. This is to ensure the meaning of natural process that happen in stockpile.

2. The method of this soil stabilization should be performed to other targeted liquefy soil, such as iron ore and other high fines content soil. This method also believed to be use in in situ replacement method.
3. Aggregate stability is the word to describe how strong the aggregate to remains its physical shape under condition of external forces including physical and chemical influences. Therefore, the chemical study on this method should expand in such to give more perspective on how it can be enhanced.



اونيورسيتي ملايسيا قهغ

UNIVERSITI MALAYSIA PAHANG

REFERENCES

- Aksakal, E., sarı, S., & Angin, I. (2015). *Effects of Vermicompost Application on Soil Aggregation and Certain Physical Properties. Land Degradation & Development* (Vol. 27). <https://doi.org/10.1002/ldr.2350>
- Al Majou, H. B. A. and D. O. 2008. (2008). Use of in situ volumetric water content at field capacity to improve prediction of soil water retention properties. *Canadian Journal of Soil Science*.
- ALANI, A. N., & Dudas, M. J. (1988). *Influence of calcium carbonate on mean weight diameter of soil. Soil & Tillage Research - SOIL TILL RES* (Vol. 11). [https://doi.org/10.1016/0167-1987\(88\)90028-1](https://doi.org/10.1016/0167-1987(88)90028-1)
- Almajmaie, A., Hardie, M., Acuna, T., & Birch, C. (2017). Evaluation of methods for determining soil aggregate stability. *Soil and Tillage Research, 167*, 39–45. <https://doi.org/10.1016/j.still.2016.11.003>
- Amezketta, E. (1999). *Soil Aggregate Stability: A Review. Journal of Sustainable Agriculture* (Vol. 14). https://doi.org/10.1300/J064v14n02_08
- An, S. S., Darboux, F., & Cheng, M. (2013). Revegetation as an efficient means of increasing soil aggregate stability on the Loess Plateau (China). *Geoderma, 209–210*, 75–85. <https://doi.org/10.1016/j.geoderma.2013.05.020>
- Anuar, A. N., Ahmad, H., Jusoh, H., & Hussain, M. (2013). *The Formation of Tourist Friendly Destination Concept in Kuala Lumpur. Asian Social Science* (Vol. 9). <https://doi.org/10.5539/ass.v9n15p166>
- Balasubramani, R., Gupta, S., Cho, W.-M., Kon Kim, J., Lee, S.-R., Jeong, K.-H., Choi, H.-
- C. (2016). *Microalgae Potential and Multiple Roles—Current Progress and Future Prospects—an Overview. Sustainability* (Vol. 8). <https://doi.org/10.3390/su8121215>
- Bashi, D., Fazly Bazzaz, B. S., Sahebkar, A., Mahdi Karimkhani, M., & Ahmadi, A. (2012). *Investigation of optimal extraction, antioxidant, and antimicrobial activities of Achillea biebersteinii and A. wilhelmsii. Pharmaceutical biology* (Vol. 50). <https://doi.org/10.3109/13880209.2012.662235>
- Bezerra, M., Santelli, R., Oliveira, E., Silveira Villar, L., & Amélia Escaleira, L. (2008). *Response Surface Methodology (RSM) as a Tool for Optimization in Analytical Chemistry. Talanta* (Vol. 76). <https://doi.org/10.1016/j.talanta.2008.05.019>
- Bishop, A. W. (1950). Undrained Triaxial Tests on Saturated Sands and Their Significance in the General Theory of Shear Strength By Part I: Theoretical Consideration.

- Burbank, M. B., Weaver, T. J., Green, T. L., Williams, B., & Crawford, R. L. (2011). Precipitation of calcite by indigenous microorganisms to strengthen liquefiable soils. *Geomicrobiology Journal*, 28(4), 301–312. <https://doi.org/10.1080/01490451.2010.499929>
- Cablík, V. (2007). Characterization and applications of red mud from bauxite processing. *The British Library "the World's Knowledge,"* 27–38.
- Captain Paul Walton. (2015). IMSBC CODE GROUP 'A' BULK CARGOES Prevention, Cause and Effect of Liquefaction.
- Cheng, X., Liu, M., & He, L. (2014). Shipwreck statistical analysis and suggestions for ships carrying liquefiable solid bulk cargoes in China. *Procedia Engineering*, 84, 188–194. <https://doi.org/10.1016/j.proeng.2014.10.425>
- Coman, M., Cecchini, C., Verdenelli, C., Silvi, S., Orpianesi, C., & Cresci, A. (2012). Functional foods as carriers for SYNBIO®, a probiotic bacteria combination. *International journal of food microbiology* (Vol. 157). <https://doi.org/10.1016/j.ijfoodmicro.2012.06.003>
- Courtney, R., & Kirwan, L. (2014). Gypsum amendment of alkaline bauxite residue – Plant available aluminium and implications for grassland restoration. *Ecological Engineering* (Vol. 42). <https://doi.org/10.1016/j.ecoleng.2012.02.025>
- Courtney RG, M. G. (2008). Soil quality and barley growth as influenced by the land application of two compost types. In *Bioresource Technology* 99: (pp. 2913–2918).
- Dashko, R., & Shidlovskaya, A. (2016). Impact of microbial activity on soil properties. *Canadian Geotechnical Journal* (Vol. 53). <https://doi.org/10.1139/cgj-2015-0649>
- Dejong, J., B. Fritzges, M., & Nüsslein, K. (2006). Microbially Induced Cementation to Control Sand Response to Undrained Shear. *Journal of Geotechnical and Geoenvironmental Engineering - J GEOTECH GEOENVIRON ENG* (Vol. 132). [https://doi.org/10.1061/\(ASCE\)1090-0241\(2006\)132:11\(1381\)](https://doi.org/10.1061/(ASCE)1090-0241(2006)132:11(1381))
- Derakhshandi, M., Rathje, E. M., Hazirbaba, K., & Mirhosseini, S. M. (2008). The effect of plastic fines on the pore pressure generation characteristics of saturated sands. *Soil Dynamics and Earthquake Engineering*, 28(5), 376–386. <https://doi.org/10.1016/j.soildyn.2007.07.002>
- Deviren Saygin, S., Cornelis, W., Erpul, G., & Gabriels, D. (2012). Comparison of different aggregate stability approaches for loamy sand soils. *Applied Soil Ecology* (Vol. 54). <https://doi.org/10.1016/j.apsoil.2011.11.012>
- Diaconescu, A., Litvak, V., Mathys, C., Kasper, L., Friston, K., & E. Stephan, K. (2017). *Computational hierarchy in human cortex.*
- Djurić, I., Mihajlović, I., Živković, Ž. & Filipović, R. (2010). Modeling the compensation effect for different bauxite types leaching in NaOH solution. *Chemical Engineering Communications*, 197(12), 1485–1499. <https://doi.org/10.1080/00986445.2010.484996>

- Duval, O., Le Bas, C., Vautier, A., Bruand, A., & Al Majou, H. (2008). Prediction of soil water retention properties after stratification by combining texture, bulk density and the type of horizon. *Soil Use and Management*, 24(4), 383–391. <https://doi.org/10.1111/j.1475-2743.2008.00180.x>
- E. Gan, H., Karim, R., Muhammad, K., Bakar, J., Hashim, D., & Abdul Rahman, R. (2007). *Optimization of the basic formulation of a traditional baked cassava cake using response surface methodology*. *Lwt - Food Science and Technology* (Vol. 40). <https://doi.org/10.1016/j.lwt.2006.05.005>
- Edwards CA, B. (1988). The potential of earthworm compost as plant growth media. In Neuhauser EF (Ed.), *Earthworms in waste and environmental management* (SPB Academ, p. pp 21–32).
- Fornes, G., Cardoza, G., & Xu, S. (2012). *The national and international expansion of Chinese SMEs: evidence from Anhui Province*. *Journal of Chinese Entrepreneurship* (Vol. 4). <https://doi.org/10.1108/17561391211262166>
- Fountain, H. (2010). *When Earthquake Liquefy Soil, Devastation Can Follow*. Retrieved from <https://www.nytimes.com/2018/10/01/world/liquefaction-earthquakes.html>
- G. Kamei, R., San Mauro, D., Gower, D., Van Bocxlaer, I., Sherratt, E., Thomas, A., S D, B. (2012). *Discovery of a new family of amphibians from Northeast India with ancient links to Africa*. *Proceedings. Biological sciences / The Royal Society* (Vol. 279). <https://doi.org/10.1098/rspb.2012.0150>
- Geeves, G. W. (1997). *Aggregate Breakdown and Soil Surface Sealing Under Agriculture*, (March).
- Gholami, L., Sadeghi, S. H., & Homaei, M. (2013). *Straw Mulching Effect on Splash Erosion, Runoff, and Sediment Yield from Eroded Plots*. *Soil Science Society of America Journal* (Vol. 77). <https://doi.org/10.2136/sssaj2012.0271>
- Goebel, M. O., Woche, S. K., & Bachmann, J. (2012). Quantitative analysis of liquid penetration kinetics and slaking of aggregates as related to solid-liquid interfacial properties. *Journal of Hydrology*, 442–443, 63–74. <https://doi.org/10.1016/j.jhydrol.2012.03.039>
- Goldman, S. J., Jackson, K., & Bursztynsky, T. A. (1986). *Erosion and Sediment Control Handbook*. XF2006261146.
- Guo, L., Breakspear, A., Zhao, G., Gao, L., Corby Kistler, H., Xu, J.-R., & Ma, L.-J. (2015, June 30). Guo et al-2015-Molecular Plant Pathology.
- Guo, Y., Hartley, W., Xue, S., Zhu, F., Zhou, J., & Wu, C. (2016). Aging of bauxite residue in association of regeneration: a comparison of methods to determine aggregate stability & erosion resistance. *Ecological Engineering*, 92, 47–54. <https://doi.org/10.1016/j.ecoleng.2016.03.025>
- Hammes, F., & Verstraete, W. (2002). *Key roles of pH and calcium metabolism in microbial carbonate precipitation*. *Reviews in Environmental Science and Bio/Technology* (Vol. 1). <https://doi.org/10.1023/A:1015135629155>

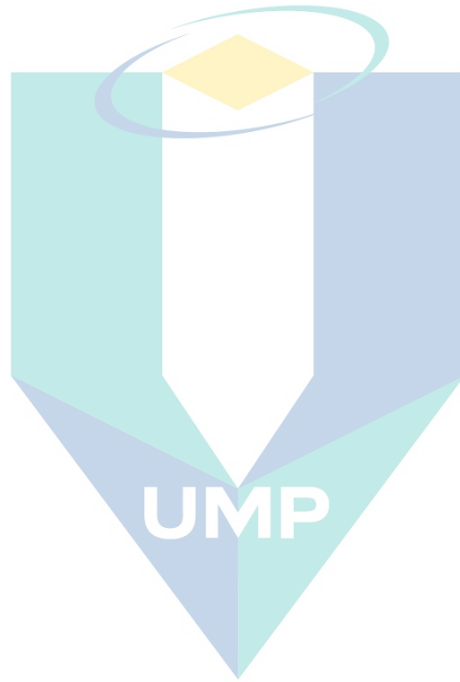
- Han, Y., Mao, W., & Wang, W. (2016). *Fire behavior of concrete-filled square steel tubular column with encased profiled steel subjected to non-uniform fires*. *Journal of Natural Disasters* (Vol. 25). <https://doi.org/10.13577/j.jnd.2016.0518>
- Hanc, A., & Dreslova, M. (2016). Effect of composting and vermicomposting on properties of particle size fractions. *Bioresource Technology*, 217, 186–189. <https://doi.org/10.1016/j.biortech.2016.02.058>
- Hazirbaba, K. (2019a). *Pore pressure generation characteristics of sands and silty sands: a strain approach*.
- Hazirbaba, K. (2019b). Stabilization of aeolian sand with combined use of geofiber and synthetic fluid. *Cogent Engineering*, 6(1), 1589895. <https://doi.org/10.1080/23311916.2019.1589895>
- Hill, G. T. et al. (2000). Methods for assessing the composition and diversity of soil microbial communities. *Appl. Soil Ecol*, 15, 25–36.
- Hisham Abdullah, N., Mohamed, N., Sulaiman, L., Zakaria, A., & Abdul Rahim, D. (2016). *Potential Health Impacts of Bauxite Mining in Kuantan*. *The Malaysian journal of medical sciences : MJMS* (Vol. 23).
- Höfer, T., Gräbsch, C., Wahrendorf, D.-S., Zeilinger, J., Grote, M., Mazurek, N., & Le Floch, S. (2016). Dry bulk cargo shipping — an overlooked threat to the marine environment? *Marine Pollution Bulletin*, 110(1), 511–519. <https://doi.org/10.1016/j.marpolbul.2016.05.066>
- Horta JC. (1989). Carbonate and gypsum soils properties and classification. In *Proceedings of the twelfth international conference on soil mechanics and foundation engineering*. (p. No. 1. p. 53–56.).
- Hou, X., Hu, H., & Silberschmidt, V. (2014). *Numerical analysis of composite structure with in-plane isotropic negative Poisson's ratio: Effects of materials properties and geometry features of inclusions*. *Composites Part B: Engineering* (Vol. 58). <https://doi.org/10.1016/j.compositesb.>
- Ivanov, V., & Chu, J. (2008). *Applications of microorganisms to geotechnical engineering for bioclogging and biocementation of soil in situ*. *Reviews in Environmental Science and Biotechnology* (Vol. 7). <https://doi.org/10.1007/s11157-007-9126-3>
- Jonas, M. (2015). Carriage of Bauxite – Liquefaction Risks. *The London Steam Ship*, (64), 1. Retrieved from <http://www.safety4sea.com/images/media/pdf/2015/London-PANDI-stoploss-Carriage-of-Bauxite>
- Ju, L., Vassalos, D., Wang, Q., Wang, Y., & Liu, Y. (2018). Numerical investigation of solid bulk cargo liquefaction. *Ocean Engineering*, 159(April), 333–347. <https://doi.org/10.1016/j.oceaneng.2018.04.030>

- Karami, A., Homaei, M., Afzalnia, S., Rouhipour, H., & Basirat, S. (2012). *Organic resource management: Impacts on soil aggregate stability and other soil physico-chemical properties. Agriculture, Ecosystems & Environment* (Vol. 148). <https://doi.org/10.1016/j.agee.2011.10.021>
- Koromila, I.A., Spandonidis, C.C., Spyrou, K.J., 2013. Experimental investigation of cargo liquefaction and impact on the stability of a bulk – Carrier. In: Proc. 13th Int. Ship Stability
- Kuttah, D., & Sato, K. (2015). Review on the effect of gypsum content on soil behavior. *Transportation Geotechnics*, 4, 28–37. <https://doi.org/10.1016/j.trgeo.2015.06.003>
- Le Bissonnais, Y. (1996). *Aggregate stability and assessment of soil crustability and erodibility: I. Theory and methodology. European Journal of Soil Science - EUR J SOIL SCI* (Vol. 47). <https://doi.org/10.1111/j.1365-2389.1996.tb01843.x>
- Li, L. Y., & Rutherford, G. K. (1996). Effect of bauxite properties on the settling of red mud. *International Journal of Mineral Processing*, 48(3–4), 169–182. [https://doi.org/10.1016/S0301-7516\(96\)00024-5](https://doi.org/10.1016/S0301-7516(96)00024-5)
- Lin, H. (Thomas, Suleiman, M., Brown, D., & Kavazanjian, E. (2015). *Mechanical Behavior of Sands Treated by Microbially Induced Carbonate Precipitation. Journal of Geotechnical and Geoenvironmental Engineering* (Vol. 142). [https://doi.org/10.1061/\(ASCE\)GT.1943-5606.0001383](https://doi.org/10.1061/(ASCE)GT.1943-5606.0001383)
- Mahmood, A. A., & Mulligan, C. (2016). Liquefaction studies: A review LIQUEFACTION STUDIES : A REVIEW, (January 2002).
- Martin Jonas. (2010). Liquefaction of unprocessed mineral ores - Iron ore fines and nickel ore. *Gard News*, 197.
- Maurer, B. W., Green, R. A., Cubrinovski, M., & Bradley, B. A. (2014). Evaluation of the Liquefaction Potential Index for Assessing Liquefaction Hazard in Christchurch, New Zealand. *Journal of Geotechnical and Geoenvironmental Engineering*, 140(7), 04014032. [https://doi.org/10.1061/\(asce\)gt.1943-5606.0001117](https://doi.org/10.1061/(asce)gt.1943-5606.0001117)
- Mitchell JK, Baxter CDP, M. T. (1995). Performance of improved ground during earthquakes. In Hryciw RD (Ed.), *Soil Improvement for Earthquake Hazard Mitigation* (p. P 1–36.). New York: Geotechnical Special Publication ASCE.
- Munro, M. C., & Mohajerani, A. (2016a). Moisture content limits of Iron Ore Fines to prevent liquefaction during transport: Review and experimental study. *International Journal of Mineral Processing*, 148, 137–146. <https://doi.org/10.1016/j.minpro.2016.01.019>
- Munro, M. C., & Mohajerani, A. (2016b). Variation of the geotechnical properties of Iron Ore Fines under cyclic loading. *Ocean Engineering*, 126(September), 411–431. <https://doi.org/10.1016/j.oceaneng.2016.09.006>

- Munro, M. C., & Mohajerani, A. (2017). Bulk cargo liquefaction incidents during marine transportation and possible causes. *Ocean Engineering*, 141(June), 125–142. <https://doi.org/10.1016/j.oceaneng.2017.06.010>
- Munro, M. C., & Mohajerani, A. (2018). Laboratory scale reproduction and analysis of the behaviour of iron ore fines under cyclic loading to investigate liquefaction during marine transportation. *Marine Structures*, 59(February), 482–509. <https://doi.org/10.1016/j.marstruc.2018.02.013>
- Nath, A., Chattopadhyay, P. K., & Majumdar, G. C. (2007). *High temperature short time air puffed ready-to-eat (RTE) potato snacks: Process parameter optimization. Journal of Food Engineering - J FOOD ENG* (Vol. 80). <https://doi.org/10.1016/j.jfoodeng.2006.07.006>
- Ni, S. H., & Fan, E. S. (2002). Fines content effects on liquefaction potential evaluation for sites liquefied during chi-chi earthquake, 1999. *Journal of the Chinese Institute of Engineers, Transactions of the Chinese Institute of Engineers, Series A/Chung-Kuo Kung Ch'eng Hsueh K'an*, 25(5), 533–542. <https://doi.org/10.1080/02533839.2002.9670728>
- Patrick Koester, J. (1994). *Influence of fines type and content on cyclic strength. Geotechnical Special Publication.*
- Paul, B., Vanlauwe, B., Ayuke, F., Gassner, A., Hoogmoed, M., Hurisso, T. T., Pulleman, M. (2013). *Medium-term impact of tillage and residue management on soil aggregate stability, soil carbon and crop productivity. Agriculture, Ecosystems & Environment* (Vol. 164). <https://doi.org/10.1016/j.agee.2012.10.003>
- Prakash, S., & K. Puri, V. (1999). *Liquefaction of Silts and Silt-Clay Mixtures. Journal of Geotechnical and Geoenvironmental Engineering - J GEOTECH GEOENVIRON ENG* (Vol. 125). [https://doi.org/10.1061/\(ASCE\)1090-0241\(1999\)125:8\(706\)](https://doi.org/10.1061/(ASCE)1090-0241(1999)125:8(706))
- Qiao, W., Ellis, C., Steffen, J., CY, W., & DJ, E. (2009). Zinc status and vacuolar zinc transporters control alkaline phosphatase accumulation and activity in *Saccharomyces cerevisiae*. *Molecular Microbiology*, 72(2), 320–334.
- Razouki, S. S., & Ibrahim, A. N. (2019). Improving the resilient modulus of a gypsum sand roadbed soil by increased compaction. *International Journal of Pavement Engineering*, 20(4), 432–438. <https://doi.org/10.1080/10298436.2017.1309190>
- Services, H. (2010). Toxicological Profile for Aluminum. *ATSDR's Toxicological Profiles*, (September). https://doi.org/10.1201/9781420061888_ch29
- Silver, M. L., & Seed, H. B. (1971). *Volume changes in sands during cyclic loading. J. Soil Mech. and Found. Div.* (Vol. 97).
- Stanchi, S., Falsone, G., & Bonifacio, E. (2015). *Soil aggregation, erodibility, and erosion rates in mountain soils (NW Alps, Italy). Solid Earth* (Vol. 6). <https://doi.org/10.5194/se-6-403-2015>

- Subhi, H. . (1987). *Properties of salt contaminated soils and their influence on the performance of roads in Iraq*. Queen Mary College, University of London.
- Teng, H., Chen, L., Huang, Q., Wang, J., Lin, Q., Liu, M., Song, H. (2016). *Ultrasonic-Assisted Extraction of Raspberry Seed Oil and Evaluation of Its Physicochemical Properties, Fatty Acid Compositions and Antioxidant Activities*. *PloS one* (Vol. 11). <https://doi.org/10.1371/journal.pone.0153457>
- Wang, C., & Dreger, D. (2004). *Liquefaction of Soils during Earthquakes*. *AGU Fall Meeting Abstracts*.
- Wang, Y., Zhang, J., & Zhang, Z. H. (2015). *Influences of intensive tillage on water-stable aggregate distribution on a steep hillslope*. *Soil and Tillage Research* (Vol. 151). <https://doi.org/10.1016/j.still.2015.03.003>
- Xiao, H., Liu, G., Zhang, Q., Fenli, Z., Zhang, X., Liu, P., Elbasit, M. A. M. A. (2018). Quantifying contributions of slaking and mechanical breakdown of soil aggregates to splash erosion for different soils from the Loess plateau of China. *Soil and Tillage Research*, 178(26), 150–158. <https://doi.org/10.1016/j.still.2017.12.026>
- Xiao, P., Liu, H., Xiao, Y., Stuedlein, A. W., & Evans, T. M. (2018). Liquefaction resistance of bio-cemented calcareous sand. *Soil Dynamics and Earthquake Engineering*, 107(November 2017), 9–19. <https://doi.org/10.1016/j.soildyn.2018.01.008>
- Yadav, A., & Garg, V. K. (2013). *Nutrient Recycling from Industrial Solid Wastes and Weeds by Vermiprocessing Using Earthworms*. *Pedosphere* (Vol. 23). [https://doi.org/10.1016/S1002-0160\(13\)60059-4](https://doi.org/10.1016/S1002-0160(13)60059-4)
- Yang, L., Yin, P., Fan, H., Xue, Q., Li, K., Li, X., Liu, Y. (2017). *Response Surface Methodology Optimization of Ultrasonic-Assisted Extraction of Acer Truncatum Leaves for Maximal Phenolic Yield and Antioxidant Activity*. *Molecules* (Vol. 22). <https://doi.org/10.3390/molecules22020232>
- Yemiş, G., Pagotto, F., Bach, S., & Delaquis, P. (2011). *Effect of Vanillin, Ethyl Vanillin, and Vanillic Acid on the Growth and Heat Resistance of Cronobacter Species*. *Journal of food Protection* (Vol. 74). <https://doi.org/10.4315/0362-028X.JFP-11-230>
- Yoder R.E., R. E. A.-Y. (1936). A direct method of aggregate analysis of soils and a study of the physical nature of erosion losses. *Agronomy Journal*, v. 28(5), 337-351–1936 v.28 no.5. <https://doi.org/10.2134/agronj1936.00021962002800050001x>
- Zhao SW, H. F. (1991). The nitrogen uptake efficiency from ¹⁵N labeled chemical fertilizer in the presence of earthworm manure. In V. C. Vereresh GK, Rajagopal D (Ed.), *Advances in management and conservation of soil fauna* (p. pp 539–542.). New Delhi: Oxford and IBH Publishing.
- Zhu, F., Hou, J., Xue, S., Wu, C., Wang, Q., & Hartley, W. (2017). Vermicompost and Gypsum Amendments Improve Aggregate Formation in Bauxite Residue. *Land Degradation and Development*, 28(7), 2109–2120. <https://doi.org/10.1002/ldr.2737>

Zhu, F., Liao, J., Xue, S., Hartley, W., Zou, Q., & Wu, H. (2016). Science of the Total Environment Evaluation of aggregate microstructures following natural regeneration in bauxite residue as characterized by synchrotron-based X-ray micro-computed tomography. *Science of the Total Environment*, 573, 155–163. <https://doi.org/10.1016/j.scitotenv.2016.08.108>



اونيورسيتي ملايسيا قهغ

UNIVERSITI MALAYSIA PAHANG

APPENDIX A

PHASE 1: SCREENING METHOD

Percentage passing %					
Sieve Size (mm)	Mass of Sieve (g)	Mass of Sieve + Soil Retained (g)	Mass Retained on Sieve (g)	Percent Retained (%)	Percent Passing (%)
10.0	592.7	711.0	118.3	12.4	87.6
6.3	515.6	682.1	166.5	17.4	70.2
5.0	508.7	619.5	110.8	11.6	58.6
3.4	540.4	730.6	190.2	19.9	38.6
1.2	514.7	732.4	217.8	22.8	15.8
0.6	390.9	441.6	50.6	5.3	10.5
0.3	448.2	476.8	28.6	3.0	7.5
0.2	421.6	434.7	13.1	1.4	6.2
0.1	299.3	306.6	7.4	0.8	5.4
Pan	243.4	294.8	51.4	5.4	0.0
			954.6	100	

Percentage passing %					
Sieve Size (mm)	Mass of Sieve (g)	Mass of Sieve + Soil Retained (g)	Mass Retained on Sieve (g)	Percent Retained (%)	Percent Passing (%)
10.0	592.7	712.0	119.3	12.7	87.3
6.3	515.6	673.5	157.9	16.9	70.4
5.0	508.7	622.4	113.7	12.1	58.3
3.4	540.4	737.1	196.8	21.0	37.3
1.2	514.7	749.7	235.0	25.1	12.2
0.6	390.9	448.5	57.5	6.1	6.0
0.3	448.2	477.0	28.8	3.1	3.0
0.2	421.6	435.5	13.9	1.5	1.5
0.1	299.3	310.7	11.4	1.2	0.3
Pan	243.4	245.8	2.4	0.3	0.0
			936.76		

Percentage passing %					
Sieve Size (mm)	Mass of Sieve (g)	Mass of Sieve + Soil Retained (g)	Mass Retained on Sieve (g)	Percent Retained (%)	Percent Passing (%)
10.0	592.7	708.5	115.8	12.0	88.0
6.3	515.6	691.8	176.2	18.3	69.7
5.0	508.7	626.3	117.7	12.2	57.5
3.4	540.4	751.5	211.1	21.9	35.6
1.2	514.7	741.9	227.2	23.6	12.0
0.6	390.9	452.2	61.3	6.4	5.7
0.3	448.2	477.2	29.0	3.0	2.7
0.2	421.6	436.3	14.7	1.5	1.1
0.1	299.3	308.8	9.5	1.0	0.1
Pan	243.4	244.8	1.4	0.1	0.0
			963.9		

Percentage passing %					
Sieve Size (mm)	Mass of Sieve (g)	Mass of Sieve + Soil Retained (g)	Mass Retained on Sieve (g)	Percent Retained (%)	Percent Passing (%)
10.0	592.7	670.0	77.3	8.4	91.6
6.3	515.6	668.3	152.7	16.5	75.2
5.0	508.7	631.1	122.5	13.2	61.9
3.4	540.4	746.0	205.7	22.2	39.7
1.2	514.7	763.1	248.5	26.8	12.8
0.6	390.9	449.6	58.7	6.3	6.5
0.3	448.2	485.2	37.0	4.0	2.5
0.2	421.6	436.0	14.4	1.6	0.9
0.1	299.3	306.4	7.2	0.8	0.2
Pan	243.4	245.0	1.6	0.2	0.0
			925.45		

Percentage passing %					
Sieve Size (mm)	Mass of Sieve (g)	Mass of Sieve + Soil Retained (g)	Mass Retained on Sieve (g)	Percent Retained (%)	Percent Passing (%)
10.0	592.7	698.8	106.2	11.7	88.3
6.3	515.6	686.9	171.3	18.9	69.4
5.0	508.7	628.0	119.4	13.2	56.2
3.4	540.4	721.0	180.6	19.9	36.2
1.2	514.7	734.8	220.1	24.3	11.9
0.6	390.9	439.9	48.9	5.4	6.5
0.3	448.2	480.4	32.2	3.6	3.0
0.2	421.6	436.8	15.2	1.7	1.3
0.1	299.3	308.7	9.4	1.0	0.3
Pan	243.4	245.8	2.4	0.3	0.0
			905.59		

Percentage passing %					
Sieve Size (mm)	Mass of Sieve (g)	Mass of Sieve + Soil Retained (g)	Mass Retained on Sieve (g)	Percent Retained (%)	Percent Passing (%)
10.0	592.7	699.9	107.2	11.3	88.7
6.3	515.6	706.4	190.8	20.1	68.5
5.0	508.7	639.7	131.1	13.8	54.7
3.4	540.4	734.0	193.6	20.4	34.2
1.2	514.7	730.2	215.6	22.8	11.5
0.6	390.9	444.7	53.8	5.7	5.8
0.3	448.2	477.5	29.3	3.1	2.7
0.2	421.6	434.7	13.1	1.4	1.3
0.1	299.3	309.5	10.2	1.1	0.2
Pan	243.4	245.6	2.2	0.2	0.0
			946.8		

Percentage passing %					
Sieve Size (mm)	Mass of Sieve (g)	Mass of Sieve + Soil Retained (g)	Mass Retained on Sieve (g)	Percent Retained (%)	Percent Passing (%)
10.0	592.7	631.4	38.7	4.2	95.8
6.3	515.6	687.0	171.4	18.7	77.1
5.0	508.7	627.1	118.5	12.9	64.2
3.4	540.4	767.0	226.6	24.7	39.6
1.2	514.7	758.9	244.2	26.6	13.0
0.6	390.9	450.4	59.5	6.5	6.5
0.3	448.2	485.4	37.2	4.0	2.5
0.2	421.6	435.9	14.3	1.6	0.9
0.1	299.3	306.0	6.8	0.7	0.2
Pan	243.4	245.2	1.8	0.2	0.0
			918.97		

Percentage passing %					
Sieve Size (mm)	Mass of Sieve (g)	Mass of Sieve + Soil Retained (g)	Mass Retained on Sieve (g)	Percent Retained (%)	Percent Passing (%)
10.0	592.7	711.1	118.4	12.2	87.8
6.3	515.6	701.9	186.3	19.2	68.6
5.0	508.7	637.4	128.8	13.3	55.3
3.4	540.4	727.5	187.1	19.3	36.0
1.2	514.7	735.8	221.1	22.8	13.2
0.6	390.9	449.6	58.6	6.0	7.1
0.3	448.2	483.1	34.9	3.6	3.5
0.2	421.6	438.4	16.9	1.7	1.8
0.1	299.3	313.0	13.8	1.4	0.3
Pan	243.4	246.7	3.3	0.3	0.0
			969.13		

Percentage passing %					
Sieve Size (mm)	Mass of Sieve (g)	Mass of Sieve + Soil Retained (g)	Mass Retained on Sieve (g)	Percent Retained (%)	Percent Passing (%)
10	592.68	714.0	121.3	13.3	86.7
6.3	515.59	687.4	171.8	18.9	67.7
5	508.65	618.1	109.5	12.0	55.7
3.35	540.39	717.0	176.6	19.4	36.3
1.18	514.67	729.5	214.8	23.6	12.6
0.6	390.94	443.9	53.0	5.8	6.8
0.3	448.2	483.8	35.6	3.9	2.9
0.15	421.58	438.0	16.4	1.8	1.1
0.063	299.25	307.4	8.2	0.9	0.2
Pan	243.38	244.9	1.6	0.2	0.0
			908.74		

Percentage passing %					
Sieve Size (mm)	Mass of Sieve (g)	Mass of Sieve + Soil Retained (g)	Mass Retained on Sieve (g)	Percent Retained (%)	Percent Passing (%)
10	592.68	666.1	73.4	7.7	92.3
6.3	515.59	726.9	211.3	22.2	70.0
5	508.65	654.8	146.2	15.4	54.7
3.35	540.39	726.3	185.9	19.6	35.1
1.18	514.67	739.7	225.0	23.7	11.4
0.6	390.94	449.5	58.6	6.2	5.3
0.3	448.2	479.7	31.5	3.3	2.0
0.15	421.58	433.8	12.2	1.3	0.7
0.063	299.25	305.6	6.3	0.7	0.0
Pan	243.38	243.4	0.1	0.0	0.0
			950.43		

Percentage passing %					
Sieve Size (mm)	Mass of Sieve (g)	Mass of Sieve + Soil Retained (g)	Mass Retained on Sieve (g)	Percent Retained (%)	Percent Passing (%)
10	592.68	670.8	78.1	8.4	91.6
6.3	515.59	701.0	185.4	19.9	71.7
5	508.65	645.1	136.5	14.6	57.1
3.35	540.39	740.0	199.6	21.4	35.6
1.18	514.67	743.6	228.9	24.6	11.1
0.6	390.94	443.5	52.6	5.6	5.4
0.3	448.2	478.4	30.2	3.2	2.2
0.15	421.58	433.8	12.3	1.3	0.9
0.063	299.25	306.2	7.0	0.7	0.1
Pan	243.38	244.7	1.3	0.1	0.0
			931.75		

Percentage passing %					
Sieve Size (mm)	Mass of Sieve (g)	Mass of Sieve + Soil Retained (g)	Mass Retained on Sieve (g)	Percent Retained (%)	Percent Passing (%)
10	592.68	713.4	120.7	12.9	87.1
6.3	515.59	690.9	175.3	18.7	68.4
5	508.65	631.2	122.5	13.1	55.3
3.35	540.39	740.5	200.1	21.4	34.0
1.18	514.67	727.7	213.1	22.7	11.2
0.6	390.94	441.9	50.9	5.4	5.8
0.3	448.2	476.3	28.1	3.0	2.8
0.15	421.58	435.9	14.3	1.5	1.3
0.063	299.25	309.6	10.3	1.1	0.2
Pan	243.38	245.1	1.8	0.2	0.0
			937.01		

Percentage passing %					
Sieve Size (mm)	Mass of Sieve (g)	Mass of Sieve + Soil Retained (g)	Mass Retained on Sieve (g)	Percent Retained (%)	Percent Passing (%)
10	592.68	744.1	151.4	16.7	83.3
6.3	515.59	681.1	165.5	18.2	65.1
5	508.65	619.3	110.6	12.2	53.0
3.35	540.39	708.1	167.7	18.4	34.5
1.18	514.67	725.6	210.9	23.2	11.3
0.6	390.94	445.1	54.2	6.0	5.4
0.3	448.2	479.8	31.6	3.5	1.9
0.15	421.58	433.0	11.4	1.3	0.6
0.063	299.25	304.3	5.1	0.6	0.1
Pan	243.38	244.0	0.6	0.1	0.0
			908.98		

Percentage passing %					
Sieve Size (mm)	Mass of Sieve (g)	Mass of Sieve + Soil Retained (g)	Mass Retained on Sieve (g)	Percent Retained (%)	Percent Passing (%)
10	592.68	723.5	130.8	14.0	86.0
6.3	515.59	691.4	175.8	18.8	67.2
5	508.65	642.9	134.2	14.4	52.9
3.35	540.39	731.2	190.8	20.4	32.5
1.18	514.67	731.0	216.3	23.1	9.3
0.6	390.94	436.5	45.5	4.9	4.5
0.3	448.2	470.6	22.4	2.4	2.1
0.15	421.58	431.8	10.3	1.1	1.0
0.063	299.25	307.1	7.9	0.8	0.1
Pan	243.38	244.6	1.2	0.1	0.0
			935.21		

Percentage passing %					
Sieve Size (mm)	Mass of Sieve (g)	Mass of Sieve + Soil Retained (g)	Mass Retained on Sieve (g)	Percent Retained (%)	Percent Passing (%)
10	592.68	714.0	121.3	12.7	87.3
6.3	515.59	732.0	216.5	22.7	64.5
5	508.65	625.5	116.9	12.3	52.3
3.35	540.39	735.7	195.3	20.5	31.8
1.18	514.67	727.3	212.6	22.3	9.5
0.6	390.94	440.9	49.9	5.2	4.2
0.3	448.2	474.0	25.8	2.7	1.5
0.15	421.58	430.0	8.4	0.9	0.6
0.063	299.25	304.2	5.0	0.5	0.1
Pan	243.38	244.3	0.9	0.1	0.0
			952.6		

Percentage passing %					
Sieve Size (mm)	Mass of Sieve (g)	Mass of Sieve + Soil Retained (g)	Mass Retained on Sieve (g)	Percent Retained (%)	Percent Passing (%)
10	592.68	738.5	145.9	14.9	85.1
6.3	515.59	665.3	149.8	15.3	69.7
5	508.65	630.1	121.5	12.4	57.3
3.35	540.39	739.3	198.9	20.4	36.9
1.18	514.67	748.2	233.5	23.9	13.0
0.6	390.94	453.3	62.4	6.4	6.7
0.3	448.2	483.4	35.2	3.6	3.1
0.15	421.58	437.9	16.3	1.7	1.4
0.063	299.25	310.2	11.0	1.1	0.3
Pan	243.38	246.0	2.6	0.3	0.0
			976.95		

SPECIFIC GRAVITY

Samples	Unamen d	1	2	3	4	5	6	7	8	9	10	11	12	13	14	15	16
S.G. Container 1	2.88	1.71	2.16	2.68	2.06	2.15	2.39	2.73	2.06	2.41	2.63	2.22	2.69	2.45	1.88	2.94	2.51
S.G. Container 2	2.99	1.69	2.25	2.75	1.98	2.07	2.47	2.88	2.01	2.23	2.51	2.19	2.75	2.51	2.01	2.74	2.67
S.G Container 3	2.97	1.85	2.04	2.88	2.08	2.02	2.07	2.94	2.05	2.53	2.81	2.49	2.63	2.3	1.81	2.81	2.47
Average S.G.	2.95	1.75	2.15	2.77	2.04	2.08	2.31	2.85	2.04	2.39	2.65	2.3	2.69	2.42	1.9	2.83	2.55

اونيورسيتي ملايسيا قهغ

UNIVERSITI MALAYSIA PAHANG

APPENDIX B

PHASE 2: CENTRE COMPOSITE DESIGN

Percentage passing %					
Sieve Size (mm)	Mass of Sieve (g)	Mass of Sieve + Soil Retained (g)	Mass Retained on Sieve (g)	Percent Retained (%)	Percent Passing (%)
10.0	592.7	673.6	80.92	8.69	91.31
6.3	515.6	702.5	186.91	20.08	71.22
5.0	508.7	643.5	134.85	14.49	56.74
3.4	540.4	739.2	198.81	21.36	35.38
1.2	514.7	742.6	227.93	24.49	10.89
0.6	390.9	445.6	54.66	5.87	5.02
0.3	448.2	477.3	29.10	3.13	1.89
0.2	421.6	432.1	10.52	1.13	0.76
0.1	299.3	305.9	6.65	0.71	0.05
Pan	243.4	243.8	0.42	0.05	0.00
			930.77	100	

Percentage passing %					
Sieve Size (mm)	Mass of Sieve (g)	Mass of Sieve + Soil Retained (g)	Mass Retained on Sieve (g)	Percent Retained (%)	Percent Passing (%)
10.0	592.7	712.6	119.92	13.10	86.90
6.3	515.6	680.5	164.91	18.02	68.88
5.0	508.7	633.5	124.85	13.64	55.23
3.4	540.4	740.9	200.51	21.91	33.32
1.2	514.7	722.6	207.93	22.72	10.60
0.6	390.9	440.2	49.26	5.38	5.22
0.3	448.2	477.3	29.10	3.18	2.04
0.2	421.6	425.1	3.52	0.38	1.66
0.1	299.3	308.7	9.45	1.03	0.63
Pan	243.4	249.1	5.72	0.63	0.00
			915.17		

Percentage passing %					
Sieve Size (mm)	Mass of Sieve (g)	Mass of Sieve + Soil Retained (g)	Mass Retained on Sieve (g)	Percent Retained (%)	Percent Passing (%)
10.0	592.7	695.6	102.92	11.46	88.54
6.3	515.6	684.3	168.71	18.79	69.75
5.0	508.7	630.1	121.45	13.52	56.23
3.4	540.4	721.6	181.21	20.18	36.05
1.2	514.7	733.6	218.93	24.38	11.68
0.6	390.9	440.2	49.26	5.49	6.19
0.3	448.2	479.3	31.10	3.46	2.73
0.2	421.6	435.6	14.02	1.56	1.17
0.1	299.3	309.5	10.25	1.14	0.02
Pan	243.4	243.6	0.22	0.02	0.00
			898.07	100.0	

Percentage passing %					
Sieve Size (mm)	Mass of Sieve (g)	Mass of Sieve + Soil Retained (g)	Mass Retained on Sieve (g)	Percent Retained (%)	Percent Passing (%)
10.0	592.7	723.5	130.82	13.84	86.16
6.3	515.6	691.2	175.61	18.58	67.59
5.0	508.7	631.8	123.15	13.03	54.56
3.4	540.4	742.2	201.81	21.35	33.21
1.2	514.7	726.1	211.43	22.36	10.85
0.6	390.9	440.6	49.66	5.25	5.59
0.3	448.2	477.5	29.30	3.10	2.50
0.2	421.6	433.2	11.62	1.23	1.27
0.1	299.3	308.6	9.35	0.99	0.28
Pan	243.4	246.0	2.62	0.28	0.00
			945.37		

Percentage passing %					
Sieve Size (mm)	Mass of Sieve (g)	Mass of Sieve + Soil Retained (g)	Mass Retained on Sieve (g)	Percent Retained (%)	Percent Passing (%)
10.0	592.7	710.2	117.52	12.13	87.87
6.3	515.6	702.8	187.21	19.33	68.53
5.0	508.7	638.6	129.95	13.42	55.12
3.4	540.4	726.4	186.01	19.21	35.91
1.2	514.7	736.2	221.53	22.87	13.04
0.6	390.9	450.6	59.66	6.16	6.88
0.3	448.2	482.6	34.40	3.55	3.32
0.2	421.6	437.1	15.52	1.60	1.72
0.1	299.3	312.0	12.75	1.32	0.40
Pan	243.4	247.3	3.92	0.40	0.00
			968.47		

Percentage passing %					
Sieve Size (mm)	Mass of Sieve (g)	Mass of Sieve + Soil Retained (g)	Mass Retained on Sieve (g)	Percent Retained (%)	Percent Passing (%)
10.0	592.7	724.1	131.42	14.10	85.90
6.3	515.6	690.2	174.61	18.70	67.20
5.0	508.7	643.1	134.45	14.40	52.80
3.4	540.4	727.2	186.81	20.00	32.80
1.2	514.7	731.0	216.33	23.16	9.64
0.6	390.9	435.6	44.66	4.78	4.85
0.3	448.2	471.0	22.80	2.44	2.41
0.2	421.6	432.1	10.52	1.13	1.29
0.1	299.3	308.2	8.95	0.96	0.33
Pan	243.4	244.8	1.42	0.15	0.17
			931.97		

Percentage passing %					
Sieve Size (mm)	Mass of Sieve (g)	Mass of Sieve + Soil Retained (g)	Mass Retained on Sieve (g)	Percent Retained (%)	Percent Passing (%)
10.0	592.7	672.8	80.12	8.63	91.37
6.3	515.6	703.2	187.61	20.21	71.16
5.0	508.7	645.3	136.65	14.72	56.45
3.4	540.4	742.6	202.21	21.78	34.67
1.2	514.7	741.0	226.33	24.38	10.29
0.6	390.9	441.8	50.86	5.48	4.81
0.3	448.2	476.3	28.10	3.03	1.79
0.2	421.6	431.8	10.22	1.10	0.69
0.1	299.3	305.1	5.85	0.63	0.06
Pan	243.4	243.9	0.52	0.06	0.00
			928.47		

Percentage passing %					
Sieve Size (mm)	Mass of Sieve (g)	Mass of Sieve + Soil Retained (g)	Mass Retained on Sieve (g)	Percent Retained (%)	Percent Passing (%)
10.0	592.7	743.2	150.52	16.52	83.48
6.3	515.6	682.1	166.51	18.28	65.20
5.0	508.7	620.3	111.65	12.26	52.94
3.4	540.4	703.1	162.71	17.86	35.08
1.2	514.7	738.1	223.43	24.53	10.55
0.6	390.9	443.1	52.16	5.73	4.83
0.3	448.2	476.1	27.90	3.06	1.77
0.2	421.6	432.6	11.02	1.21	0.56
0.1	299.3	303.5	4.25	0.47	0.09
Pan	243.4	244.2	0.82	0.09	0.00
			910.97		

Percentage passing %					
Sieve Size (mm)	Mass of Sieve (g)	Mass of Sieve + Soil Retained (g)	Mass Retained on Sieve (g)	Percent Retained (%)	Percent Passing (%)
10	592.68	712.5	119.82	12.75	87.25
6.3	515.59	691.2	175.61	18.69	68.56
5	508.65	632.1	123.45	13.14	55.42
3.35	540.39	751.9	211.51	22.51	32.91
1.18	514.67	718.2	203.53	21.66	11.24
0.6	390.94	440.1	49.16	5.23	6.01
0.3	448.2	477.3	29.10	3.10	2.92
0.15	421.58	436.2	14.62	1.56	1.36
0.063	299.25	310.8	11.55	1.23	0.13
Pan	243.38	244.6	1.22	0.13	0.00
			939.57		

Percentage passing %					
Sieve Size (mm)	Mass of Sieve (g)	Mass of Sieve + Soil Retained (g)	Mass Retained on Sieve (g)	Percent Retained (%)	Percent Passing (%)
10	592.68	712.4	119.72	12.69	87.31
6.3	515.59	691.2	175.61	18.62	68.68
5	508.65	632.1	123.45	13.09	55.59
3.35	540.39	740.6	200.21	21.23	34.36
1.18	514.67	734.1	219.43	23.27	11.10
0.6	390.94	440.3	49.36	5.23	5.86
0.3	448.2	477.5	29.30	3.11	2.76
0.15	421.58	434.1	12.52	1.33	1.43
0.063	299.25	310.2	10.95	1.16	0.27
Pan	243.38	245.9	2.52	0.27	0.00
			943.07		

Percentage passing %					
Sieve Size (mm)	Mass of Sieve (g)	Mass of Sieve + Soil Retained (g)	Mass Retained on Sieve (g)	Percent Retained (%)	Percent Passing (%)
10	592.68	712.5	119.82	12.73	87.27
6.3	515.59	691.2	175.61	18.66	68.60
5	508.65	632.1	123.45	13.12	55.48
3.35	540.39	748.1	207.71	22.07	33.41
1.18	514.67	722.9	208.23	22.13	11.28
0.6	390.94	440.2	49.26	5.24	6.05
0.3	448.2	477.3	29.10	3.09	2.95
0.15	421.58	436.1	14.52	1.54	1.41
0.063	299.25	308.6	9.35	0.99	0.42
Pan	243.38	247.3	3.92	0.42	0.00
			940.97		

Percentage passing %					
Sieve Size (mm)	Mass of Sieve (g)	Mass of Sieve + Soil Retained (g)	Mass Retained on Sieve (g)	Percent Retained (%)	Percent Passing (%)
10	592.68	712.9	120.22	12.88	87.12
6.3	515.59	690.1	174.51	18.70	68.42
5	508.65	632.6	123.95	13.28	55.14
3.35	540.39	748.3	207.91	22.28	32.86
1.18	514.67	718.3	203.63	21.82	11.04
0.6	390.94	440.2	49.26	5.28	5.76
0.3	448.2	477.3	29.10	3.12	2.65
0.15	421.58	436.2	14.62	1.57	1.08
0.063	299.25	308.6	9.35	1.00	0.08
Pan	243.38	244.1	0.72	0.08	0.00
			933.27		

Percentage passing %					
Sieve Size (mm)	Mass of Sieve (g)	Mass of Sieve + Soil Retained (g)	Mass Retained on Sieve (g)	Percent Retained (%)	Percent Passing (%)
10	592.68	710.3	117.62	12.58	87.42
6.3	515.59	688.2	172.61	18.46	68.96
5	508.65	633.1	124.45	13.31	55.64
3.35	540.39	745.1	204.71	21.90	33.75
1.18	514.67	724.3	209.63	22.42	11.32
0.6	390.94	440.8	49.86	5.33	5.99
0.3	448.2	475.3	27.10	2.90	3.09
0.15	421.58	436.2	14.62	1.56	1.53
0.063	299.25	310.6	11.35	1.21	0.31
Pan	243.38	246.3	2.92	0.31	0.00
			934.87		

SPECIFIC GRAVITY

Samples	1	2	3	4	5	6	7	8	9	10	11	12	13
S.G. Container 1	2.41	2.45	1.98	2.15	2.12	2.33	2.48	2.10	2.38	2.27	2.32	2.34	2.34
S.G. Container 2	2.36	2.38	2.11	2.06	2.07	2.41	2.57	2.24	2.43	2.41	2.41	2.25	2.26
S.G. Container 3	2.19	2.40	1.94	2.09	1.96	2.31	2.51	2.20	2.42	2.49	2.35	2.28	2.12
Average S.G.	2.32	2.41	2.01	2.10	2.05	2.35	2.52	2.18	2.41	2.39	2.36	2.29	2.24

اونيورسيتي ملايسيا قهغ

UNIVERSITI MALAYSIA PAHANG

APPENDIX C

PHASE 3: VALIDATION AND MODELLING

Bauxite Sample (B-10503)

Disruptive test	Size	ID	Net Weight	Percentage (%)	X_i	W_i
Fast Wetting (Slaking)	2-1.18	35F	13.95	93.25	1.59	0.9325
	1.18-0.212	37F	0.51	3.41	0.696	0.0341
	0.212-0.063	39F	0.46	3.1	0.1375	0.031
	<0.063		0.04	0.2674		
Slow Wetting (Clay Swelling)	2-1.18	31F	7.86	83.24	1.59	0.8324
	1.18-0.212	29F	0.78	8.251	0.696	0.08251
	0.212-0.063	33F	0.39	4.08	0.1375	0.0408
	<0.063		0.42	4.46		
Wet Stirring (Breakdown)	2-1.18	15A	8.46	86.64	1.59	0.8664
	1.18-0.212	13F	0.782	8.01	0.696	0.0801
	0.212-0.063	55A	0.251	2.57	0.1375	0.0257
	<0.063		0.271	2.78		

Bauxite Sample (B-10505)

Disruptive test	Size	ID	Net Weight	Percentage (%)	X_i	W_i
Fast Wetting (Slaking)	2-1.18	31F	15.72	93.10	1.59	0.9310
	1.18-0.212	29F	0.49	2.9	0.696	0.029
	0.212-0.063	33F	0.59	3.47	0.1375	0.0347
	<0.063		0.09	0.53		
Slow Wetting (Clay Swelling)	2-1.18	55A	9.76	89.8	1.59	0.898
	1.18-0.212	13F	0.16	1.47	0.696	0.0147
	0.212-0.063	15A	0.41	3.77	0.1375	0.0377
	<0.063		0.54	4.96		
Wet Stirring (Breakdown)	2-1.18	39F	8.31	83.1	1.59	0.831
	1.18-0.212	37F	0.9	9	0.696	0.09
	0.212-0.063	35F	0.38	3.8	0.1375	0.038
	<0.063		0.41	4.1		

Bauxite Sample (B-10705)

Disruptive test	Size	ID	Net Weight	Percentage (%)	X_i	W_i
Fast Wetting (Slaking)	2-1.18	37F	14.13	97.85	1.59	0.9785
	1.18-0.212	55A	0.08	0.554	0.696	0.00554
	0.212-0.063	29F	0.19	1.32	0.1375	0.0132
	<0.063		0.04	0.277		
Slow Wetting (Clay Swelling)	2-1.18	39F	10.07	94.32	1.59	0.9432
	1.18-0.212	35F	0.4368	4.09	0.696	0.0409
	0.212-0.063	15A	0.1411	1.32	0.1375	0.01321
	<0.063		0.029	0.27		
Wet Stirring (Breakdown)	2-1.18	31F	8.71	88.62	1.59	0.8862
	1.18-0.212	33F	0.62	6.31	0.696	0.0631
	0.212-0.063	13F	0.24	2.46	0.1375	0.0246
	<0.063		0.26	2.61		

Bauxite Sample (B-10404)

Disruptive test	Size	ID	Net Weight	Percentage (%)	X_i	W_i
Fast Wetting (Slaking)	2-1.18	15A	13.41	87.5	1.59	0.875
	1.18-0.212	13F	0.23	1.52	0.696	0.0152
	0.212-0.063	35F	0.62	4.06	0.1375	0.0406
	<0.063		1.06	6.92		
Slow Wetting (Clay Swelling)	2-1.18	29F	8.26	84.72	1.59	0.8472
	1.18-0.212	55A	0.83	8.51	0.696	0.08513
	0.212-0.063	37F	0.35	3.59	0.1375	0.0359
	<0.063		0.31	3.18		
Wet Stirring (Breakdown)	2-1.18	39F	8.43	87.72	1.59	0.8772
	1.18-0.212	33F	0.76	7.91	0.696	0.0791
	0.212-0.063	31F	0.26	2.71	0.1375	0.0271
	<0.063		0.16	1.65		

UNIVERSITI MALAYSIA PAHANG

Bauxite Sample (B-10606)

Disruptive test	Size	ID	Net Weight	Percentage (%)	X_i	W_i
Fast Wetting (Slaking)	2-1.18	37F	16.32	97.67	1.59	0.9767
	1.18-0.212	55A	0.12	0.718	0.696	0.00718
	0.212-0.063	29F	0.21	1.26	0.1375	0.0126
	<0.063		0.06	0.3591		
Slow Wetting (Clay Swelling)	2-1.18	39F	9.82	89.27	1.59	0.8927
	1.18-0.212	35F	0.2	1.82	0.696	0.0182
	0.212-0.063	15A	0.39	3.55	0.1375	0.0355
	<0.063		0.59	5.36		
Wet Stirring (Breakdown)	2-1.18	31F	9.29	93.09	1.59	0.9309
	1.18-0.212	33F	0.25	2.5	0.696	0.0250
	0.212-0.063	13F	0.34	3.41	0.1375	0.0341
	<0.063		0.1	0.010		

Bauxite Sample (B-A10604)

Disruptive test	Size	ID	Net Weight	Percentage (%)	X_i	W_i
Fast Wetting (Slaking)	2-1.18	31F	15.48	96.66	1.59	0.9656
	1.18-0.212	29F	0.15	0.935	0.696	0.00935
	0.212-0.063	33F	0.30	1.871	0.1375	0.01871
	<0.063		0.1	0.6238		
Slow Wetting (Clay Swelling)	2-1.18	39F	9.63	95.35	1.59	0.9535
	1.18-0.212	35F	0.3	2.97	0.696	0.0297
	0.212-0.063	15A	0.12	1.19	0.1375	0.0119
	<0.063		0.05	0.5		
Wet Stirring (Breakdown)	2-1.18	31F	9.69	95.94	1.59	0.9594
	1.18-0.212	33F	0.14	1.39	0.696	0.0139
	0.212-0.063	13F	0.15	1.49	0.1375	0.0149
	<0.063		0.12	1.19		

UNIVERSITI MALAYSIA PAHANG

Bauxite Sample (B-B10604)

Disruptive test	Size	ID	Net Weight	Percentage (%)	X_i	W_i
Fast Wetting (Slaking)	2-1.18	37F	14.58	96.62	1.59	0.9662
	1.18-0.212	55A	0.14	0.9278	0.696	0.009278
	0.212-0.063	29F	0.29	1.922	0.1375	0.01922
	<0.063		0.08	0.530		
Slow Wetting (Clay Swelling)	2-1.18	39F	9.85	94.08	1.59	0.9408
	1.18-0.212	35F	0.45	4.298	0.696	0.04298
	0.212-0.063	15A	0.14	1.337	0.1375	0.01337
	<0.063		0.03	0.287		
Wet Stirring (Breakdown)	2-1.18	31F	9.52	95.2	1.59	0.952
	1.18-0.212	33F	0.13	1.3	0.696	0.013
	0.212-0.063	13F	0.21	2.1	0.1375	0.021
	<0.063		0.14	1.4		

Bauxite Sample (B-C10604)

Disruptive test	Size	ID	Net Weight	Percentage (%)	X_i	W_i
Fast Wetting (Slaking)	2-1.18	37F	15.16	96.684	1.59	0.96684
	1.18-0.212	55A	0.21	1.34	0.696	0.0134
	0.212-0.063	29F	0.19	1.21	0.1375	0.0121
	<0.063		0.12	0.7653		
Slow Wetting (Clay Swelling)	2-1.18	39F	9.73	93.288	1.59	0.9328
	1.18-0.212	35F	0.41	3.931	0.696	0.03931
	0.212-0.063	15A	0.19	1.822	0.1375	0.01822
	<0.063		0.1	0.9587		
Wet Stirring (Breakdown)	2-1.18	31F	9.56	94.94	1.59	0.9494
	1.18-0.212	33F	0.19	1.887	0.696	0.01887
	0.212-0.063	13F	0.24	2.383	0.1375	0.02383
	<0.063		0.08	0.7944		

UNIVERSITI MALAYSIA PAHANG

Bauxite Sample (B-10204)

Disruptive test	Size	ID	Net Weight	Percentage (%)	X_i	W_i
Fast Wetting (Slaking)	2-1.18	37F	7.93	75.4	1.59	0.754
	1.18-0.212	55A	0.82	7.79	0.696	0.0779
	0.212-0.063	29F	1.24	11.79	0.1375	0.1179
	<0.063		0.53	5.04		
Slow Wetting (Clay Swelling)	2-1.18	39F	8.93	77.25	1.59	0.7725
	1.18-0.212	35F	1.42	12.28	0.696	0.1228
	0.212-0.063	15A	0.8	6.92	0.1375	0.0692
	<0.063		0.41	3.55		
Wet Stirring (Breakdown)	2-1.18	31F	7.96	73.4	1.59	0.734
	1.18-0.212	33F	1.23	11.36	0.696	0.1136
	0.212-0.063	13F	0.58	5.31	0.1375	0.0531
	<0.063		1.077	9.93		

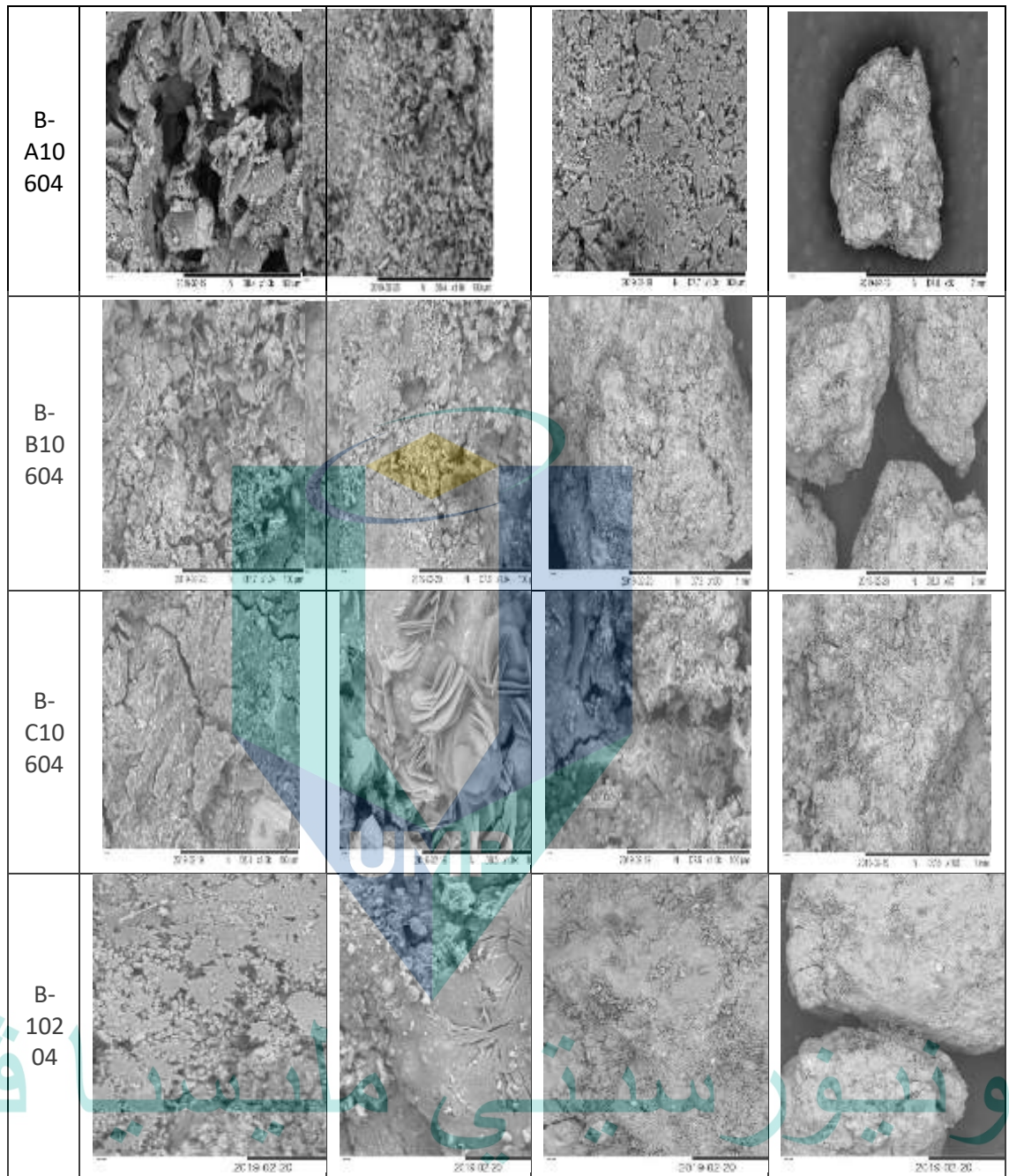
Bauxite Sample (B-100)

Disruptive test	Size	ID	Net Weight	Percentage (%)	X_i	W_i
Fast Wetting (Slaking)	2-1.18	37F	8.05	67.08	1.59	0.6708
	1.18-0.212	55A	0.9	7.5	0.696	0.075
	0.212-0.063	29F	2.44	20.33	0.1375	0.203
	<0.063		0.61	5.08		
Slow Wetting (Clay Swelling)	2-1.18	39F	9.03	75.25	1.59	0.7525
	1.18-0.212	35F	1.59	13.25	0.696	0.1325
	0.212-0.063	15A	0.93	7.75	0.1375	0.0775
	<0.063		0.45	3.75		
Wet Stirring (Breakdown)	2-1.18	31F	8.12	67.67	1.59	0.67
	1.18-0.212	33F	1.92	16	0.696	0.16
	0.212-0.063	13F	0.92	7.7	0.1375	0.077
	<0.063		1.04	8.67		

Samples	B-10503	B-10505	B-10705	B-10404	B-10606	B-A10604	B-B10604	B-C10604	B-10204	B-100
Mass above the flow state	330.53	329.39	326.45	323.16	369.24	310.52	308.14	306.79	302.13	397.98
Mass above the flow state after drying	239.13	237.65	235.48	236.93	285.12	225.43	221.59	220.74	230.87	301.89
Mass below the flow state	344.89	343.96	350.42	334.12	364.24	339.35	337.61	336.49	330.46	381.22
Mass below the flow state after drying	262.17	259.64	265.34	253.76	247.21	235.14	231.96	229.17	250.68	298.13
Flow moisture point (%)	25.82%	26.18%	26.07%	25.37%	27.46%	29.06%	29.69%	29.97%	23.86%	22.97%
Transportable moisture limit	23.24%	23.56%	23.47%	22.83%	24.71%	26.15%	26.72%	26.97%	21.48%	20.67%

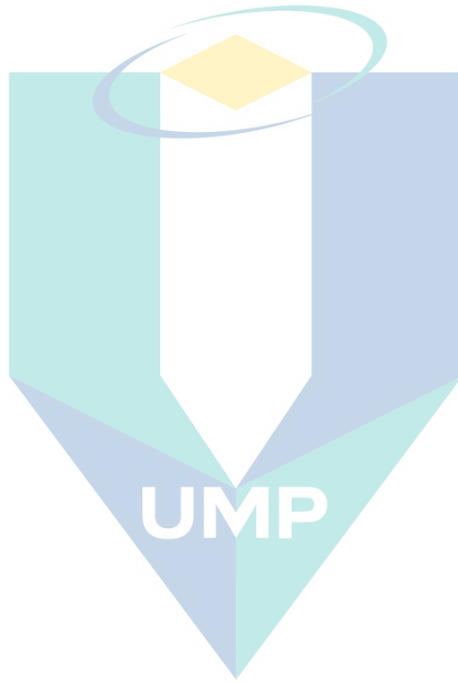
spl	1st	2nd	3rd	4th
B-10503				
B-10505				
B-10705				
B-10404				
B-10606				

UNIVERSITI MALAYSIA PAHANG



اوپن سٹیٹ یونیورسٹی

UNIVERSITI MALAYSIA PAHANG



اونيورسيتي ملايسيا قهغ

UNIVERSITI MALAYSIA PAHANG